Identification of Markers to Predict Benefit from Trastuzumab Treatment

Thesis

Identification of markers to predict benefit from trastuzumab treatment

Student: **Tiziana Triulzi**

OU personal identifier: C8584713

Director of studies: Dr. Elda Tagliabue

Supervisor: Dr. Aleix Prat

Registered degree: Doctor of Philosophy

Sponsoring establishment: Fondazione IRCSS, Istituto Nazionale dei Tumori, Milan, Italy

Submission date: February 2017

TABLE OF CONTENTS

ABSTRACT

Despite the clinical benefit of trastuzumab, some patients do not respond to this therapy. Aims of this study are to identify new predictive biomarkers to distinguish responsive from *de novo* resistant tumours and to have new insights into the biological characterisation of trastuzumab activity.

Whole-transcriptome analysis of primary HER2-positive breast carcinomas (BCs) treated with adjuvant trastuzumab identified a tumour subgroup, characterised by high *ERBB2*/low *ESR1* expression, with good clinical outcome, and allowed the development of a trastuzumab risk model (TRAR) able to identify patients with high- and low-risk of relapse. Application of TRAR model to available datasets and to a new series of HER2-positive BC patients treated with neoadjuvant trastuzumab designated TRAR as predictive of response rather than associated to low aggressiveness. Our analyses showed that tumours exquisitely sensitive to treatment are addicted to HER2, enriched in immune pathways and have a peculiar circulating NK profile, characterised by high expression of the NKG2D receptor. Enrichment of immune system- and tyrosine kinase receptor signaling-related pathways was found associated also with response to trastuzumab monotherapy in clinical samples, suggesting the possibility to treat HER2-addicted tumours with trastuzumab monotherapy. Accordingly TRAR-low, high-NKG2D- and -MHC-II-expressing tumours were associated with response to one cycle of trastuzumab alone. In addition, increase of MHC-II gene expression upon a single cycle of trastuzumab characterised patients who benefit from the following combination with chemotherapy. Characterisation of biological features of TRAR-low tumours showed high infiltration of macrophages and CD8+ T cells, together with the expression of chemokines involved in

their recruitment and of immune checkpoint ligands. *In vitro* analysis demonstrated a direct regulation of CCL2 and PD-L1 by HER2 signals.

Overall, we described a tool able to identify BCs responsive to trastuzumab and understood that in these tumours HER2 is crucial for tumour growth, for infiltration of pro-trastuzumab immune cells and their suppression.

LIST OF FIGURES AND TABLES

ABBREVIATIONS

ADCC	Antibody dependent cell mediated cytotoxicity
ADCP	Antibody dependent cell mediated phagocitosys
APC	Antigen presenting cells
AT	Adriamycin plus taxotere
AUC	Area under the ROC curve
BC	Breast cancer
CEP17	Chromosome 17
CISH	Cromogenic in situ hybridization
CK	Citokeratins
CTL	CD8+ cytotoxic T cell
d16HER2	Delta 16 HER2
DASL	DNA-mediated annealing, selection, extension and ligation
DFS	Disease free survival
DH	Docetaxel and trastuzumab
DPz	Docetaxel and pertuzumab
ECD	Extracellular domain
ECM	Extracellular matrix
EGF	Epidermal growth factor
EGFR	Epidermal growth factor receptor
ER	Estrogen receptor
FFPE	Formalin-fixed paraffin-embedded
FISH	Fluorescent in situ hybridization
GEP	Gene expression profile
GHEA	Group HErceptin in Adjuvant therapy
HCK	Hematopoietic cell kinase
HDPP	HER2-derived prognostic predictor
HER	Human epidermal growth factor receptor
HER2-E	HER2-enriched
HPz	Trastuzumab and pertuzumab
HRG	Heregulin
ICD	Immunogenic cell death
IDC	Infiltrating ductal carcinoma
IF	Immunofluorescence
IFN	Interferon
IGF1R	Insulin growth factor receptor
IHC	Immunohistochemistry
IRE	Immune response-enriched
LCK	Lymphocyte-specific kinase
LPBC	Lymphocyte-predominant BC
Mab	Monoclonal antibody
MAPK	Mitogen-activated protein kinase
Metabric	MolEcular TAxonomy of Breast Cancer International Consortium

MDSC	Myeloid-derived suppressor cell
MFI	Median fluorescent intensity
MHC	Major histocompatibility complex
NF-kB	Nuclear factor-κB
NK	Natural killer
NKG2D	NK Group 2 member D
NIRE	Non-mmune response-enriched
NRG	Neuregulins
PAM	Prediction analysis of microarray
PBMCs	Peripheral blood mononuclear cells
pCR	Pathologic complete response
PD-1	Programmed cell death protein 1
PD-L	Programmed cell death potein ligand
PI3K	Phosphatidylinositol 3-kinase
PIK3CA	Phosphatidylinositol 3-kinase catalytic subunit alpha
pCR	Pathological complete response
PR	Progesteron receptor
PTEN	Phosphatase and tensin homolog
qRT-PCR	Quantitative real time PCR
ROC	Receiver Operator Characteristic
RTK	Tyrosine kinase receptor
TAM	Tumour associated macrophages
TCA	The citric acid cycle
TCGA	The Cancer Genome Atlas
TCR	T cell receptor
TIL	Tumour infiltrating lymphocytes
TKI	Tyrosine kinase inhibitor
TME	Tumour microenvironment
TNBC	Triple negative breast cancer
TRAR	TRastuzumab Advantage Risk
Treg	Regulatory T cell
TRUP	TRastuzumab UPfront

CHAPTER 1: INTRODUCTION

1.1 Breast cancer

Breast cancer (BC) is the second most common cancer worldwide after lung cancer, the fifth most common cause of cancer death, and the principal cause of cancer death in women. The incidence rates of BC are increasing [Jemal et al., 2010], but mortality rate has been decreasing, reaching a total reduction of about 35% over the last three decades [Kohler et al., 2015].

1.1.1 Breast cancer histopathological classification

BC is not a single disease, but comprises many biologically different entities with distinct pathological features and clinical implications [Rivenbark et al., 2013].

From a histological point of view BCs are classified based on the degree of invasion of cancer in the surrounding tissue [Weigelt et al., 2010]. Cancer that does not extend beyond the involved duct or the lobule is called in-situ carcinoma and based on the cell of origin is called Ductal Carcinoma in Situ or Lobular Carcinoma in Situ. Cancer that infiltrates the surroundings is called invasive carcinoma. The major invasive tumour types include infiltrating ductal (IDC), invasive lobular, mucinous, tubular, medullary and papillary carcinomas. Of these, IDC is the most common subtype, accounting for 70–80% of all invasive lesions [Li et al., 2005].

The severity of the disease is evaluated examining physical and anatomical properties of the cancer using histological grading and TNM staging. The histological grade is the description of the neoplasia according to abnormalities of tumour cells compared to normal cells when observed under a microscope and, depending on their extent, a numerical score of 1, 2 or 3 is assigned. It is based on three factors: i) the amount of tubule formation; ii) the nuclear pleomorphism and iii) the mitotic activity. Grade1 score corresponds to neoplastic cells which appear highly similar to normal cells, in contrast,

cells with higher dissimilarities from normal cells identify Grade3 tumours, which have a poorer prognosis than lower-grade tumours [Rakha et al., 2010].

In the TNM system, T (1-4) is used to describe the size of the tumour, N (0-3) accounts for the lymph node invasion and M measures the spread of the tumour to distant sites. T grows according to increase dimension, with T1 tumours that have size lower than 2 cm, T2 2-5 cm, T3 >5cm. T4 tumours have any size and have grown into the chest wall or skin. N0 indicates that no cancer cells are found in the lymph nodes; N1-the cancer has spread up to three nodes; N2- the cancer has spread to four to nine nodes; N3- the cancer has spread to more than ten nodes. M0 indicates that the cancer has not metastasised, whereas M1 that there is evidence of metastasis to another part of the body. The cancer is then staged by combining T, N and M classifications.

These clinico-pathological variables together with immunohistochemical markers are conventionally used to predict patient prognosis and for disease management [Senkus et al., 2015]. Estrogen receptor (ER) and progesterone receptor (PR) assays are performed on paraffin sections of all invasive BCs by immunohistochemistry (IHC) [Hammond et al., 2010]. They are weak prognostic factors but are the strongest predictive factors for endocrine therapy response. The nuclear staining positivity of any intensity in at least 1% of tumour cells is the cut-off of positivity used in the clinic based on data showing that patients with even 1% ER/PR-positive tumours may benefit from hormonal therapy. About 70% of all BCs are ER-positive and 60% to 65% are PR-positive.

The human epidermal growth factor receptor (HER) 2 is usually assessed by IHC according to ASCO guideline recommendation [Wolff et al., 2007;Wolff et al., 2013]. The IHC scoring criteria are shown in figure 1. Tumours are scored negative when no staining (score 0, Fig. 1A) or a faint incomplete membrane staining (score 1+, Fig. 1C) is visualised in at least 10% tumour cells; positive when a weak to moderate complete membrane

staining is observed and the staining ring is thin (score 2+, Fig. 1B) or when a strong complete membrane staining (score 3+, Fig. 1D) is observed. In situ hybridization assay of HER2 expression is usually performed in tumours that are scored as 2+ by IHC.

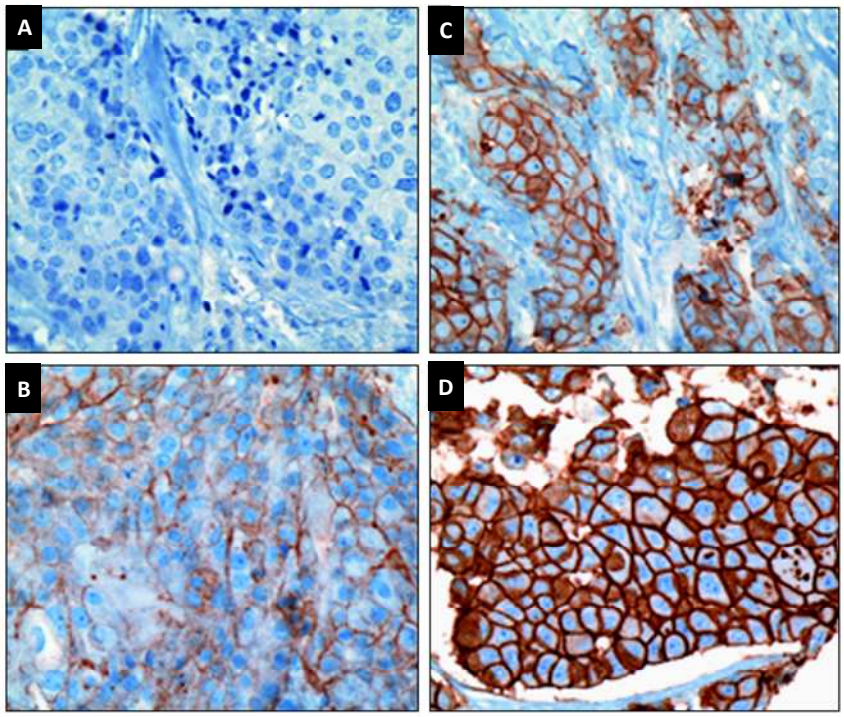

Figure 1. IHC assessment of the level of HER2 protein expression at the tumour cell membrane

Images of tumour staining using the US Food and Drug Administration–approved DAKO HercepTest kit according to the manufacturer's instructions**. A:** IHC score 0; **B:** IHC score 1+; **C:** IHC score 2+; **D:** IHC score 3+ (**A**-**D**, ×400). Modified from [Hicks and Kulkarni, 2008]

In situ hybridization techniques, like fluorescence and chromogenic in situ hybridization (FISH and CISH, respectively), allowed the determination of *ERBB2* gene copy number using DNA probes conjugated with a fluorophore or a peroxidase [Penault-Llorca et al., 2009]. To evaluate *ERBB2* amplification in FISH assay 2 probes conjugated with two different fluorophores are used: one complementary to *ERBB2* gene and the other to the centromere of chromosome 17 (CEP17). Carcinomas are considered amplified when the ratio between the HER2 specific signals and the one of CEP17 is >2.2 (Fig. 2A) and negative when this ratio is <= 2.2 (Fig. 2B). CISH used only one probe directed against HER2 and is visualised with an optical microscope (Fig. 2C).

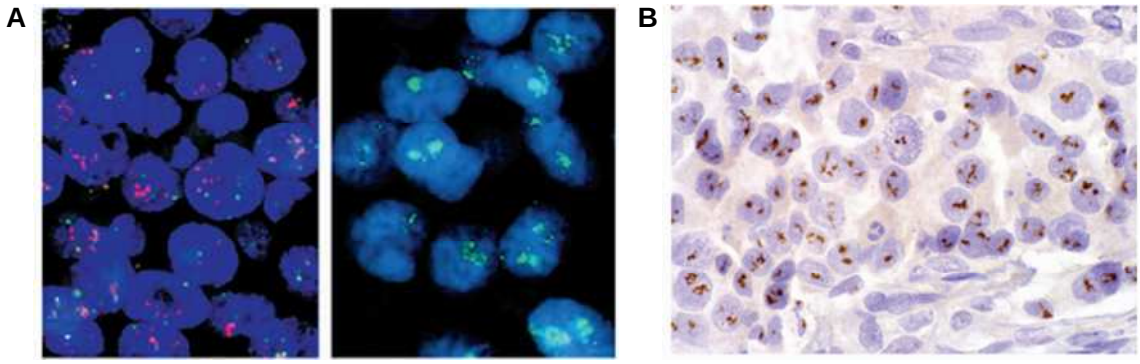

Figure 2. Evaluation of HER2 amplification status
A) Fluorescence in situ hybridization (FISH) of a case of IDC, on the left, negative for HER2 gene amplification and a case of HER2 gene-amplified BC, on the right. **B)** Chromogenic in situ hybridization (CISH) of an IDC with significant HER2 gene amplification. Adapted from [Ross et al., 2009].

Testing criteria define HER2-positive tumours when there is evidence of protein overexpression (IHC 3+) or gene amplification. Overexpression/amplification of HER2 is reported in 10% to 34% of invasive BCs [Ross et al., 2009].

1.1.2 Breast cancer molecular classification

With the development of microarrays, gene expression profiling (GEP) has been used to extricate the heterogeneity of BCs. The pioneer studies conducted by Sorlie et al. reported a typical 'molecular portrait' of BCs using 456 cDNA clones, according to which tumours were classified into five intrinsic subtypes with distinct clinical outcomes, i.e., luminal A, luminal B, HER2, basal and normal-like tumours [Perou et al., 2000;Sorlie et al., 2001]. In 2007 another BC subgroup was identified: claudin low [Herschkowitz et al., 2007] that share some gene expression features of basal-like tumours but with low expression of cell-cell adhesion molecules like claudins 3-4-7 and E-cadherin (Fig. 3A)[Prat and Perou, 2011].

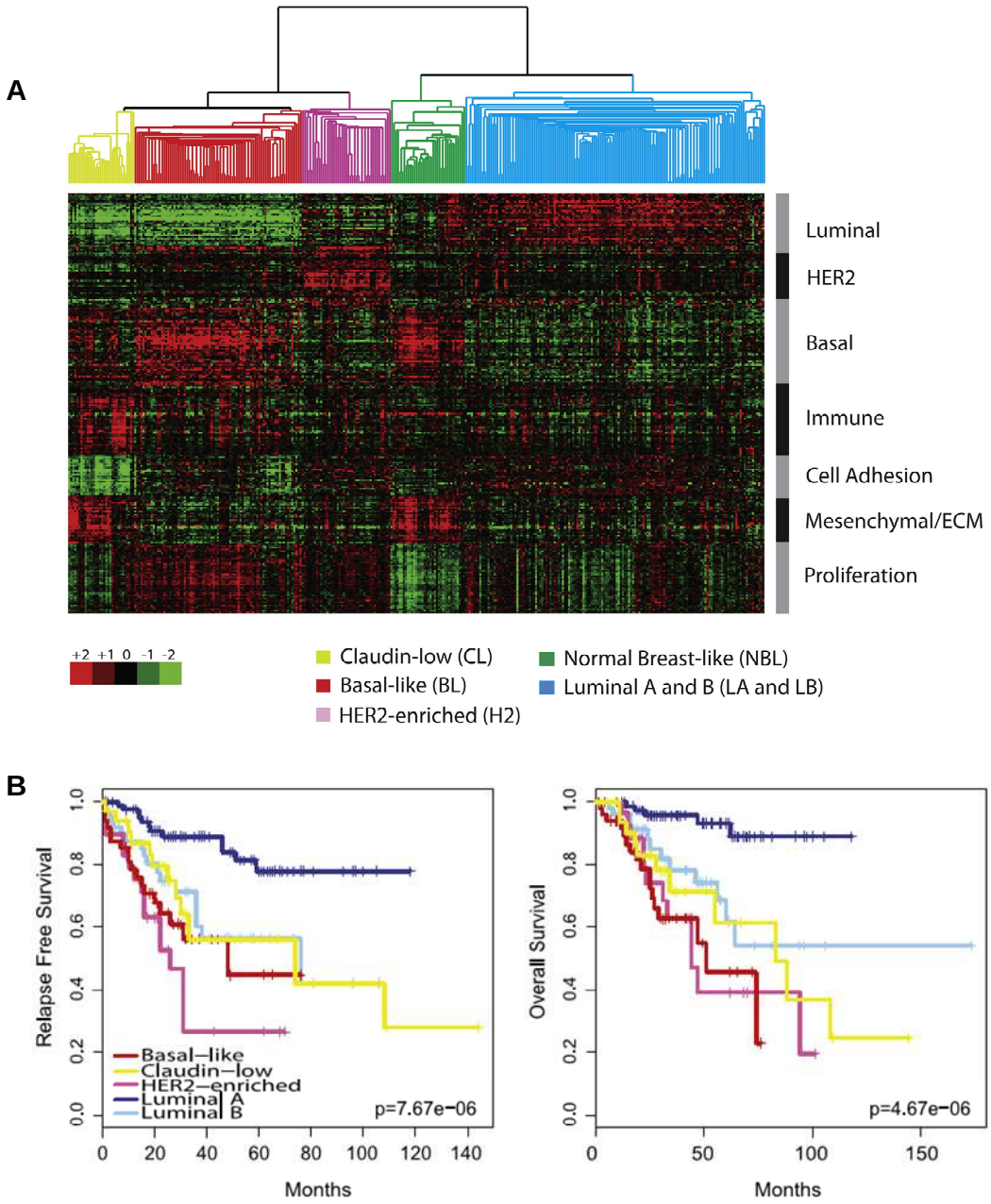

Figure 3. Breast cancer intrinsic subtype characterisation and prognosis
A) Intrinsic hierarchical clustering and selected gene expression patterns of UNC337 BCs dataset (GSE18229) using the intrinsic gene list from [Parker et al., 2009]. Sample-associated dendrogram is coloured according to intrinsic subtype. **B)** Kaplan Meier DFS survival and overall survival curves according to intrinsic partition with Normal-like samples excluded. [Prat and Perou, 2011]

The most reproducible identified molecular subtypes among the hormone receptor-positive cancers are the luminal A and luminal B groups. The HER2 and basal-like groups are the major molecular subtypes identified among hormone receptor-negative BCs. Other molecular subtypes such as luminal C, claudin-low and normal breast-like groups have been identified in some studies, but are less well-characterised than the luminal A, luminal B, HER2, and basal-like types. Also The Cancer Genome Atlas (TCGA) study

considered only these 4 subgroups due to low size of normal-like and claudin-low subgroups [Cancer Genome Atlas Network, 2012].

Luminal tumours

Luminal subset is the most common subtype among BCs. The luminal-like tumours have expression profiles reminiscent of the luminal epithelial component of the breast [Perou et al., 2000]. Indeed, these tumours express luminal cytokeratins 8/18, *ESR1* and genes associated with ER activation such as *LIV1* and *CCND1* [Sotiriou et al., 2003]. Luminal tumours are stratified in luminal A and luminal B. Luminal A tumours, that represent 50-60% of total BCs [Eroles et al., 2012], are mainly characterised by low pathological grade and proliferation rate. Luminal B tumours (10-20% of total BCs [Eroles et al., 2012]) are more aggressive, showing higher grade and proliferation index than subgroup A [Sorlie et al., 2003]. Approximately 20% of luminal B BCs also overexpresses HER2 and epidermal growth factor receptor (EGFR) tyrosine kinase receptors (RTKs) [Wirapati et al., 2008;Eroles et al., 2012].

In general, the luminal subtypes have a good prognosis even if luminal B tumours have a significantly worse prognosis than the luminal A (Fig. 3B). Luminal A tumours are adequately treated with endocrine therapy [Eroles et al., 2012], while luminal B tumours benefit more from chemotherapy and hormonal treatment.

HER2-positive tumours

The HER2-positive tumours are characterised by overexpression of HER2 and other genes in its amplicon such as *GRB7* [Perou et al., 2000]. They are characterised by high expression of HER2-regulated genes, proliferation/cell cycle-related genes and repression of luminal related genes. It is a highly proliferative subtype which accounts for 15-20% of all BC and is characterised by poor prognosis and higher risk of early relapse (Fig. 3B). They are sensitive to trastuzumab combined with chemotherapy.

Basal tumours

The basal subtype, including from 8 to 13% of BC has expression profiles mimicking that of the normal breast myo-epithelial cells [Perou et al., 2000]. Such expression patterns comprise low expression of hormone receptors and HER2, and high expression of basal markers [such as cytokeratins (CK) 5, 6, 14, 17, EGFR] and proliferation related genes [Sotiriou et al., 2003]. They have aggressive clinical course (Fig. 3B) and they are sensitive to conventional chemotherapies such as anthracycline and taxane [Brenton et al., 2005; Rouzier et al., 2005].

Further refinement of the BC molecular taxonomy was achieved through the studies performed by TCGA network [Cancer Genome Atlas Network, 2012] and the Molecular Taxonomy Of Breast Cancer International Consortium (METABRIC) [Curtis et al., 2012]. The TCGA investigated BC heterogeneity by incorporating information from multiple platforms, i.e., genomic DNA copy number arrays, DNA methylation, exome sequencing, mRNA arrays, miRNA sequencing and reverse-phase protein arrays. They found that diverse genetic and epigenetic alterations converge phenotypically into the four major BC subgroups (*i.e.,* luminal A, luminal B, HER2 positive, triple negative) previously identified using mRNA profiling. The METABRIC study by integrating mRNA profiling with copy number analysis of 2000 breast tumours, revealed refined BC molecular taxonomy, i.e., 10 integrative clusters which are named IntClust 1 to 10, [Curtis et al., 2012] with only a partial overlapping with the instrinsic subtypes.

The utility of these new molecular classifications to predict outcomes has raised hopes of its adaptation in clinical practice; however, routine use of microarray analysis or genome sequencing is still cost prohibitive. An attempt was made by researchers who narrowed down the intrinsic classification to a 50-gene signature that can effectively differentiate the molecular subtypes using quantitative real time PCR (qRT-PCR)[Parker et

al., 2009]. This 50-gene signature, termed prediction analysis of microarray 50 (PAM50), has been shown to be an effective replacement for full microarray analysis with an ability to classify tumours into one of the intrinsic subtypes [Parker et al., 2009]. Furthermore, it has been demonstrated that classification by PAM50 had a significantly improved ability to predict the risk of relapse compared to clinical variables (tumour size, node status and histological grade) [Parker et al., 2009]. However, its use in clinical practice is still uncommon and the approximation of the molecular category by a four biomarker profile (ER, PR, HER2, and KI67) evaluated by IHC is preferred (Table 1). In 2013, the evaluation of these markers was recommended in the St Gallen guidelines for clinical decision making [Goldhirsch et al., 2013b]. Using this approach, tumours that are ER- positive and/or PR-positive, HER2-negative and low proliferative (Ki67<14%) are most likely luminal A; those that are ER-positive and/or PR-positive, and HER2-positive or KI67-positive are most likely luminal B; those that are ER-negative, PR-negative, and HER2-positive are most likely HER2-enriched (HER2-E), and those that are ER-negative, PR-negative, and HER2-negative are most likely basal-like. CK5/6 and EGFR are now used to distinguish more precisely basal-like BC group among triple negative BC (TNBC)[Cheang et al., 2008]. Indeed, the overlap between histological TNBC and RNA-defined basal-like subtype is incomplete and the two terms do not unequivocally identify the same tumours [Kreike et al., 2007], even if the majority of basal-like BCs (80-85%) are also TNBCs and the majority of TNBCs (80-85%) are also basal-like BCs.

Thus, at the present time, this IHC-based profile seems to be the most useful panel for approximating the molecular subtype of BCs and to decide the treatment schedule in the clinical practice. Of note, the molecular intrinsic classification has been demonstrated to still provide clinically relevant information beyond current pathology-based classifications [Prat et al., 2015].

Table 1. Approximation of intrinsic molecular subtypes using IHC biomarkers. Adapted from [Guiu et al., 2012]

Intrinsic subtypes (GEP)	IHC classification (St. Gallen)	Agreement IHC/GEP
Luminal A	**'Luminal A'** ER- and/or PR-positive HER2-negative Ki-67<14%	73%-100%
Luminal B	**'Luminal B (HER2-negative)'** ER- and/or PR-positive HER2-negative Ki-67 >=14% **'Luminal B (HER2-positive)'** ER- and/or PR-positive HER2-positive Any Ki-67	73%-100%
HER2-enriched	**'HER2-positive (non-luminal)'** ER and PR absent HER2-positive	41%-69%
Basal-like	**'Triple negative'** ER and PR absent HER2-negative	80%

1.2 HER2-positive breast cancer

1.2.1 The HER receptor family

HER2 receptor is a member of the ERBB/HER family of transmembrane RTKs together with EGFR, HER3 and HER4. These proteins are type I transmembrane growth factor receptors that respond to extracellular signals activating intracellular signaling pathways. They are made of a large extracellular ligand-binding domain, which has four subdomains (I–IV), followed by a transmembrane domain, and an intracellular domain composed of a small intracellular juxta-membrane domain preceding the kinase domain, and a C-terminal tail, on which the docking sites for phospho-tyrosine binding effector molecules are present (Fig. 4). The extracellular domain of HER proteins is usually in a closed inactive conformation and when the ligand binds to the receptor it induces its conformational change to the open, active form (Fig. 4). At this state, receptors dimerise and a transphosphorylation of their intracellular domains occurs [Burgess et al., 2003]. This is true for the EGFR, HER3 and HER4 that bind specific ligands [Yarden, 2001], while HER2, an orphan receptor, has always a conformation that resembles a ligand-activated state favouring its dimerization [Citri and Yarden, 2006] (Fig. 4).

Thirteen polypeptide extracellular ligands have been identified, which contain a conserved epidermal growth factor (EGF) domain that consists of six cysteine residues. These ligands are divided into four groups on the basis of their receptor specificity (Fig. 5). The first one includes EGF, transforming growth factor alpha, amphiregulin and epigen, which bind specifically to EGFR; the second group includes heparin-binding EGF, epiregulin and betacellulin which bind both EGFR and HER3. The third one, the neuregulins (NRGs), are divided into two subgroups on the basis of their capacity to bind HER3 and HER4 (NRG-1 and NRG- 2) or only HER4 (NRG-3 and NRG-4). Heregulin (HRG) is one of the NRG-1 subgroup.

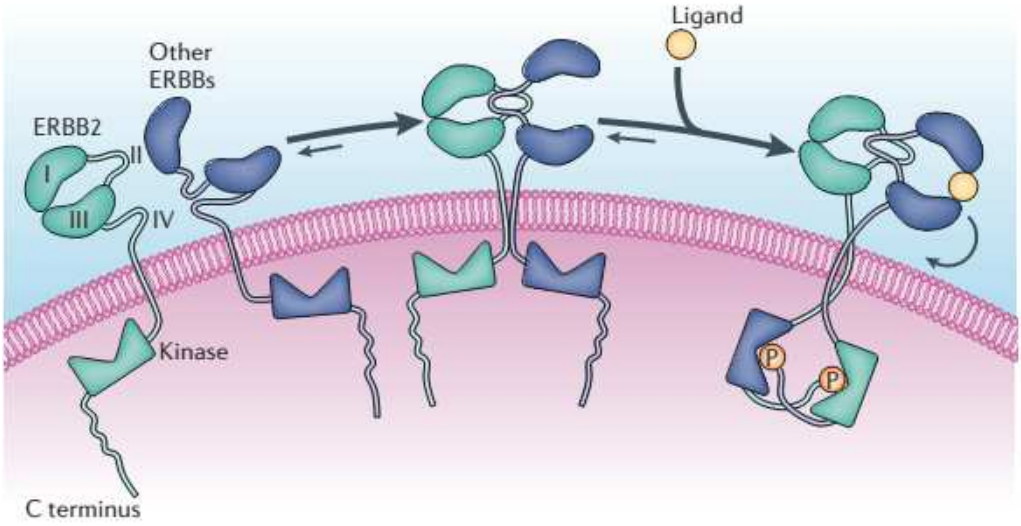

Figure 4. Structural bases for ERBB-receptor dimerisation and activation
The dimerisation loop of HER2 is constitutively extended, even in the monomeric state and the strong interaction between domains I and III closes the binding pocket, which abolishes accessibility to ligands. P: phosphate. Other members of the ERBB family in their monomeric state are autoinhibited through an interaction of domain II with domain IV. This interaction keeps subdomains I and III at a distance that does not allow the simultaneous binding of a ligand to both subdomains, and at the same time sequesters the dimerisation loop. By stabilising a dimer and forcing a rotation in the vicinity of the membrane, ERBB ligands activate the kinase activity of the receptor. [Citri and Yarden, 2006]

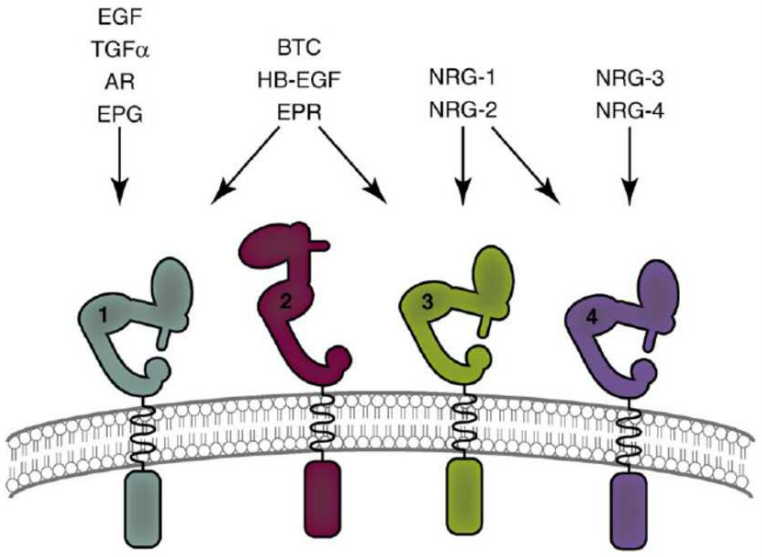

Figure 5. The HER receptors and their ligands
The four groups of HER ligands and their specificity EGFR (1), HER2 (2), HER3 (3) and HER4 (4) are shown. TGFa: transforming growth factor alpha; AR: amphiregulin; EPG: epigen; HB-EGF: heparin-binding; EPR: epiregulin; BTC: betacellulin; NRG: neuregulin. [Hynes and MacDonald, 2009]

Once phosphorylated in the tyrosine residues, many intracellular phosphotyrosine-binding proteins are recruited to the docking site of the HER receptors leading to

activation of a plethora of downstream second messenger pathways that induce several biological effects (Fig. 6) (reviewed in [Yarden and Sliwkowski, 2001]). Partner selection among HER proteins, as well as ligand identity, appear to be key determinants of the specificity and potency of intracellular signals. HER2 has the strongest catalytic kinase activity and thus HER2-containing heterodimers have the strongest signaling functions [Citri et al., 2003]. On the other hand HER3 lacks ATP binding within its catalytic domain and is catalytically inactive [Citri et al., 2003]. For this reason, the signaling functions of HER3 are entirely mediated by the kinase activity of its heterodimeric partners, that in the majority of cases is HER2 [Citri et al., 2003]. Notably, the HER2-HER3 heterodimers are the most transforming and mitogenic receptor complex [Siegel et al., 1999; Holbro et al., 2003; Waterman et al., 1999].

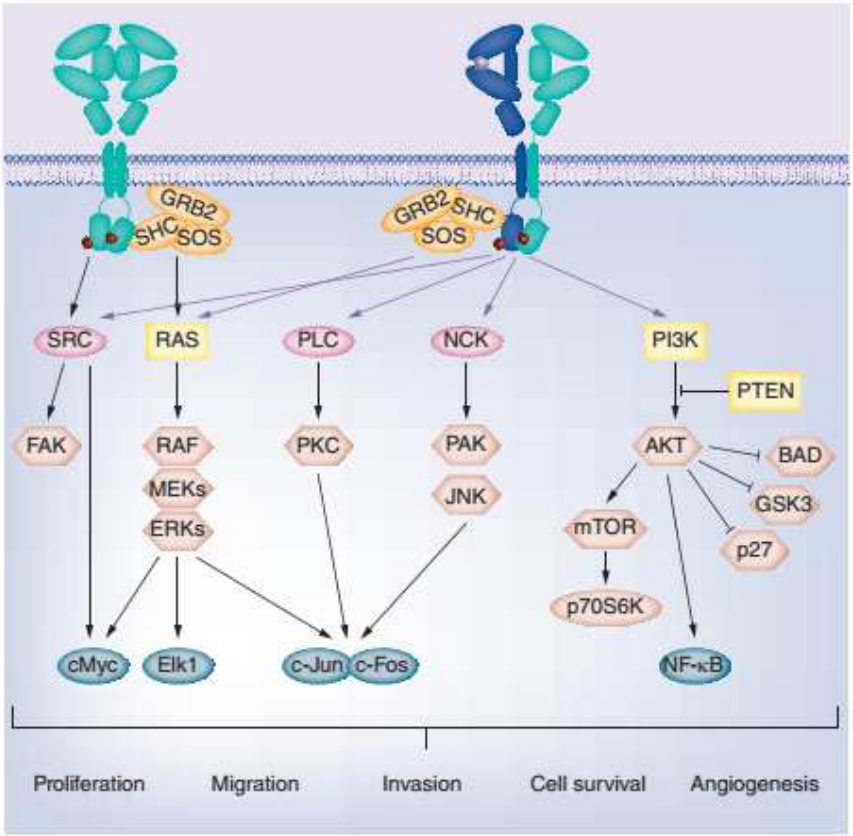

Figure 6. The HER receptors signaling cascade

The figure illustrates the HER2 (light blue) homodimer, the ligand- (grey dot) induced heterodimer with other members of the HER family (HER1, HER3 or HER4) (blue) and the downstream signaling pathways. Red dot showed phosphate. BAD: BCL2-associated agonist of cell death; ERK: extracellular signal-regulated kinases; FAK, focal adhesion kinase; GRB2: growth factor receptor-

bound protein 2; GSK3: glycogen synthase kinase 3; JNK: c-Jun N-terminal kinases; NCK: non-catalytic region of tyrosine kinase adaptor protein 1; NFκB: nuclear factor κB; MEK: mitogen-activated protein kinases; mTOR: mammalian target of rapamycin; p27: cyclin-dependent kinase inhibitor; PAK: p21-activated kinase; PI3K: phosphatidylinositol 3-kinase; PLC: phospholipase C; PKC: protein kinase C; PTEN: phosphatase and tensin homolog; SHC: Src homology 2 domain-containing; SOS: son of sevenless. [Triulzi et al., 2016]

The canonical signals downstream HER2 mediate cell proliferation through Ras- and Shc-activated mitogen-activated protein kinase axis (RAS-MAPK), and inhibit apoptosis, thereby fostering cell survival through activation of the phosphatidylinositol 3-kinases v-akt (PI3K-AKT) pathway, which is regulated by phosphatase and tensin homolog (PTEN) and involves key effectors such as the nuclear factor κB (NF-kB) and the mammalian target of rapamycin [Marmor et al., 2004]. The potency and kinetics of PI3K activation differ according to heterodimerization partner, probably because it couples directly to HER3 and HER4 and indirectly with HER1 and HER2 [Yarden and Sliwkowski, 2001]. Other important factors in the HER2 signaling network are the protein kinase C, which is activated by the phospholipase C [Marmor et al., 2004] and the c-Jun N-terminal kinases, which is activated by the non-catalytic region of tyrosine kinase adaptor protein 1 [Marmor et al., 2004; Yarden and Sliwkowski, 2001]. c-Src is also activated upon activation of HERs and is the main downstream signal of HER2 homodimers; the transcription factors STAT1, STAT3, and STAT5 can be directly phosphorylated by HERs, subsequent to which they dimerise and translocate to the nucleus to activate gene transcription critical for proliferation [Marmor et al., 2004]. This complex signaling cascade translates in the nucleus into distinct transcriptional programs through the recruitment of nuclear factors as the proto-oncogenes FOS, JUN and MYC, but also a family of zinc-finger containing transcription factors that includes SP1 and EGR1, as well as ETS family members such as GA-binding protein [Marmor et al., 2004].

HER-receptors can be also phosphorilated by other signals, including hormones, neurotransmitters, lymphokines and stress inducers [Yarden and Sliwkowski, 2001]. The

most studied mechanism involves the G-protein-coupled receptors, that have mitogenic activity transactivating HER-receptors through stimulation of Src kinases which phosphorilates the intracellular domains of HERs. Another mechanism of activation of HER network, independent from its own inputs, derives from the activation of the transcription of genes encoding their ligands downstream steroid hormones and the RAS-MAPK activation. In particular, the bi-directional cross-talk between HER2 and ER have been extensively investigated (reviewed in [Giuliano et al., 2013]), since almost the 50% of HER2-positive BCs also express ER [Osborne and Schiff, 2005]. On one hand, HER2 signaling could repress the expression of both ERα and ERβ receptors through multiple mechanisms, as the inactivation of FOXO3a or the activation of p42/44 MAPK. Moreover, the HER2 activation could positively regulate ER signalling and its estrogen dependency (Fig. 7). ER can in turn activate or inhibit HER2 through its signaling and activity as transcription factor [Giuliano et al., 2013]. Indeed, genes downregulated by estrogens include EGFR and HER2.

The strenght of the signals derived from HER-receptors depends also from the persistance of the receptor on the cell membrane. HER-receptors are regulated through internalization and degradation or recycling. The recognition of the tyrosine 1045 of HER1 by the ubiquitin ligase Cbl is fundamental in the shut down of the signaling and is a determinant of the receptor degradation in the lysosome [Yarden, 2001]. After receptor endocytosis, stability of the activated ligand-receptor complex in the endosomal environment is a determinant of the receptor fate: high stability, as those observed for EGFR homodimers, induces its ubiquitination and degradation, whereas less stable heterodimerisation between EGFR and HER2 causes Cbl dissociation from the receptor complex in the endosome and recycling of the receptors to the cell membrane. Activation of some pathways, like PKC, induced by certain growth factors and hormones (for

example PDGF, LPA and EGF itself) increases threonine and serine phosphorilation of HER1 and HER2 which decreases tyrosine phosphorilation and ligand binding affinity, inducing a rapid recycling of the receptor. HER3 and HER4 do not recruit Cbl and thus they are constitutively recycled, whereas Cbl can link the tyrosine 1112 of the HER2 receptor [Yarden, 2001;Rubin and Yarden, 2001], even if this link is very weak and localization studies demonstrated that the receptor is localised mainly on the cell membrane, suggesting that it is resistant to endocytosis or it is internalised but very efficiently recycled [Bertelsen and Stang, 2014].

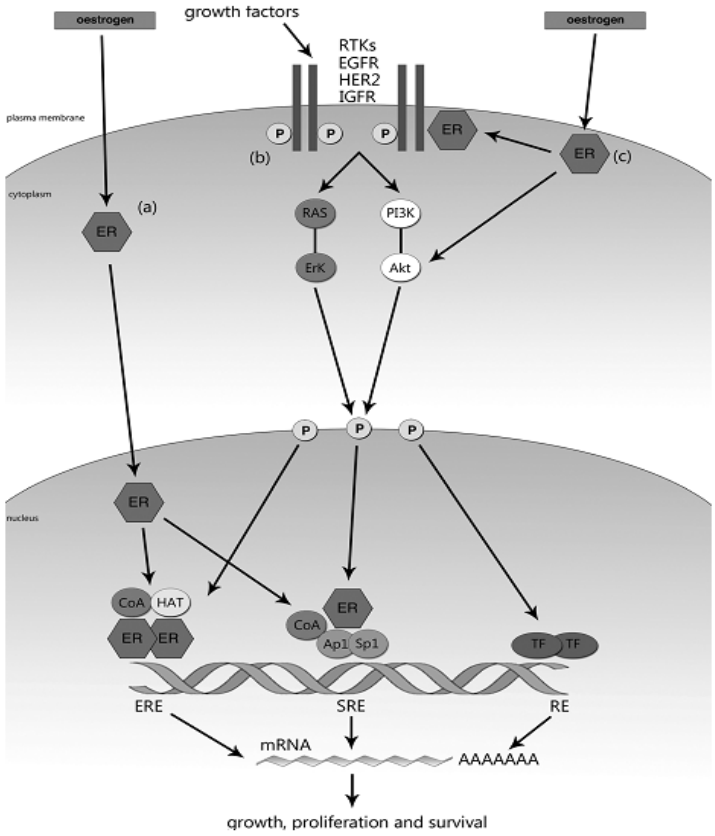

Figure 7. Mechanisms of action of estrogen receptor in breast cancer
ER regulates gene expression trough three ways. In classic estrogen signalling, ligand-bound ER activates gene expression binding to estrogen receptor elements (EREs), serum response elements (SRE) (A). ER can also be activated as a consequence of signalling events downstream of RTKs such as EGFR, HER2 and the insulin-like growth factor receptor (IGFR). Phosphorylation (P) of transcription factors (TFs) and co-regulators, including components of the ER pathway leads to ligand-independent activation of the ER enhancing gene expression on EREs and other response elements (REs) by the Erk or Akt kinases (B). Moreover, signalling can be mediated through non-genomic mechanisms by ER that is localised at the cell membrane or in the cytoplasm (C). CoA: co-activators; HAT: histone acetyl transferases; Ap1: activation protein 1; Sp1: specificity protein 1. [Montemurro et al., 2013]

1.2.2 Treatments of HER2-positive breast cancers

In accordance with the involvement of HER2 in the modulation of a plethora of signals that culminate in tumour proliferation, resistance to apoptosis and invasiveness, tumours with amplification of this oncogene are very aggressive, and develop early relapses [Ménard et al., 2003]. Indeed, before the introduction of trastuzumab in the clinical setting, women with HER2-positive BC were expected to have bad outcomes [Ménard et al., 2003]. Over the past 15 years, significant progress has been made [Engel and Kaklamani, 2007], with the introduction of rationally designed targeted agents in the clinical management of BC patients [De et al., 2013;Krop, 2013]. Patients with HER2-positive BC treated with trastuzumab typically experience better outcomes than people with HER2-negative disease [Dawood et al., 2010].

So far, two strategies have been adopted: on one hand, monoclonal antibodies (MAbs) which bind to extracellular domain of HER2 (such as trastuzumab, pertuzumab, T-DM1); on the other hand, tyrosine kinase inhibitors (TKIs) (such as lapatinib, afatinib) compete with the ATP binding site of the catalytic domain of the receptors. The recombinant humanised MAb trastuzumab (Herceptin, Genentech, South San Francisco, CA, USA) binds to the juxtamembrane region (subdomain IV) of the HER2 receptor. It was introduced in the treatment of HER2 positive BCs in 1998 when it was approved by the food and drug administration for metastatic BC after demonstration in a Phase III trial that its addition to standard chemotherapy extended patients' time to progression from 4.6 to 7.4 months and reduced their relative risk of death by 20% [Slamon et al., 2001]. Nowadays with or without chemotherapy it is the backbone of systemic treatment of metastatic and early HER2-positive BC [Callahan and Hurvitz, 2011].

Neoadjuvant treatment with trastuzumab and chemotherapy has been evaluated in three Phase III trials (Table 2). Concurrent administration of trastuzumab and paclitaxel followed by anthracycline-based chemotherapy ± trastuzumab produced a higher pathologic complete response (pCR) rate than the same chemotherapy alone (65.2% vs 26.3%, p=0.016) [Buzdar et al., 2007]. An improvement in 3-year disease free survival (DFS) of patients with the addition of trastuzumab (100% vs 85.3%, p=0.041) was observed [Buzdar et al., 2007]. The Neoadjuvant Herceptin (NOAH) trial compared treatment with trastuzumab (for 1 year, starting preoperatively) with no trastuzumab, in women with HER2-positive locally advanced or inflammatory BC treated with a neoadjuvant chemotherapy regimen containing doxorubicin, cyclophosphamide, paclitaxel, methotrexate, and fluorouracil. The pCR rate was significantly higher in the trastuzumab arm and also 3-year DFS was significantly improved (HR=0.59, 95%CI=0.38–0.90, p=0.013) [Gianni et al., 2010]. In the phase III German Breast Group/Gynecologic Oncologic Study Group (GeparQuattro) trial, the combination of trastuzumab and anthracycline-based chemotherapy in patients with HER2-positive BC produced a greater pCR rate than chemotherapy alone in a reference group of patients with HER2-negative BC (pCR 31.7% vs 15.7% respectively) [Untch et al., 2010].

Table 2. Neoadjuvant trials comparing the addition of trastuzumab to chemotherapy

Trial	Treatment	pCR, %	p-value	Reference
Buzdar et al	P>FEC PH>FECH	26 65	0.016	[Buzdar et al., 2007]
GeparQuattro	EC>Da ECH>DaH	16* 32	<0.001	[Untch et al., 2010]
NOAH	AP>P>CMF APH>PH>CMFH	22 43	0.002	[Gianni et al., 2010]

A: Adriamycin; C: Cyclophosphamide; D: Docetaxel; Da: Dacarbazin; E: epirubicin; F: fluorouracil; M: metotrexate; H: Trastuzumab; P: paclitaxel; pCR: Pathological complete response; V: Vinorelbine

*Refers to a cohort of HER2-negative BC.

In the adjuvant setting, based on results of four large trials (Table 3), trastuzumab is recommended for use as monotherapy after completion of chemotherapy, and in

combination with taxanes (paclitaxel or docetaxel) after completion of doxorubicin plus cyclophosphamide, or given concurrently with carboplatin and docetaxel [Goldhirsch et al., 2011]. HERA study, analysing the comparison between 2-years vs 1-year trastuzumab, demonstrated that treatment provides a significant DFS benefit (HR=0.76, p<0.0001) compared to observation, but 2-years of adjuvant treatment is not more effective than one [Goldhirsch et al., 2013a]. Regarding treatment duration, another study, the FinHER trial, tested the efficacy of short durations (9 weeks) instead of the standard treatment (1 year). This trial provided evidence that 9 weeks of adjuvant trastuzumab with chemotherapy (docetaxel followed by a combination of fluorouracil, epirubicin and cyclophosphamide) has improved efficacy in terms of DFS compared with chemotherapy alone, but this was not compared with the standard duration of trastuzumab treatment [Joensuu et al., 2009]. Data from the NCCTG N9831 and the NSABP B-31 trials confirmed the efficacy of adjuvant trastuzumab and paclitaxel compared to chemotherapy alone and data from the N9831 trial, evaluating the timing of the introduction of trastuzumab, suggested that trastuzumab can be more effective if started concurrently with the taxane component (trastuzumab and paclitaxel) rather than at the end of adjuvant chemotherapy (trastuzumab after paclitaxel) [Perez et al., 2011]. The BCIRG 006 trial again confirmed the efficacy of trastuzumab and docetaxel *versus* chemotherapy alone and the similar efficacy between patients treated with adryamicin-based treatment (adryamicin, cyclophosphamide followed by docetaxel and trastuzumab) with non anthracycline (docetaxel, carboplatin and trastuzumab) regimen, favouring the last one due to lower risk-benefit ratio [Slamon et al., 2011].

Table 3. Adjuvant trials comparing the addition of trastuzumab to chemotherapy

Trial	Treatment	DFS, HR (95%CI)	p-value	Reference
BCIRG 006	AC>D AC>DH +DCaH	1 0.64 (0.53-0.78)	<0.001	[Slamon et al., 2011]
FinHER	D(V)>FEC D(V)H>FEC	1 0.42 (0.21-0.83)	0.01	[Joensuu et al., 2006]
HERA	CT CT>H	1 0.76 (0.67-0.86)	<0.001	[Goldhirsch et al., 2013a]
NSABP B-31+ NCCTG N9831	AC>P AC>PH	1 0.52 (0.45-0.6)	<0.001	[Perez et al., 2011]

A: Adriamycin; C: Cyclophosphamide; Ca: Carboplatin; CT: chemotherapy; D: Docetaxel; E: epirubicin; F: fluorouracil; H: Trastuzumab; P: paclitaxel; DFS: disease free survival; V: Vinorelbine

1.2.3 Beyond trastuzumab treatment in the clinical setting

While trastuzumab remains the milestone of treatment, other anti-HER2 agents have now been approved: pertuzumab, a recombinant humanised MAb that blocks HER2 dimerization with HER1 and HER3; lapatinib, a reversible TKI of HER2 and EGFR which competes with ATP to enter in the ATP binding pocket [Konecny et al., 2006]; and TDM1, which is trastuzumab linked to the cytotoxic agent emtansine (DM1). While in adjuvant setting trastuzumab is currently used as therapy, these new drugs have now changed the scenario of treatment of metastatic BC. As first-line treatment, most patients with metastatic BCs receive a combination of pertuzumab, trastuzumab and taxanes. TDM1 is typically a second-line choice, but capecitabine and lapatinib, lapatinib and trastuzumab, or other chemotherapeutic agents with trastuzumab offer further options for treatment of metastatic disease. Lapatinib is used in combination with trastuzumab due to several findings demonstrating that lapatinib in combination with chemotherapy was less active than trastuzumab plus chemotherapy both in HER2-positive MBC and in neoadjuvant setting [Eroglu et al., 2014].

Dual-blockade of HER2 has also been introduced in neoadjuvant treatment setting further improving pCR rates (Table 4). The NeoALTTO and the randomised phase II CHER-LOB studies, comparing the activity of paclitaxel plus trastuzumab (arm i) or lapatinib (arm ii) or both (arm iii) followed in the CHER-LOB study by the same biological therapies

with chemotherapy (fluorouracil, epirubicin and cyclophosphamide), revealed a significantly higher pCR rate in the group treated with lapatinib and trastuzumab than in the group treated with trastuzumab alone, independently from the chemotherapy used [Baselga et al., 2012;Guarneri et al., 2012].

In the phase III NSABP B-41 study, the pCR rate in the dual-blockade arm with lapatinib and trastuzumab in addition to paclitaxel was higher than in the trastuzumab arm but with only a trend toward statistically significance [Robidoux et al., 2013]. The pCR rates did not differ significantly between the lapatinib alone arm and the trastuzumab alone arm in these three studies. In the NeoSphere phase II study, it has been demonstrated that also the double blockade with trastuzumab and pertuzumab with docetaxel increases the pCR rates compared to trastuzumab and docetaxel. Notably, the pCR rate in patients treated with a combination of antibodies (pertuzumab and trastuzumab) without chemotherapy was 16.8% [Gianni et al., 2012]. Positive results of the combination of trastuzumab and pertuzumab in NeoSphere trial are supported by TRYPHAENA phase II study that revealed pCR rates of 57-66% with different chemotherapeutic regimen in addition to trastuzumab and pertuzumab (arm i: fluorouracil, epirubicin and cyclophosphamide followed by docetaxel, trastuzumab and pertuzumab; arm ii: fluorouracil, epirubicin, cyclophosphamide, trastuzumab and pertuzumab followed by docetaxel, trastuzumab and pertuzumab; arm iii: cyclophosphamide, docetaxel, trastuzumab and pertuzumab) [Schneeweiss et al., 2013].

Double-blockade in the adjuvant setting with trastuzumab and lapatinib in combination with taxanes was tested in 8381 women in the phase III ALTTO trial, but the 16% improvement in DFS (HR=0.84, 95%CI=0.70-1.12, p=0.0480) observed with the concomitant dual blockade compared to trastuzumab alone was not statistically significant ($p \leq 0.025$ was required for statistical significance in the test for superiority of

L+H vs. H arms) [Piccart-Gebhart et al., 2014]. Results from the phase III Aphinity trial promise to shed further light on the role of pertuzumab and trastuzumab in the adjuvant setting.

Table 4. Neoadjuvant studies of HER2 double blockade

Trial	Treatment	pCR, %	p-value*	Reference
CHER-LOB	PH>FECH PL>FECL PHL>FECHL	25 26 47	p=0.019†	[Guarneri et al., 2012]
NEOALTTO	PH PL PHL	29 25 51	p=0.0001	[Baselga et al., 2012]
NeoSphere	DH DPz HPz DHPz	29 24 17 46	p=0.0141	[Gianni et al., 2012]
NSABP B-41	AC>PH AC>PL AC>PHL	52 53 62	p=0.095	[Robidoux et al., 2013]
TRYPHAENA	FEC>DHPz FECHPz>DHPz CDHPz	57 62 66	n.s	[Schneeweiss et al., 2013]

*p-value is related to the comparison between double blockade arm vs trastuzumab containing arm. †p-value obtained comparing arm C vs A+B (double blockade vs trastuzumab or lapatinib).
A: Adriamycin; C: Cyclophosphamide; D: Docetaxel; E: epirubicin; F: fluorouracil; H: Trastuzumab; L: lapatinib; P: paclitaxel; pCR: pathological complete reasponse; Pz: pertuzumab.

1.2.4 Mechanisms of trastuzumab action

Numerous studies have been performed in preclinical models in the effort to define how trastuzumab exerts its activity as anti-tumour agent in tumours overexpressing HER2 (reviewed in [Spector and Blackwell, 2009]). These preclinical studies have indicated at least two major mechanisms of trastuzumab action (Fig. 8): i) cytostatic activity through the blockade of HER2 proliferation pathways, extracellular domain (ECD) shedding and consequent formation of the activating HER2 truncated form and tumour angiogenesis; and ii) cytotoxic activity by antibody dependent cell-mediated cytotoxicity (ADCC) and inhibition of HER2-mediated DNA repair of damage induced by radiotherapy or chemotherapy [Tagliabue et al., 2011].

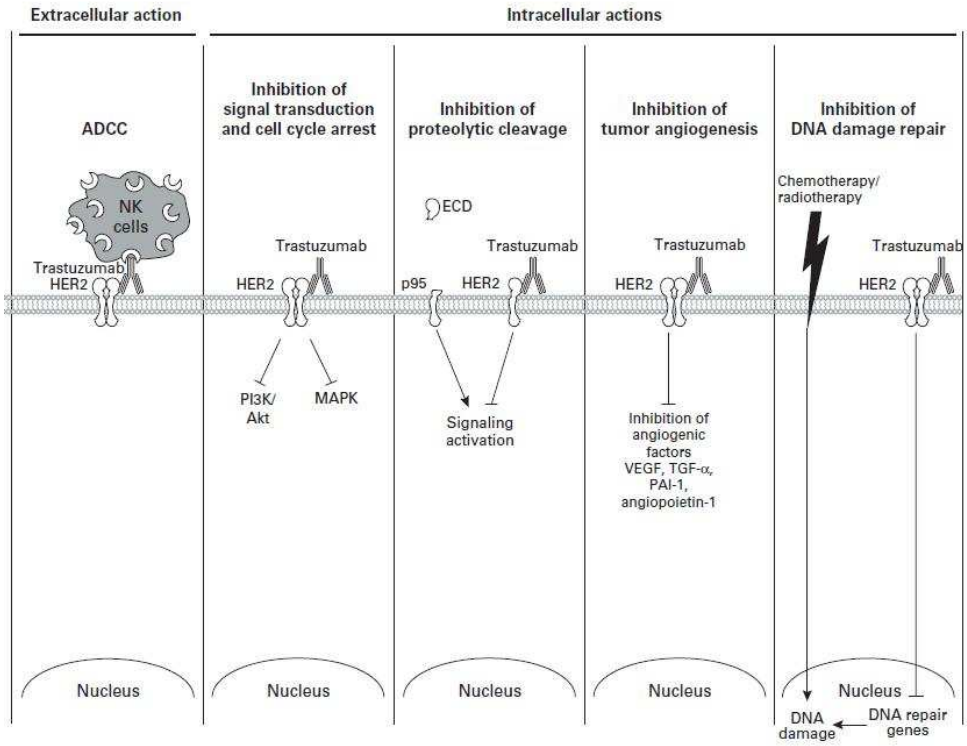

Figure 8. Mechanisms of action of trastuzumab
Possible extracellular and intracellular mechanisms of action of trastuzumab are shown. ADCC: antibody-dependent cellular cytotoxicity; Akt: RAC-α serine/threonine-protein kinase or protein kinase B; ECD: extracellular domain; MAPK: mitogen-activated protein kinase; NK: natural-killer cell; PAI-1: plasminogen activator inhibitor-1; PI3K: phosphatidylinositol triphosphate kinase; TGF-α: transforming growth factor α; VEGF: vascular endothelial growth factor. [Spector and Blackwell, 2009]

In details, i*n vitro* analyses showed that trastuzumab inhibits colony formation, downregulates expression of HER2 and cyclin D1, and increases p27 protein levels in the HER2-amplified BT474 and SKBR3 human BC cells; these effects were temporally associated with the inhibition of PI3K and AKT function [Yakes et al., 2002]. Inhibition of HER2 signal was also accompanied by induction of the Rb-related protein p130, with consequent reduction in the number of cells in S-phase [Sliwkowski et al., 1999]. Trastuzumab was also found to inhibit the cleavage of the HER2 ECD by proteolytic enzymes, thereby inhibiting the generation of phosphorylated HER2 truncated p95 receptor implicated in tumour growth and progression [Molina et al., 2001]. Antiangiogenesis activity of trastuzumab was demonstrated in mice with severe combined immunodeficiency disease and transplanted with human HER2-positive BC

cells. Trastuzumab-mediated reduction of tumour growth was accompanied by a reduction in vessel volume, consistent with the involvement of HER2 signal in controlling the expression of pro- and anti-angiogenic factors [Izumi et al., 2002;Pegram and Reese, 2002].

Incubation of BC cell lines with trastuzumab delayed the repair of DNA inter-strand crosslinks produced by cisplatin [Lee et al., 1991;Boone et al., 2009]. Therapy with cisplatin and trastuzumab antibody in mice xenotransplanted with human breast or ovarian HER2-positive cancer cells induced complete tumour remissions if antibody and drug were given in close temporal proximity; treatment with cisplatin increased unscheduled DNA synthesis that was reduced by combined therapy with trastuzumab [Pietras et al., 1998].

In FcRγ +/+ nude mice injected subcutaneously with HER2-overexpressing human BC cells, trastuzumab inhibited tumour growth, while its effect was reduced by more than 50% in FcRγ -/- mice or after disrupting the antibody engagement of FcRγ, supporting the role of ADCC in drug activity [Clynes et al., 2000]. Other than ADCC, the antibody dependent cell mediated phagocytosis (ADCP), in which activated macrophages phagocytose and kill trastuzumab-coated cancer cells, is today recognised as another FcRγ mediated possibility that the immune system uses to kill tumour cells in the presence of trastuzumab [Shi et al., 2015] (Fig. 9).

Recently, *in vivo* studies aimed at clarifying the role of the immune system in trastuzumab activity not only confirmed the relevance of innate immune cells in trastuzumab activity, but also revealed the critical role of adaptive immune cells [Stagg et al., 2011; Park et al., 2010; Mortenson et al., 2013]. In particular, in these studies a role for CD8+ T cells, CD4+ T cells and NK cells in trastuzumab activity has been demonstrated using MAbs depleting these immune subpopulations. Moreover, Stagg and coworkers

[Stagg et al., 2011] demonstrated that neutralization of interferon (IFN) of type I and II, High Mobility Group Box 1 and of myeloid differentiation primary response gene 88, that encode a signal transducer acting downstream of many Toll-like receptors, abrogates the therapeutic activity of trastuzumab. These data supported also a role of macrophages, as mediators of ADCP, and an induction of immunogenic cell death (ICD) by trastuzumab [Kroemer et al., 2015] (Fig. 9).

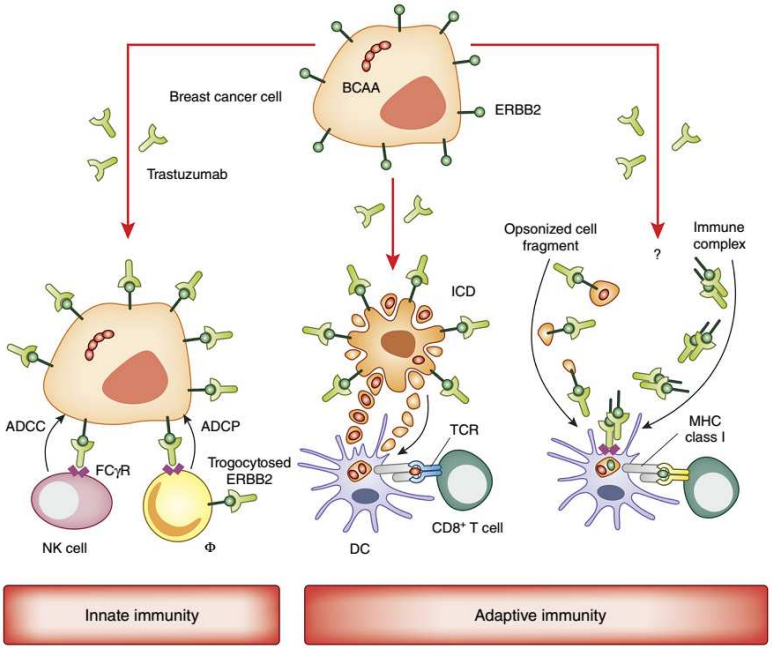

Figure 9. Key mechanisms of the immune system involvement in response to trastuzumab

Trastuzumab mediates multipronged immunostimulatory effects involving both innate and adaptive immunity. Cancer cells opsonised by trastuzumab can be recognised by natural killer (NK) cells or monocytes/macrophages (Φ) via FcRγs, resulting in the activation of ADCC or ADCP. Trastuzumab may also promote ICD, resulting in the uptake of BC–associated antigens (BCAAs) by dendritic cells (DCs), their presentation on MHC-I molecules and hence the elicitation of a CD8+ T cell–dependent immune response. CD8+ T cells can also recognize BCAA-derived peptides presented on MHC-I molecules by cancer cells themselves. Finally, it cannot be excluded that DCs engulfing trastuzumab–ERBB2 immune complexes (or cancer cell fragments opsonised by trastuzumab) may prime ERBB2-targeting CD8+ T cells and/or CD4+ T cells (not shown). ADCC: Antibody-derived cell mediated cytotoxicity; ADCP: Antibody-derived cell mediated phagocytosis; ICD: immunogenic cell death; MHC-I: major histocompatibility complex class I; TCR: T cell receptor. Question mark indicates that the pathway cannot be excluded (but remains to be formally demonstrated). [Kroemer et al., 2015]

It is reasonable, as proposed by Bianchini et al [Bianchini and Gianni, 2014], that the debris of dying cells due to the activity of innate immune cells in the presence of

trastuzumab, are uptaken by antigen presenting cells (APC), like dendritic cells or macrophages that processed and presented tumour antigens through the major histocompatibility complex (MHC) molecules. Antigens presented by MHC class II molecules on APCs mainly activate CD4 cells, whereas ingested apoptotic and necrotic cellular material can also be processed and presented on MHC class I molecules, thus contributing significantly to initiation of the cytotoxic T-cell response. Cytotoxic T-cells, that ultimately recognise and lyse antigen-expressing tumours, are also triggered by CD4 Th1 cells, generated in the presence of IFN-γ (Fig. 10).

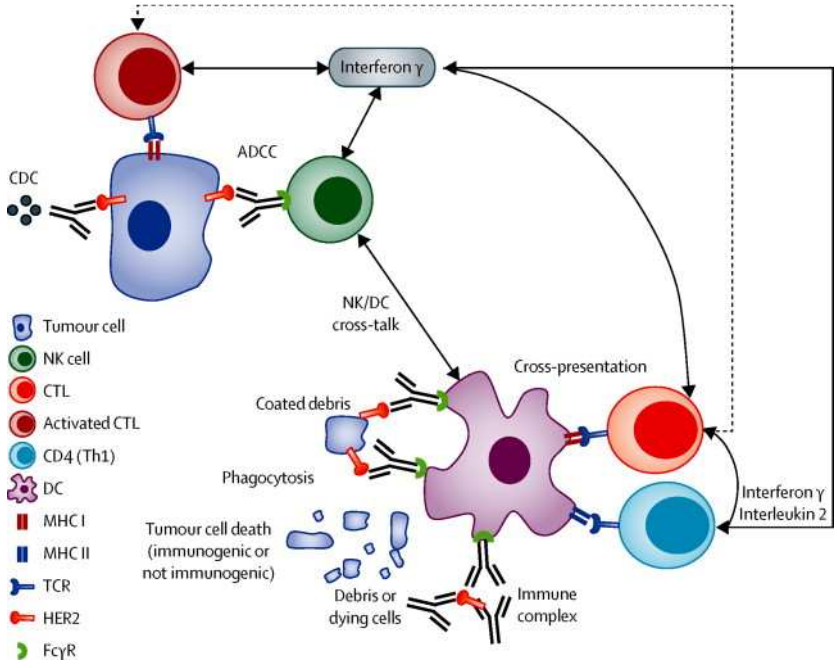

Figure 10. Participation of innate and adaptive immune cells in trastuzumab activity
Involvement of the innate and adaptive system in trastuzumab mechanisms of action. ADCC: antibody-dependent cell-mediated cytotoxicity; CDC: complement-dependent cytotoxicity; CTL: cytotoxic T lymphocyte; DC: dendritic cell; FcγR:Fcγ receptor; NK: natural killer; TCR:T-cell receptor; Th1:T helper 1 cell. [Bianchini and Gianni, 2014]

Few studies have been conducted on tumour samples of patients to verify the mechanism(s) of trastuzumab action found in preclinical models. An IHC study of women treated with preoperative trastuzumab and paclitaxel for 12 weeks showed a loss of HER2 expression in a subset of patients, suggesting downregulation of HER2 expression with consequent blockage of oncoprotein-supported tumour growth as reported in preclinical

studies [Burstein et al., 2003]. However, the observed HER2 downregulation could be just the mirror of trastuzumab cytotoxic activity on HER2-positive cells with a consequent enrichment of HER2 negative cells. Analysis of pre- and post-operative breast tissue samples obtained from 23 patients who underwent neoadjuvant trastuzumab plus docetaxel treatment showed significantly increased NK cell infiltration of tumours and increased lymphocyte activity as compared with samples obtained from patients treated with chemotherapy alone [Arnould et al., 2006]. Consistent with these results, patients with primary BC treated preoperatively with 4 weekly doses of trastuzumab in monotherapy achieved complete or partial remission if they presented high *in situ* tumour infiltration by leukocytes and peripheral blood mononuclear cells (PBMCs) able to mediate *in vitro* ADCC [Gennari et al., 2004; Varchetta et al., 2007].

1.2.5 Markers of trastuzumab activity

Several studies carried out mainly in experimental models have identified single molecules whose expression or loss of expression leads to trastuzumab resistance (Table 5). The most obvious candidate biomarker predictive of trastuzumab efficacy is HER2 itself. Indeed, the capacity of trastuzumab to engage the HER2 receptor represents the first step in antibody activity. Altered forms of HER2 derived from alternative initiation of HER2 gene translation from methionines 611 and 687 [Anido et al., 2006], as well as p95HER2 derived by proteolytic shedding of the HER2 ECD [Arribas and Borroto, 2002] are differentially present on the surface of HER2-overexpressing tumour cells. Thus, tumours harbouring high levels of these forms, which retain HER2 kinase activity but not the trastuzumab-specific epitope, exhibited a lower response rate to trastuzumab than cancers expressing full-length HER2 *in vitro*, in xenografted models and in the metastatic setting [Scaltriti et al., 2007]. However, two pre-operative studies did not validate the association between p95HER2 expression and resistance to trastuzumab: analysis of 153

patients of the GeparQuattro study found that p95HER2 expression was associated with response to neoadjuvant trastuzumab rather than resistance [Loibl et al., 2015a]; in the CHER-LOB trial the pCR rates did not differ between p95HER2-positive and -negative tumours in any treatment group [Guarneri et al., 2015].

The splice variant lacking exon 16 (d16HER2), identified in almost all human HER2-positive primary BCs [Castiglioni et al., 2006] and characterised by an imbalance in the number of cysteines in the ECD portion and by the constitutive generation of stable HER2 homodimers [Siegel et al., 1999], decreases trastuzumab binding *in vitro* [Castiglioni et al., 2006] and promotes resistance to trastuzumab in multiple cell lines [Mitra et al., 2009]. Recent data using xenografted [Alajati et al., 2013] or spontaneous [Castagnoli et al., 2014] BC mouse models demonstrated that tumours expressing this isoform are instead responsive to trastuzumab treatment. Accordingly, patients with the highest expression of this isoform in the activated form benefit from trastuzumab treatment in the adjuvant setting [Castagnoli et al., 2014].

Table 5. Markers of trastuzumab response

			Clinical settings		
Marker	***In vitro***	***Mice***	**Neoadjuvant**	**Adjuvant**	**Metastatic**
p95HER2	Resistance	Resistance	No-predictive* Response*	--	Resistance
d16HER2	Resistance	Response	--	Response	--
ER	Resistance	--	Resistance*	Resistance*	Resistance
EGFR	Resistance	Resistance	--	Resistance	No-predictive
MET	Resistance	--	--	--	Resistance
IGFR	Resistance	--	Resistance*	Resistance	No-predictive
HER3	Resistance	--	--	--	Resistance
EphA2	Resistance	Resistance	--	--	--
PI3K/PTEN	Resistance	--	Resistance*	No-predictive*	Resistance
MUC4	Resistance	Resistance	--	Resistance	--

*Data derived from analyses in clinical trials

An escape mechanism from trastuzumab action is the loss of dependence on HER2 for tumour growth. Studies carried out in *in vitro* models expressing both the ER, which can induce resistance to HER2 inhibitory reagents, and HER2 demonstrated an intricate

crosstalk between the two pathways. Consistent with those findings, all clinical trials thus far showed a higher rate of pCR in HER2-positive/ER-negative than in ER-positive tumours (reviewed in [von et al., 2012], Table 6), and in the NOAH trial, negative PR, a downstream transcriptional target of ER, was associated with higher pCR rates after addition of trastuzumab compared to chemotherapy alone [Gianni et al., 2015]. Moreover, a recent meta-analysis [Cortazar et al., 2014] showed that the association between pCR and long-term outcomes was greatest in patients with HER2-positive/ER-negative disease receiving trastuzumab.

Other transmembrane receptors, such as EGFR, c-Met, insulin-like growth factor receptor (IGF1R), and HER3, were found to contribute to trastuzumab resistance through activation of their downstream intracellular signaling cascades. Human BT474 HER2-positive BC cells selected for resistance to trastuzumab exhibited higher levels of phosphorylated EGFR and EGFR/HER2 heterodimers than sensitive cells. Phosphorylation of HER2 in resistant cells was inhibited by the EGFR TKIs erlotinib and gefitinib [Ritter et al., 2007]. EGFR association with trastuzumab resistance was observed in HER2-positive tumours treated with adjuvant-trastuzumab but not in the metastatic setting [Lee et al., 2015]. Hepatocyte growth factor-induced activation of c-Met was shown to impair trastuzumab anti-tumour activity by abrogating p27 induction. Remarkably, HER2-overexpressing BC cells can upregulate Met expression after trastuzumab treatment, promoting their own resistance [Shattuck et al., 2008]. Accordingly, patients with *MET*-FISH-positive human metastatic BC had a significantly higher trastuzumab failure rate and a significantly shorter time to progression than FISH-negative cases [Minuti et al., 2012]. In BC cell models that overexpress HER2, an increased level of IGF1R signaling appeared to interfere with the action of trastuzumab [Lu et al., 2004]. An IGF1R/HER2/HER3 heterotrimeric complex was demonstrated exclusively in trastuzumab-resistant SKBR3

and BT474 cells, and knockdown of HER3 or IGF1R resensitised resistant cells to trastuzumab [Huang et al., 2010], consistent with the ability of lapatinib to impair IGF1R-mediated signaling in trastuzumab-resistant cells and induce apoptosis even in the presence of IGF1 [Nahta et al., 2007]. HER2-positive, operable stage II/III BCs expressing IGF1R were found more likely to be resistant to preoperative trastuzumab plus chemotherapy (vinorelbine) [Harris et al., 2007]. In the NOAH trial, overexpression of membranous IGF1R in 171 patients was associated with higher likelihood of residual disease after trastuzumab plus chemotherapy [Gianni et al., 2015]. Also in adjuvant setting patients receiving trastuzumab with IGF1R overexpressing tumours presented shorter DFS [Gallardo et al., 2012].

Other RTKs have been described to mediate resistance to trastuzumab activity. Trastuzumab-resistant cell lines overexpress Eph receptor A2, and inhibition of this receptor restores sensitivity to trastuzumab treatment *in vivo* [Zhuang et al., 2010]. Somatic alterations in the PI3K/AKT pathways downstream of HER2, found in ~30% of HER2-positive tumours, also resulted in resistance to trastuzumab in cell culture based on constitutive activation of downstream signaling [Cescon and Bedard, 2015]. A study of a small retrospective series also reported that patients with a phosphatidylinositol 3-kinase catalytic subunit alpha (PIK3CA) mutation or low expression of PTEN have poor response to trastuzumab and shorter DFS [Cescon and Bedard, 2015]. By contrast, results from large clinical trials using trastuzumab in adjuvant settings showed no difference in trastuzumab benefit as a function of PIK3CA mutations (FinHER, NSABP B-31) or PTEN expression (NCCTG N9831)[Engelman, 2009] (Table 6).

Table 6. Predictive biomarker analyses in trials of HER2-targeted therapies. Adopted from [Triulzi et al., 2016]

		Estrogen receptor (ER)		PIK3CA/PTEN	
Trial	**End point**	ER+	ER-	PIK3CA Mut PTEN Low	PIK3CA WT PTEN High
NOAH CT CT+H	pCR	29 30	22 51		
		p=0.095$^{\Delta}$			
Neosphere DH DPz HPz DHPz	pCR	20 17 6 26	37 30 27 63	23 17 9 38	29* 24* 17* 46*
CherLOB CT+H CT+L CT+HL	pCR	24 21 36	27^{a} 38^{b} 59^{c}	33 25 12	21^{a} 27^{b} 48^{c}
		^{a}p=0.84, ^{b}p=0.25, ^{c}p=0.13		^{a}p=0.44, ^{b}p=0.51, ^{c}p=0.06	
NeoALTTO PH PL PHL	pCR	1	2.44(1.45-4.03)$^{\mp}$	20 15 29	28^{a} 20^{b} 53^{c}
		p<0.001		^{a}p=0.44, ^{b}p=0.51, ^{c}p=0.01	
Tryphaena FECHPz>DHPz FEC>DHPz DCHPz	pCR	46 48 50	79 65 84	48.7$^{\mp}$	64.3$^{\mp}$
				p=0.17	
Gepar Sixto CT+LH	pCR	0.40(0.21-075)	1	0.35(0.16-0.81)	1
		p=0.004		p=0.013	
CALGB 40601 CT+H CT+L CT+HL	pCR	41 29 41	54 37 79	39$^{\mp}$	47$^{\mp}$
		p=0.09$^{\Delta}$		p=0.5	
FinHER D(V)>FEC D(V)H>FEC	DFS			1 0.19(0.04-1.04)	1 0.98(0.47-2.8)
				p=0.14$^{\Delta}$	
NSABP B-31 AC>P AC>PH	DFS	1 0.44(0.32-0.61)$^{\approx}$	1 0.51(0.39-0.67)$^{\approx}$	1 0.44(0.24-0.82)	1 0.51(0.37-0.71)
				p=0.64$^{\Delta}$	
NCCTG-N9831 AC>P AC> P>H AC>PH	DFS	1 0.44(0.32-0.61)$^{\approx}$	1 0.51(0.39-0.67)$^{\approx}$	1 0.85(0.55-1.30) 0.47(0.28-0.79)	1 0.71(0.54-0.92)^{a} 0.65(0.49-0.87)^{b}
				^{a}p=0.47$^{\Delta}$, ^{b}p=0.16$^{\Delta}$	
HERA O H	DFS	1 0.63(0.50-0.78)	1 0.63(0.43-0.93)		

For studies in which DFS is the end point hazard ratio are reported, whereas for studies in which pCR is the end point percentages or odd ratios to predict pCR are reported. *Shown are results for all patients not for PIK3CA WT subgroup; $^{\mp}$ Reported data refers to all arms together; $^{\approx}$ Results

derived from NSABP B-31 and NCCTG-N9831 trials merged; [Δ] Interaction p-value. A: Adriamycin; C: Cyclophosphamide; CT: Chemotherapy; D: Docetaxel; DFS: Disease-free survival; ER: Estrogen receptor; FEC: fluorouracil/epirubicin/cyclophosphasmide; H: Trastuzumab; L: Lapatinib; O: Observation only; P: paclitaxel; pCR: Pathological complete response; Pz: Pertuzumab; V: Vinorelbine.

In a large-scale RNA interference screen to identify genes involved in trastuzumab resistance in BC, only PTEN gene knockdown conferred trastuzumab resistance [Berns et al., 2007]. However, an association between loss of PTEN expression and trastuzumab resistance appeared less clear in the clinical setting, with lower antibody response in tumours with PTEN loss in metastatic [Nagata et al., 2004], but not early stage, BC patients [Perez et al., 2013]. In a recent study carried out in two large adjuvant BC trials (BCIRG-005 and BCIRG-006), the absence of PTEN IHC staining in tumour cells was associated with poor clinical outcome in HER2-positive disease, although trastuzumab appeared to provide clinical benefit for patients lacking PTEN staining, suggesting that PTEN loss is associated with worse outcome rather than resistance to antibody treatment [Stern et al., 2015]. Application of this marker to trials of double blockade (GeparSixto) showed that PIK3CA mutation was significantly associated with a lower pCR rate (p=0.013), although disease-free and overall survival did not differ significantly between patients with mutant and wild-type PIK3CA [Loibl et al., 2014]. These findings were confirmed in tumours of patients in the NeoALTTO trial [Majewski et al., 2015] (Table 6), and in a meta-analysis where the pCR rate was significantly lower in HER2-positive PIK3CA mutant tumours after anti-HER2 treatment; patients with a HER2+/ER+/PIK3CA mutant tumour had a pCR rate of 5.5% only when treated with double-blockade and might be considered for alternative treatment [Loibl et al., 2015b].

Alterations in cell cycle, such as down-regulation of p27 [Nahta et al., 2004;Yakes et al., 2002] and amplification of cyclin E2 [Scaltriti et al., 2011] have also been found associated with trastuzumab resistance *in vitro*. Some cell surface proteins, such as CD44, a

transmembrane receptor that binds to ECM-associated hyaluronan and enhances HER2 signaling [Ghatak et al., 2005], and the membrane-associated MUC-4 glycoprotein, may interact with HER2 and block access of trastuzumab to the HER2 ECD [Nagy et al., 2005; Mercogliano et al, 2017].

While the overall experimental results above suggest mechanisms of resistance related to molecular features of HER2-overexpressing tumour cells, analyses of tumour samples from the major clinical studies have failed to definitively demonstrate the predictive value of most of these biomarkers (Table 5), with the exception of ER, which has been negatively associated to trastuzumab benefit in all clinical trials.

1.2.6 The 'new generation' predictive biomarkers of trastuzumab activity

New high-throughput genomic technologies have increased the rate of discovery of potential markers with prognostic or predictive ability, even in the HER2-positive cohort (Table 7). These technologies have enabled the detection of the molecular intrinsic heterogeneity using the PAM50 classification among clinically HER2-positive BCs. Indeed, all of the intrinsic subtypes were identified within HER2-amplified BCs, with 50% classified as HER2-enriched (HER2-E) [Prat et al., 2014b]. Analysis of PAM50 in the TCGA BC cohort showed that HER2-E tumours have the highest activation of the HER2/EGFR signaling pathway [Cancer Genome Atlas Network, 2012], suggesting that they may benefit the most from trastuzumab treatment. In patients of the NOAH trial, Prat and co-workers [Prat et al., 2014a] demonstrated that those with HER2-E tumours benefit substantially from trastuzumab-based treatment, achieving a higher rate of pCR than with other tumours (Table 7). Application of this predictor to another neoadjuvant setting trial CALGB found that 70% of patients with HER2-E tumours had pCR with neoadjuvant chemotherapy plus HER2-targeted therapies, whereas the pCR rate was 34-36% in the other subtypes, similar to the pCR rate in the chemotherapy arm [Carey et al., 2013]. The

predictive ability of this classifier was validated also in NeoALLTO trial [Fumagalli et al., 2016]. However, application of this predictor to the phase III NSABP B-31 trial failed to identify subgroups that benefit differentially from trastuzumab treatment [Pogue-Geile et al., 2015], suggesting the need for further evaluation of this predictor in the adjuvant setting. In this dataset, PAM50 classification was not found to be prognostic too [Prat et al., 2015]. In NCCTG-N9831 trial patients with HER2-E tumors were the only who benefit from the addition of trastuzumab to chemotherapy [Perez et al., 2016]. Pogue-Geile and coworkers [Pogue-Geile et al., 2013] developed an 8-gene predictive algorithm that identified subgroups of patients in the NSABP B-31 trial with different benefit from trastuzumab-based chemotherapy (Table 7). In particular, tumours of patients with a large benefit from the addition of trastuzumab to chemotherapy expressed high levels of HER2-related genes (*ERBB2*, *c17orf37*, *GRB7*) and low levels of ER-related genes (*ESR1*, *NAT1*, *GATA3*, *CA12*, *IGF1R*), whereas tumours of patients who did not benefit from trastuzumab expressed high levels of ER-related genes and intermediate levels of HER2-related genes. The group that benefitted moderately from trastuzumab expressed low HER2 and intermediate ER-related gene levels.

The relevant role of the immune system in trastuzumab activity [Bianchini and Gianni, 2014] has prompted some groups to explore the possibility of using immune information as biomarkers to identify patients likely to benefit from trastuzumab. Recently, Perez and coworkers [Perez et al., 2015] developed a genomic signature that predicts benefit from trastuzumab using samples of the NCCTG N9831 trial. The predictive signature consists of 14 genes related to immune function and classifies tumours as immune response-enriched (IRE) and non-immune response-enriched (NIRE). IRE tumours had an increased DFS when treated with trastuzumab, whereas the DFS of NIRE tumours was independent of trastuzumab treatment (Table 7). IRE tumours are enriched in genes related to T and B

cell responses, chemokine signaling and inflammation. This signature predictive power was validated in the NeoALTTO trial [Fumagalli et al., 2016], but failed to predict trastuzumab benefit in the NSABP B-31 trial [Gavin et al., 2015], profiled on the Affymetrix platform versus DNA-based annealing, selection, extension and ligation (DASL) used to develop the signature. The expression of immune genes/metagenes has been also correlated to pCR in the Neosphere trial: in the docetaxel and trastuzumab arm (DH) combined with docetaxel plus pertuzumab (DPz) and pertuzumab plus trastuzumab arms (HPz), multivariate analysis linked higher expression of PD-1, MHC-II and STAT1 metagenes with pCR, while higher PD-L1, MHC-I or IFN-I metagenes were linked to lower pCR [Bianchini et al., 2015] (Table 7). In the NOAH trial, a similar association of higher STAT1 with higher pCR and of higher MHC-I and IFN-I with lower pCR was found for trastuzumab/chemotherapy but not for chemotherapy only [Bianchini et al., 2015]. Accordingly, Loi and coworkers [Loi et al., 2014b] recently demonstrated an association between stromal tumour-infiltrating lymphocytes (sTIL), as evaluated by histopathology, and benefit from trastruzumab treatment in terms of DFS in the FinHER trial [Loi et al., 2014b] (Table 7). Each 10% increase in lymphocytic infiltration was associated with increased DFS in patients treated with trastuzumab (interaction p= 0.025). These data were validated in the NeoALTTO trial, in which the presence of sTIL at diagnosis was an independent, positive prognostic marker for both pCR and DFS endpoints [Salgado et al., 2015a]. In the NCCTG N9831 trial, sTIL pathological evaluation was not predictive of trastuzumab benefit, but instead associated with chemotherapy benefit [Perez et al., 2016]. In the Neosphere trial patients with low sTIL levels (<5%) in the three combined arms (DH, DPz and HPz) had the lowest rate of pCR (4.3%) compared to patients with intermediate or high sTIL levels (p=0.018) [Bianchini et al., 2015].

Table 7. New generation predictive biomarker analyses in trials of HER2-targeted therapies. Modified from [Triulzi et al., 2016]

		PAM50/8genes		**Immune genes and cells**	
Trial	**End point**	HER2-E ESR1^{high}/ERBB2^{int}	Non-HER2-E ESR1^{low}/ERBB2^{high}	IRE STAT1 high **TIL high**	NIRE STAT1 low **TIL low**
NOAH CT CT+H	pCR	28 53	18 34	1.29(0.49-3.42) 6.44(1.9-21.81)	1[a] 1[b]
		p=0.053$^{\Delta}$		[a]p=0.6059, [b]p=0.0028	
Neosphere DH DPz TPz DHPz	pCR			3.06(1.60-5.84)$^{\mp}$ 0.45(0.25-0.79)	1[a] 1[b]
				[a]p=0.0007, [b]p=0.0057	
NeoALTTO PH PL PHL	pCR	4(2.3-6.9)$^{\mp}$	1	1.4(1.1-1.8)$^{\mp}$ **2.6(1.26-5.39)$^{\mp\perp}$**	1 **1**
		p<0.001		p=0.02**, p=0.01**	
CALGB 40601 CT+H CT+L CT+HL	pCR	70$^{\mp}$	35$^{\mp}$		
		p<0.001			
FinHER D(V)>FEC D(V)H>FEC	DFS			**1.22(1.00-1.47)** **0.82(0.58-1.16)**	**1** **1**
				p=0.02$^{\Delta}$	
NSABP B-31 AC>P AC>PH	DFS	1 1.58 (0.67-3.69) 0.44(0.34-0.58)	1 0.28 (0.20-0.41) 0.47 (0.35-0.61)	1 0.57	1 0.48
		p<0.001$^{\Delta}$, p=0.67$^{\Delta}$		p=0.47$^{\Delta}$	
NCCTG-N9831 AC>P AC> P>H and AC>PH	DFS	1 0.68 (0.52-0.89)	1* 1.06 (0.53-2.13)	1 0.35(0.22-0.35)	1 0.89(0.62-1.28)
		p=0.0005	p=0.87	p<0.001$^{\Delta}$	

For studies in which recurrence-free survival is the end point hazard ratio are reported, whereas for studies in which pCR is the end point percentages or odd ratios to predict pCR are reported.
$^{\mp}$ Reported data refers to all arms together. In the Neosphere trial it refers to D+T, D+Pz and T+Pz together; $^{\perp}$ Positivity cut-off was set at sTIL >5%; $^{\Delta}$ Interaction p-value. *Shown are results for basal-like tumors. A: Adriamycin; C: Cyclophosphamide, CT: Chemotherapy; D: Docetaxel; FEC: Fluorouracil/epirubicin/cyclophosphasmide; H: Trastuzumab; HER2-E: HER2-enriched; IRE: Immune response-enriched; L: Lapatinib; NIRE: Non-immune response-enriched; P: Paclitaxel; Pz: Pertuzumab; TIL: tumour-infiltrating lymphocyte; V: Vinorelbin.

1.3 The immune system

1.3.1 The immune contexture of breast carcinomas

A tumour grows in a complex microenvironment composed of stromal cells, lymphoid and myeloid cells, vascular and lymphatic vessels [Egeblad et al., 2010] (Fig. 11). It is created by and at all times shaped and dominated by the tumour, which orchestrates molecular and cellular events taking place in surrounding tissues. Infiltrates of inflammatory cells can differ in size and composition from tumour to tumour, and their presence has been taken as evidence that the host is not unaware of the developing tumour, but rather attempts to interfere with tumour progression, a process referred to immune surveillance [Varfolomeev et al., 2008].

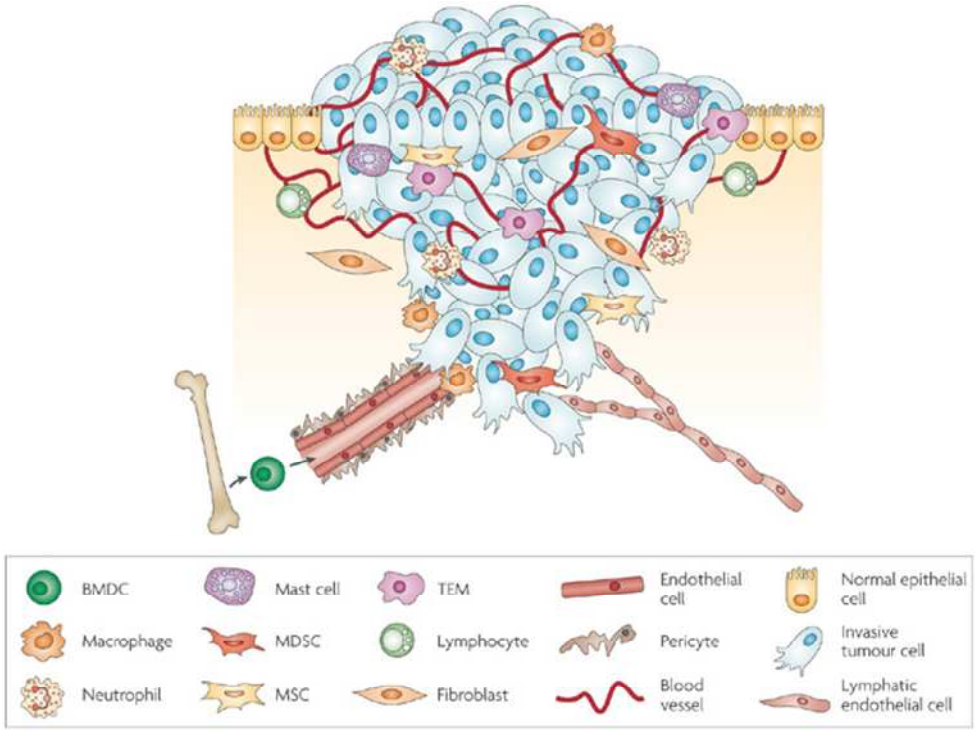

Figure 11. The primary tumour microenvironment
Cancer cells in primary tumours are surrounded by a complex microenvironment comprising endothelial cells of the blood and lymphatic circulation, stromal fibroblasts and a variety of bone marrow-derived cells (BMDCs) including macrophages, myeloid-derived suppressor cells (MDSCs), TIE2-expressing monocytes (TEMs) and mesenchymal stem cells (MSCs). [Joyce and Pollard, 2009]

A median of 11% (range, 5%-26%) of BC are highly infiltrated by immune cells and are classified as lymphocyte-predominant BC (LPBC), and approximately 16% of cancers have no evidence of TILs [Stanton et al., 2016]. TNBC and HER2-positive BC demonstrated the highest, while ER-positive tumours showed the lowest incidence of LPBC. Accordingly, luminal BCs were found less infiltrated by immune cells than non-luminal BCs [Miyan et al., 2016]. The same distribution in tumours belonging to different intrinsic subtypes was demonstrated for specific immune populations like CD8+ T and regulatory T (Treg) cells. Tumours contains all immune cell types, including effectors of innate immunity like macrophages, mast cells, NK cells, and those mediating adaptive immunity like dendritic cells, B cells and effector T cells [including various subsets of T cell: T helper cells, T helper 1 (Th1) cells, Th2 cells, Th17 cells, Treg cells, T follicular helper (Tfh) cells and cytotoxic T cells] (Fig. 12) [Whiteside, 2008]. NK cells, which mediate innate immunity and are rich in perforin- or granzyme-containing granules, are visibly absent from most tumour infiltrates, while CD3+CD4+ and CD3+CD8+ T cells, are usually a major component of the tumour microenvironment (TME) [Whiteside, 2008]. Another copious member of the TME is represented by B cells and macrophages that are known as tumour-associated macrophages or TAMs. It is known that CD4+ Th1 cells, CD8+ cytotoxic T cells, NK and NKT cells, M1 macrophages, and mature DCs are protective against tumour growth [Dushyanthen et al., 2015]. On the contrary, CD4+ Th2 cells, immature DC, M2 macrophages, Tregs and myeloid-derived suppressor cells (MDSCs) suppress anti-tumour immunity and promote tumour growth. The role of Th17 cells like that of B cells is still under debate [Salgado et al., 2015b], while the infiltration of Tfh cells in BCs suggested that they are an important immune element whose present in the tumour is a positive prognostic factor [Gu-Trantien et al., 2013].

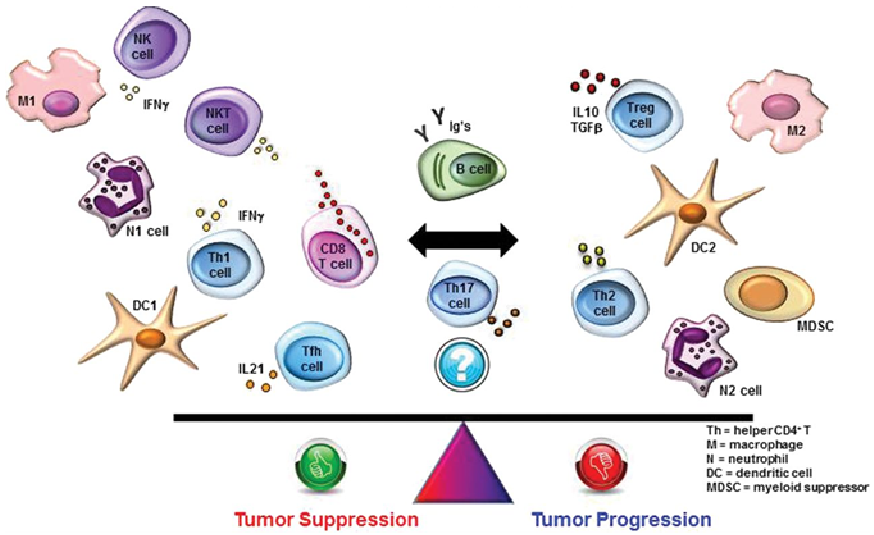

Figure 12. Tumour-infiltrating lymphocytes in cancer
Leukocyte subsets present in the TME and their contribution to pro- or anti-tumour activities. [Salgado et al., 2015b]

1.3.2 Chemokine-induced infiltration of immune cells in the tumour microenvironment

Development of an effective antitumour immune response relies on the coordinated interaction of immunocompetent cells, the spatio-temporal distribution of which is in part orchestrated by chemokines. Chemokines coordinate circulation, homing, and retention of immune cells in different sites during inflammation and immunity and regulate immune cell development and effectors function (reviewed in [Franciszkiewicz et al., 2012]). Chemokines constitute a large family of small, mostly secreted proteins comprising more than 50 members (Fig. 13) [Lazennec and Richmond, 2010]. They are classified based on the position of the first two conserved cysteine in the N-terminal of the mature proteins. The first group of chemokines, named the CC subfamily has adjacent cysteines and is composed of 28 members, whereas the CXC subfamily, which possesses a single variable aminoacid between the first two cysteines, comprises 17 members. Two minor subfamilies are represented by the CX3C family that has three amino acids separating the two cysteines, and the XC family, which lacks the first cysteine. The CXC

chemokines can be further classified into ELR- and ELR+ subgroups based on the presence or absence of the motif 'glu-leu-arg (ELR)'. ELR+ CXC chemokines (CXCL1, 2, 3, 5, 6, 7 and 8) are angiogenic factors, whereas ELR- members (except CXCL12) are angiostatic factors and inhibit the formation of blood vessels [Lazennec and Richmond, 2010].

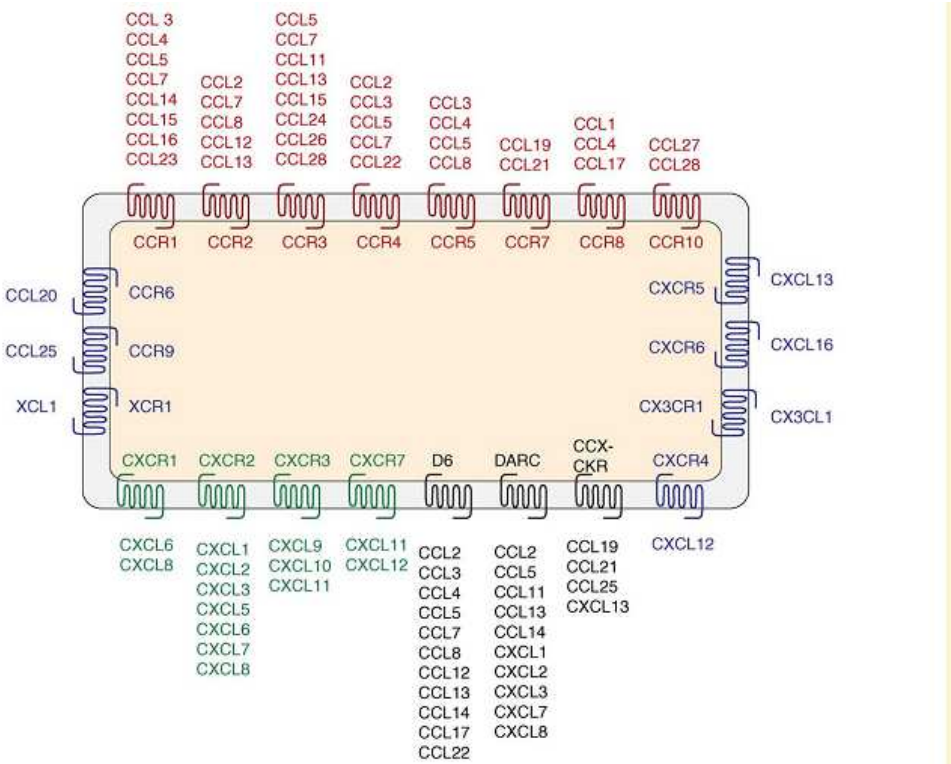

Figure 13. Chemokine and chemokine receptor families
CC and CXC chemokines that interact with multiple receptors are shown in red and green respectively. In blue are shown receptors that recognize only one ligand. Decoy receptors are shown in black. [Lazennec and Richmond, 2010]

Chemokine receptors are 7 transmembrane domain receptors coupled with G proteins (GPCR) and are responsible not only for triggering intracellular signals resulting in cell polarization, migration, and adhesion, but also for contributing to gene expression, cell proliferation, and survival of immune cells. There are ten CCR family members and seven CXCR family members in addition to XCR1 and CX3CR1. Moreover, there are three decoy receptors (D6, DARC and CCX-CKR) that bind ligands with high affinity but do not elicit signal transduction. Many chemokines bind multiple receptors and most receptors bind multiple chemokines, suggesting functional redundancy (Fig. 13).

Chemokines commonly associated with activated T-cell trafficking in the tumour tissue, include the CXCR3 ligands CXCL9, CXCL10, and CXCL11 and the CCR5 ligands CCL3, CCL4, and CCL5 (Fig. 14) [Franciszkiewicz et al., 2012]. Recruitment of innate immune cells (MΦ, NK, and NKT cells) in the tumour burden depends mainly on CCL2, CCL5, CXCL9 and CX3CL1. Tumour-derived chemokines are also responsible for recruitment of Treg cells and MDSC: Tregs are mostly recruited through CCL22-CCR4 while MDSCs are recruited within tumours in a CCR2, CXCR4, or CXCR2-dependent manner [Franciszkiewicz et al., 2012].

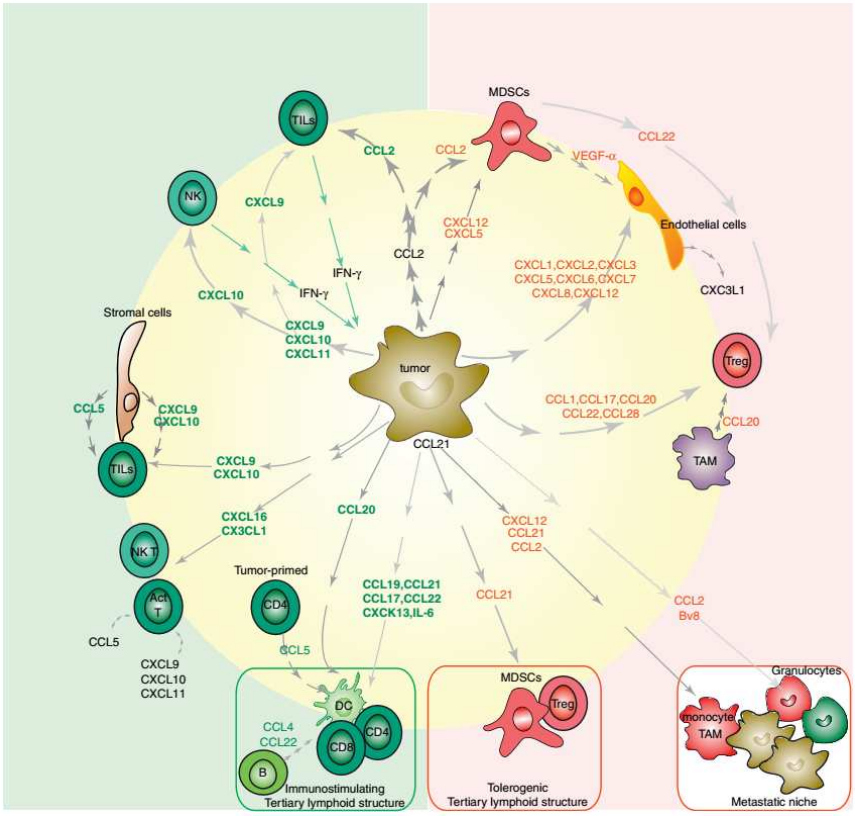

Figure 14. Chemokines and cellular networks in cancer progression
Chemokines directly released by primary tumours act on cells of innate and adaptive immunity to either support (right part, red) or control (left part, green) tumour development and metastatic spreading. MDSCs: myeloid-derived suppressor cells; TAMs: tumour-associated macrophages; TILs: tumour-infiltrating lymphocytes; ActT: activated T lymphocytes; DC: dendritic cells; Treg: regulatory T lymphocytes. [Viola et al., 2012]

Effector cells are mainly attracted in the tumour burden by CXCR3 ligands CXCL9 and CXCL10. In addition to their angiostatic activity, these chemokines participate in the

antitumour immune response through recruitment of T and NK cells. In renal cell carcinoma and in melanoma, intratumoural expression of CXCL9 and CXCL10 coincided with a high degree of CD8+ T cell infiltration [Franciszkiewicz et al., 2012]. Importantly, tumour infiltration by NK cells, Th1 CD4+ T cells and CD8+ T cells creates a positive feedback loop within the TME because IFN-γ, they release, enhances the production of CXCL9, 10 and 11 by tumour cells (Fig. 14)[Viola et al., 2012].

Chemokine (CC-motif) ligand 2 (CCL2), also referred to as monocyte chemoattractant protein-1, is one of the many inflammatory chemokines released by both tumour and stromal cells. CCL2 expression is a poor prognostic marker in BC: it has a strong tumourigenic role through its effects on monocyte/macrophage recruitment and activation, direct and indirect induction of angiogenesis, and promotion of metastasis, but it can also recruit TILs (reviewed in [Steiner and Murphy, 2012]). It has also been reported to directly upregulate pro-tumourigenic inflammatory mediators, including CCL5 and tumour necrosis factor-alpha (TNF-α). CCL5, like CCL2, is significantly correlated with poor prognosis and more advanced disease stage. The activities of CCL2 and CCL5 appear to be both co-dependent and exclusive: while both enhance tumour macrophage recruitment, CCL2 induces angiogenesis, and CCL5 is primarily implicated in BC cell invasion and metastases through its promotion of tumour cell motility and matrix metalloproteinase activity [Soria and Ben-Baruch, 2008].

1.3.3 The anti tumour immune response

The antitumour immune response is dependent upon NK and NKT recognition of tumour cells and CD4+ (Th1) IFN-γ production, which in turn mediates the expansion, differentiation, and activation of tumour-specific CD8+ T cells [Gu-Trantien et al., 2013].

NK cells are primarily viewed as cytotoxic lymphocytes playing a relevant role in innate immunity, mainly in tumour surveillance and in defenses against viruses; upon activation, NK cells release cytotoxic granules containing perforin and various granzymes, leading to the perforation of target cells and subsequent death [Vivier et al., 2008]. A second effector mechanism of NK cells is exerted by secretion of a variety of cytokines and chemokines, including IFN-γ, TNF, GM-CSF (granulocyte-macrophage colony stimulating factor), MIP-1α (macrophage inflammatory protein-1α) and CCL5. NK cells are considered as the major source of IFN-γ *in vivo*, and NK-derived IFN-γ is also crucial in priming Th1 T-cell responses. In humans, NK cells are usually defined as CD3−CD56+ lymphocytes and comprise about 5–20% of peripheral blood lymphocytes. They can be divided into two major sub-populations, namely $CD56_{dim}$CD16+ and $CD56_{bright}$CD16− [Bellora et al., 2014]. The $CD56_{dim}$ population predominates in the blood (~95% of NK cells) and at sites of inflammation, exhibits a high cytotoxic potential and broadly expresses MHC-I specific inhibitory receptors. In contrast, the $CD56_{bright}$ subset prevails in lymph nodes (~75% of NK cells), mainly produces cytokines upon activation and displays little cytotoxicity [Bellora et al., 2014].

The NK cell detection system, in addition to the low-affinity Fc receptor CD16, which permits NK cells to kill antibody-coated target cells through ADCC, includes a variety of cell surface activating and inhibitory receptors, the engagement of which by ligands expressed on tumour cells regulates immune effector cell activities [Vivier et al., 2008]. In humans, major activating NK receptors are the natural cytotoxicity receptors NKp30, NKp44 and NKp46, and the NK Group 2 member D (NKG2D), a type II transmembrane C-type lectin like receptor [Moretta et al., 2001]. It binds multiple ligands, including MHC-I chain-related A (MICA), MICB and several UL-16 binding proteins (ULBPs), which are induced after cellular stress [Gasser et al., 2005] and are the most

common ligands for NK cell receptors in BCs together with DNAM-1 ligands [Mamessier et al., 2011]. NKG2D, other than NK cells, is expressed also by NKT and CD8+ T cells and, through activation of its downstream signalling pathway induced by binding to its ligands, participates in the activation and induction of degranulation of NK and T cells [Nausch and Cerwenka, 2008].

CD8+ cytotoxic T cells (CTLs) induce cell lysis via recognition of specific tumour associated antigens on the surface of cancer cells. To have an effective killing of cancer cells by CTL, a series of stepwise events must be initiated and allowed to proceed. These steps are described as the cancer immunity cycle (Fig. 15) [Chen and Mellman, 2013]. In the first step, neoantigens created by oncogenesis are released and captured by APCs for processing. Next, APCs present the captured antigens on MHC-I and MHC-II molecules to T cells with B7 molecules (CD80 and CD86) in the lymph node, resulting in the priming and activation of effector T cell responses against the cancer-specific antigens. Finally, the activated effector T cells migrate to and infiltrate the tumour site, specifically recognize and bind to cancer cells through the interaction between their T cell receptor (TCR) and its cognate antigen bound to MHC-I, and kill the cell through the release of high levels of granzymes, IFN-γ, and perforin. Killing of the cancer cell releases additional tumour-associated antigens to increase the extent and strength of the response in subsequent revolutions of the cycle.

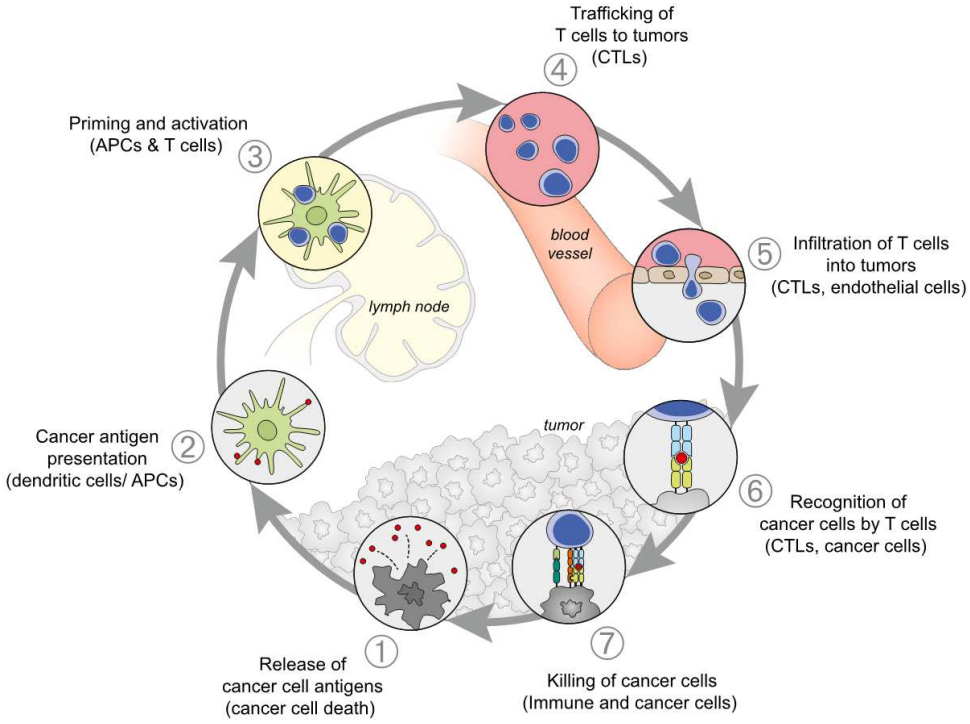

Figure 15. The Cancer immunity cycle
The generation of immunity to cancer is a cyclic process that can be self propagating. It can be divided into seven major steps, starting with the release of antigens from cancer cells and ending with the killing of cancer cells. Each step is represented with the primary cell types involved and the anatomic location of the activity listed. APCs: antigen presenting cells; CTLs: cytotoxic T lymphocytes. [Chen and Mellman, 2013]

1.3.4 Mechanisms adopted by tumours to escape immunosurveillance

The tumour manages to escape the host immune system and contrives to benefit from infiltrating cells by modifing their functions to create a TME favourable to its progression. The interaction between tumour and immune cells during tumour progression is described by the immunoediting process that goes forward through three phases: i) elimination, where cancerous cells are eliminated following immunosurveillance; ii) equilibrium, where transformed cells are held in control but are not eliminated by the immune system; and iii) escape, where tumour cell modifications shape disease progression inducing immune subversion and escaping from their control [Varfolomeev et al., 2008] (Fig. 16). Immune evasion, i.e. the ability of the tumour to avoid or escape detection and elimination by the immune system, has been highlighted as one the

emerging hallmarks of cancer, necessary for tumour progression and metastasis [Hanahan and Weinberg, 2011].

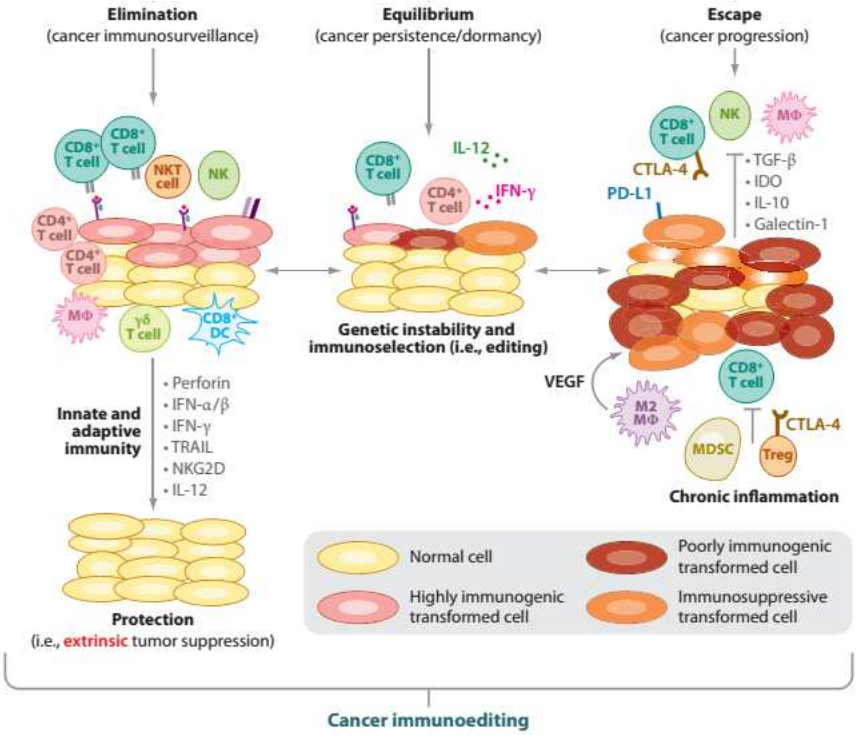

Figure 16. The three phases of cancer immunoediting
Once normal cells are transformed into tumour cells the immune system may function as an extrinsic tumour suppressor by eliminating tumour cells or preventing their outgrowth. In the first phase, elimination, innate and adaptive immune cells recognize transformed cells and destroy them, resulting in a return to normal physiological tissue. However, when antitumour immunity is unable to completely eliminate transformed cells, tumour variants may enter into the equilibrium phase, where cells and molecules of adaptive immunity prevent tumour outgrowth. These variants may eventually acquire further mutations that result in the evasion of tumour cell control by immune cells and progress to clinically detectable malignancies in the escape phase. CTLA-4: cytotoxic T lymphocyte associated protein-4; IDO: indoleamine 2,3-deoxygenase; IFN: interferon; IL: interleukin; M: macrophage; MDSC: myeloid-derived suppressor cells; NK: natural killer; NKG2D: NK group 2, member D; PD-L1: programmed cell death 1 ligand 1; TGF-β: transforming growth factor-β; TRAIL: tumour necrosis factor-related apoptosis-inducing ligand; Treg: regulatory T cell; VEGF: vascular endothelial growth factor. Modified from [Vesely et al., 2011].

In cancer patients, the cancer immunity cycle does not accomplish optimally. Tumour antigens may not be detected, dendritic cells and T cells may treat antigens as self rather than foreign, thereby creating Treg cell responses rather than effector responses, and T cells may be inhibited from infiltrating the tumour and suppressed by tumour cells (reviewed by [Motz and Coukos, 2013]). Tumours are known to employ a number of

mechanisms to suppress antitumour immune responses and to promote tumour progression [Vesely et al., 2011;Topfer et al., 2011]. They borrow four possible mechanism to evade the existing activated antitumour immune response: i) to alter the expression of cell surface markers like MHC-I and antigenic molecules through which the immune system recognised and kill them; ii) to acquire resistance to apoptotic mechanisms normally induced by cytotoxic cells through upregulation of apoptosis inhibitors (Bcl-XL, FLIP); iii) to alter the balance of immune cell populations in the TME; iv) to directly suppress the immune cells.

Tumour cells directly recruit regulatory cells, like Tregs and MDSCs, to generate an immunosuppressive microenvironment through the release of specific chemokines and IL-4, IL-13, GM-CSF, IL-1β, VEGF, or PGE2 [Vesely et al., 2011]. Recruited Treg cells have inhibitory action on CD8+ T cells, APCs, NKs, and CD4+ Th1 T cells through contact-dependent mechanisms or IL-10 and TGF-β secretion. MDSC accumulating in human tumours are CD34+CD33+CD13+CD15− bone marrow derived immature dendritic cells, an equivalent to CD11b+/Gr1+ cells in mice [Serafini et al., 2006]. They promote tumour growth and suppress immune cell functions through copious production of an enzyme involved in L-arginine metabolism, arginase 1, which synergizes with iNOS as well as ROS production blunting lymphocyte [Gabrilovich and Nagaraj, 2009]. M2 macrophages, polarised from myeloid precursor by IL-4 and IL-13, inhibit T cells through release of TGF-β, IL-10, and PDGF [Vesely et al., 2011].

One mechanism through which tumour cells inhibit effector immune cell functions is the release of TGF-β, IL-10, VEGF, LXR-L, IDO or soluble MICA, or expression of molecule that are usually used by immune system to regulate itself (i.e. PD-L1 and PD-L2). Programmed cell death protein 1 (PD-1) is expressed on the cell membrane of the majority of CD4+ T cells and CD8+ T cells infiltrating the TME. If PD-1 interact with its

ligands (PD-L1 or PD-L2) concurrently with TCR binding to an antigen presented by MHC, T cell encounter 'exhaustion' (Fig. 17)[Damgaard et al., 2012].

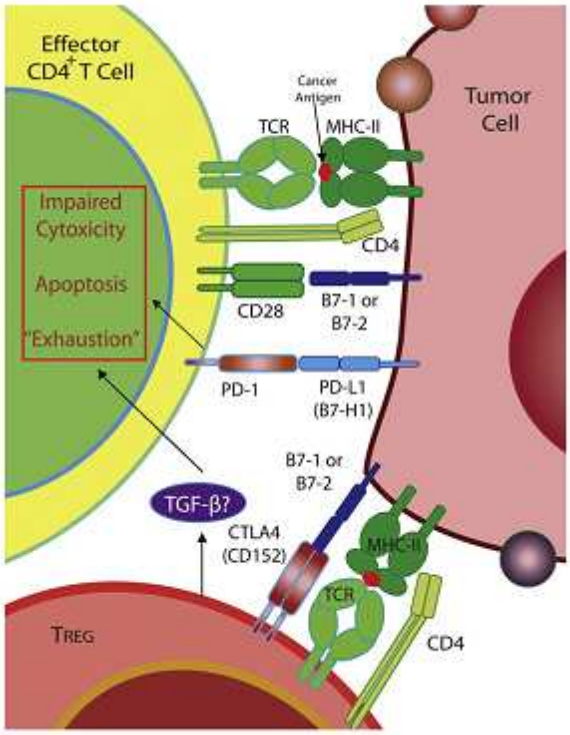

Figure 17. T cell 'exhaustion' via PD-1
Effector cells can be inactivated when PD-1 on their membrane binds its ligands on target tumour cells. Also Treg can induce exhaustion of activated T cells by releasing cytokines that have direct immunosuppressive effects, like TGFβ. [Burkholder et al., 2014]

In glioblastoma it has been demonstrated that oncogenic stress could induce constitutive expression of PD-L1 on the tumour cell membrane through the deletion of PTEN [Parsa et al., 2007]. In lymphoma, anaplastic lymphoma kinase (ALK) addiction drives PD-L1 expression through STAT3 [Marzec et al., 2008]. The other mechanism of PD-L1 modulation on tumour cells derives from their adaptation to the tumour-specific immune responses: the tumour uses the natural physiology of the PD-L1 expression modulating its expression upon interferons (mainly IFN-γ) produced by immune cells (Fig. 18).

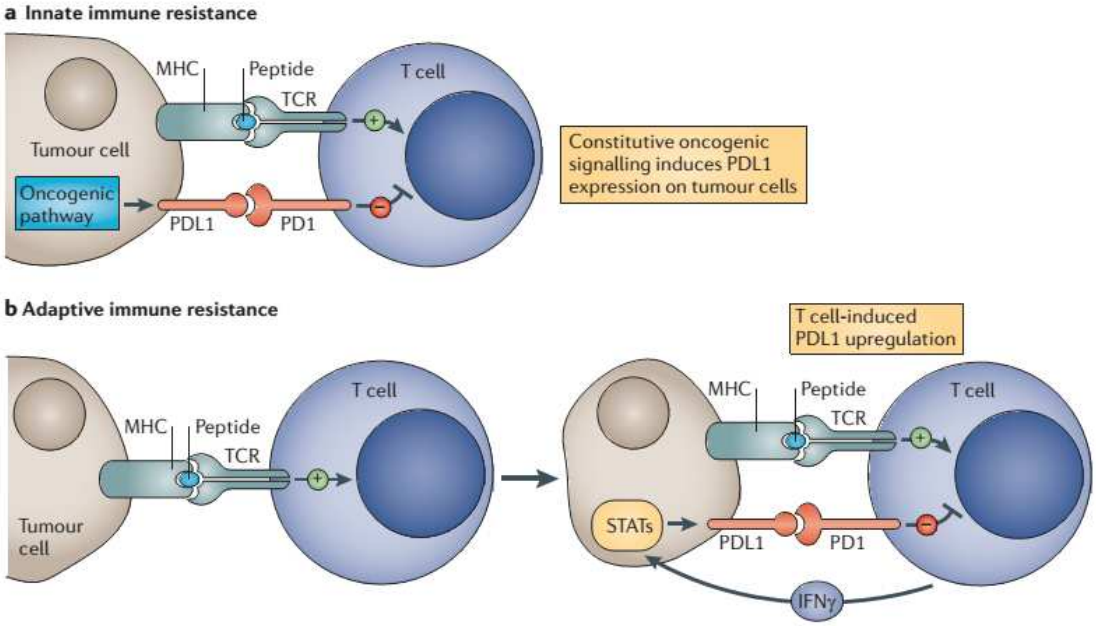

Figure 18. Mechanisms of expression of immune-checkpoint ligands on tumour cells
PD-L1 expression on tumour cells could derive by (a) constitutive oncogenic signaling independently from the TME or (b) by induction mediated by inflammatory signals that are produced by an active antitumour immune response. IFN-γ: interferon γ; MHC: major histocompatibility complex, TCR: T cell receptor. [Damgaard et al., 2012]

1.4 Aim and significance of the thesis

Trastuzumab is the standard of care treatment for patients with HER2-positive BCs that represent almost 20-25% of all BCs. Selection of patients to receive this targeted agent in the clinical practice occurs through evaluation of HER2 positivity by IHC and/or FISH. Several clinical trials demonstrated trastuzumab therapeutic effectiveness; indeed the addition of trastuzumab to chemotherapy almost doubled the probability to reach the pCR in neoadjuvant setting and reduced the probability of relapse of almost 40% in adjuvant setting. However, the treatment is not effective in every patient pointing to the relevance of identifying biomarkers to distinguish patients sensitive to this therapy from those suited for novel targeted approach. In this context HER2-positive BCs are known to be heterogeneous and all intrinsic subtypes are found in clinically positive HER2 disease, with HER2-E tumours as those most sensitive to trastuzumab treatment. Later on, based on increasing evidences of the role of the immune system in trastuzumab mechanism of action, also immune-related informations were explored and found predictive of trastuzumab benefit in several studies.

Aim of this study was to identify new predictive biomarker of trastuzumab benefit and to characterise responsive tumours in order to have new insights into the biological characterisation of trastuzumab activity.

Starting from patients treated in the clinical practice with trastuzumab, we performed whole gene expression profile analysis of 53 HER2-positive tumours treated with adjuvant trastuzumab in our institute. We developed a Trastuzumab Advantage Risk (TRAR) model able to stratify patients according to their sensitivity to trastuzumab. Molecular and biological characterisation of tumours sensitive to trastuzumab showed that they are addicted to HER2 and are enriched in immune pathways and cells. *In vitro* analyses

allowed us to determine a direct relationship between HER2 activity and CCL2 and PD-1 ligands expression, indicating that in HER2-addicted tumours the oncogene molds its tumour microenviroment. Moreover, analyzing two cohorts of patients treated with neoadjuvant trastuzumab we observed an association between tumour HER2 dependence and the expression of NKG2D activating receptor in circulating NK cells.

Overall, we described a tool able to identify BCs responsive to trastuzumab and understood that in these tumours HER2 is crucial for tumour growth, for infiltration of pro-trastuzumab immune cells and their suppression.

CHAPTER 2: MATERIALS AND METHODS

2.1 Breast cancer patients

2.1.1 GHEA cohort

The 53 BCs of the Group HErceptin in Adjuvant therapy (GHEA) cohort were selected from our recently published multicenter Italian observational study cohort [Campiglio et al., 2013], composed by 295 HER2-positive BC patients treated with adjuvant chemotherapy plus trastuzumab between 2005 and 2009 in Fondazione IRCCS Istituto Nazionale dei tumouri of Milan. Of all 32 relapsed tumours within the 4-year follow-up, 23 samples with good quality RNA were selected for this study and matched 1:1 with non-relapsed tumours for patient age, ER positivity, lymph node involvement and tumour size. To increase the size of the GHEA cohort, 7 additional non-relapsed tumours, which matched to relapsed tumour for the same parameters, were selected and included. Table 8 lists the patients' clinico-pathological characteristics.

Histological grade was determined by the Nottingham grading system. The HER2 positivity was assigned following the 2013 ASCO/CAP Guidelines [Wolff et al., 2013]. Tumours were considered Ki67- and ER-positive if they showed at least 14% and 10% immunoreactive cells, respectively, according to institutional guidelines. All procedures were in accordance with the Helsinki Declaration (World Medical Association, 2013). Tumour specimens used for research consisted of leftover material of samples collected during standard surgical and medical approaches at Fondazione IRCCS Istituto Nazionale dei tumouri of Milan. Aliquots were allocated to this study after approval by the Independent Ethical Committee of Fondazione IRCCS Istituto Nazionale dei tumori of Milan.

Table 8. Frequency of clinico-pathological features of GHEA patients according to relapse. Adopted from [Triulzi et al., 2015]

Variable	Relapsed (*n*=23)	Non-relapsed (*n*=30)	₮ *p-value*
Median age, y (range)	52 (32-67)	55 (35-69)	0.451
Tumour size			
T1	8 (35%)	13 (43%)	0.581
T2	8 (35%)	11 (37%)	
T3 and T4	7 (30%)	6 (20%)	
Lymph node status			
Positive	21 (91%)	25 (83%)	0.685
Histological grade			
III	18 (78%)	21 (70%)	0.547
Estrogen receptor			
Positive	13 (57%)	19 (63%)	0.778
Progesteron receptor			
Positive	9 (39%)	15 (50%)	0.579
Ki67			
Positive	19 (83%)	20 (67%)	0.225
Neo-adjuvant chemotherapy			
A+T+CMF	9 (39%)	7 (23%)	
CMF	0	1 (3%)	0.366
Adjuvant chemotherapy			
A	0	5 (17%)	
T	0	2 (7%)	
A+T	12 (52%)	15 (50%)	0.088
CMF	2 (9%)	0	
Hormone therapy			
Yes	12 (52%)	16 (53%)	1.000
Median trastuzumab duration, cycles (range)	18(5-30)	18(12-19)	0.974

₮ p-value is calculated by Fisher exact test.
A: Adryamicin; T: Taxanes; CMF: Cyclophosphamide, methotrexate, 5'-fluorouracil

2.1.2 TRUP cohort

The 24 breast carcinomas of the trastuzumab-upfront-in-HER2-positive-locally-advanced- BC (TRUP) cohort were retrieved from TRUP window-of-opportunity trial [Koukourakis et al., 2014] composed by 28 locally advanced primary BC diagnosed using incisional biopsy at A.O. Istituti Ospitalieri di Cremona. Table 9 lists the patients' clinical and pathological characteristics. Patients were treated with one cycle of trastuzumab alone followed by 4 cycles of paclitaxel and trastuzumab till definitive surgery. After one

cycle of trastuzumab treatment (21 days) a tru-cut biopsy was performed and tumour dimensions were measured by FDG PET/CT scan and by clinicians. pCR was defined as no residual invasive tumour or *in situ* carcinoma in the primary tumour and in the nodes.

Table 9. Frequency of clinico-pathological features of TRUP patients according to response. Adopted from [Triulzi et al., 2015]

Variable	**Responders* (*n*=6)**	**Non-responders (*n*=18)**	**ǂ *p-value***
Tumour size			
T1 and T2	5 (83%)	11 (61%)	0.6214
Lymph node status			
Positive	2 (50%)	6 (37%)	1.0000
Histological grade			
III	5 (83%)	14 (78%)	1.0000
Estrogen receptor			
Positive	1 (17%)	11 (61%)	0.1550
Progesteron receptor			
Positive	1 (17%)	6 (33%)	0.6287

***** Response is defined as pCR; ǂ p-value is calculated by Fisher exact test.

Human peripheral blood and tumour specimens were obtained at A.O. Istituti Ospitalieri di Cremona after written informed consent from patients in accordance with the Helsinki Declaration and after institutional approval from our ethics committee (Comitato Etico Indipendente, Fondazione IRCCS, Istituto Nazionale dei tumouri) for the conduct of the study.

2.1.3 Neo-INT cohort

HER2-positive BC core biopsies were obtained from 8 patients before a treatment protocol consisting of 3 or 4 cycles of AT (adriamycin plus taxotere) followed by 4 cycles of CMF (cyclophosphamide, methotrexate and fluorouracil) and trastuzumab at Fondazione IRCCS, Istituto Nazionale dei tumouri of Milan. pCR was defined as no residual invasive tumour or *in situ* carcinoma in the primary tumour. Table 10 lists the patients' clinico-pathological characteristics.

Blood samples of these patients were collected at two time points during neoadjuvant treatment: pre, before any treatment; post, after AT cycles. Human peripheral blood and tumour specimens were obtained after written informed consent from patients in accordance with the Helsinki Declaration and after institutional approval from our ethics committee (Comitato Etico Indipendente, Fondazione IRCCS, Istituto Nazionale dei tumouri) for the conduct of the study.

Table 10. Frequency of clinico-pathological features of TRUP patients according to response

Variable	**Responders (*n*=2)**	**Non-responders (*n*=6)**
tumour size *T1 and T2*	2 (100%)	5 (83%)
Lymph node status *Positive*	2 (100%)	4 (67%)
Histological grade *III*	2 (100%)	4 (67%)
Estrogen receptor *Positive*	1 (50%)	2 (33%)
Progesteron receptor *Positive*	1 (50%)	2 (33%)
Ki67 *Positive*	2 (100%)	6 (100%)

2.2 Cellular biology

2.2.1 Breast carcinoma cell lines

In this study we have used the following human HER2-positive BC cell lines purchased from the American Type Culture Collection (ATCC, Rockville, MD): SKBR3, HCC1954, MDAMB361, MDAMB453, BT474 and ZR75.30. SKBR3 and HCC1954 cell line were cultured in Roswell Park Memorial Institute (RPMI) 1610 medium (Euroclone, Milan, IT), MDAMB361, MDAMB453 and BT474 in Dulbecco's modified Eagle medium (DMEM) (Euroclone) and ZR75.30 in DMEM-F12 (Euroclone), all supplemented with 10% fetal bovine serum (FBS) (Thermo Fisher, Waltham, MA, USA) and 1 mM L-glutamine (Euroclone). All cell lines were grown in a humidified chamber (95% air, 5% CO_2) at 37 °C and were authenticated using the Short Tandem Repeat Profiling method in our institute facility.

2.2.2 Cell treatments

For the stimulation of HER2 downstream signals, cells were treated with 20 ng/ml EGF or heregulin (HRG) (Peprotech, Rocky Hill, NJ) in serum-free medium. These ligands induce HER1-HER2 and HER3-HER2 heterodimerisation, respectively, triggering downstream signalling cascade. For the blocking of HER2 signals, cells were treated with 10 μg/ml trastuzumab (Roche, Basel, Switzerland) or 0.3 μM lapatinib (LC Laboratories, Woburn, MA, USA). 10 μM LY294002 (BioMol, Hamburg, Germany) a PI3K inhibitor, 10 μM UO126 (Sigma-Aldrich, Saint Loius, MO, USA), a MEK inhibitor, and 10 μM BAY 11-7082 (Santacruz Biotechnology, Dallas, TX, USA), a NF-kB inhibitor, were used to block HER2 downstream signals in standard culture condition alone or upon serum deprivation with EGF and HRG. For IFN-γ stimulation, cells were treated with 100 ng/mL IFN-γ

(Peprotech) in standard culture conditions. Details concerning treatment schedules are reported for each experiment in the "Results" section.

Drug titration curves were obtained by treating HER2-positive cells grown as monolayers in 96-well plates (n=6 wells/treatment) with lapatinib (from 0.015 to 10 μM) for 72 h. Control cells were treated with 0.01% DMSO. Cell growth was measured using the sulforhodamine B (SRB) assay: cells were fixed with trichloroacetic acid 10% and then stained with SRB. Absorbance was evaluated at 550 nm, and cell growth in treated cells was calculated as a percentage of that in untreated cells.

2.2.3 ADCC assay

$1*10^6$ BC cells (BT474, SKBR3, MDAMB453 and MDAMB361) were labeled with 100 μCi ^{51}Cr (Perkin-Elmer, Waltham, MA, USA) in FBS for 1 hour at 37°C. After 3 washes with PBS-5% FBS, cells were co-incubated for 4 hours at 37°C with PBMCs isolated by density-gradient separation using Ficoll-Paque PLUS (Amersham Biosciences, Piscataway, NJ, USA) from healthy donors (effector: target ratio 50:1) in 200 μl RPMI 1640 complete medium in triplicate 96-well U-bottomed plates in the presence of saturating concentrations of trastuzumab (4 μg/ml). To evaluate the modulation of ADCC activity of PBMCs modified by plasma treatment, PBMCs from healthy donors were cultured in plasma (diluited 1:10 with RPMI 1640 without serum) obtained from INT-Neo patients for 24 hours and then used in ADCC assay against BT474 cells in the presence of trastuzumab. Radioactivity of the supernatant was measured with a Trilux Beta Scintillation Counter (Perkin-Elmer). Maximum and spontaneous release of chromium by BC cells was measured in supernatant of cells cultured alone for 4 h in the presence or not respectively of 1% Triton X-100. Percent specific lysis was calculated as: 100 × (experimental cpm - spontaneous cpm)/ (maximum cpm - spontaneous cpm).

2.2.4 ELISA assay

Soluble CCL2 were quantified in BC cell supernatants using DuoSet ELISA kits (R&D Systems, Minneapolis, MN, USA), following the manufacturer's instructions. Cell culture supernatants were collected at different time points after treatments and stored at -80°C until use. ELISA detection was performed using 100 µl of each supernatant.

2.2.5 Western blot and immunoprecipitation analyses

Protein fractions were solubilised from BC cell lines for 40 min at 0°C with lysis buffer containing 50 mM Tris-HCl pH 7.4, 150 mM NaCl, 1% Triton X-100, 2 mM Na-orthovanadate, protease inhibitor cocktail (Complete Mini, Roche). Proteins were resolved by electrophoresis on pre-cast 7% Tris-acetate polyacrylamide gels and 4-12% bis-tris gels (Thermo Fisher Scientific), transferred on PDVF membranes (Millipore, Jaffrey, NH) and then incubated with primary antibodies. The following primary mouse MAbs were used:

- 1:300 Ab3 c-erbB-2/HER2/neu IgG1 (Calbiochem, Darmstadt, Germany);
- 1:1000 Anti-Vinculin antibody (clone hVIN-1, Sigma-Aldrich);
- 1:200 anti-STAT1 (Santa Cruz Biotechnology).

The following primary rabbit polyclonal antibodies were used:

- 1:6000 anti-phospho-HER2, p-Neu (Tyr 1248) (Santa Cruz Biotechnology)
- 1:1000 anti-phospho-p44/42 MAPK (Erk1/2, Thr202/Tyr204) (Cell Signalling Technology, Danvers, MA, USA);
- 1:1000 anti-p44/42 MAPK (Erk1/2) (Cell Signalling Technology);
- 1:1000 anti-phospho-AKT (Ser473) (Cell Signalling Technology);
- 1:1000 anti-AKT (Cell Signalling Technology);
- 1:1000 anti NF-kB (Santa Cruz Biotechnology);
- 1:1000 anti-phospho-NF-kB (Ser536) (Santa Cruz Biotechnology);

- 1:1000 anti-phospho-STAT1 (Tyr701) (Cell Signalling Technology);
- 1:800 anti-EGFR (1005, Santa Cruz Biotechnology);
- 1:200 anti-HER3 (C-17, Santa Cruz Biotechnology)

Filters were then incubated with secondary rabbit or mouse anti-IgG antibodies conjugated with horseradish peroxidase (1:10000, Amersham GE Healthcare, Little Chalfont, UK) and proteins visualised by enhanced chemiluminescence detection system (Sigma-Aldrich). Quantification was performed with Quantity One 4.6.6 software (Bio-Rad, Hercules, CA).

For immunoprecipitation, $4x10^6$ BC cells were seeded in 10 mm petri dishes, cultured for 48 h and lysed as described above. 1 mg of the cell extract were pre-cleared by incubation with 80 µl of sepharose protein A/G (Thermo Fisher Scientific) and 30 µl of normal mouse serum under rocking conditions for 30 minutes at 4°C. Then, lysate was incubated under rocking conditions with 1 µg anti-HER2 antibodies produced in our labouratory (MGR2 [Tagliabue et al., 1991]) for 2 h at 4°C, followed by incubation with sepharose protein A/G (Thermo Fisher Scientific) for 3 h under rocking conditions. Immunoprecipitates were separated, electrophoretically transferred onto nitrocellulose filters, probed and revealed as described above.

2.2.6 Immunohistochemistry

IHC was performed on formalin-fixed paraffin embedded (FFPE) tissue. Slides were deparaffinised in xilol, serially rehydrated and, after antigen retrieval using autoclave at 121 °C for 6 minutes using the appropriate antigen retrieval solution, stained with primary antibodies. Then, slides were incubated with the appropriate secondary antibodies (Dako, Agilent Technologies, Santa Clara, CA, USA). Immunoreactions were visualised using streptavidin-biotin-peroxidase (Thermo Fisher Scientific) and the DAB (3,3'Diaminobenzidine) Chromogen System (Dako) followed by counterstaining with

Carazzi hematoxylin. Table 11 lists the molecules detected and the antigen unmasking used.

Table 11. List of molecules evaluated by IHC

Molecule	Host	Clone	Dilution	Brand	Antigen Retrieval
CD45	Mouse	2B11	1:200	Dako	Target Retrieval Solution pH9, Dako
CD20	Mouse	L26	1:400	Dako	Target Retrieval Solution pH9, Dako
CD3	Mouse	F7.2.38	1:400	Dako	Target Retrieval Solution pH9, Dako
CD8	Mouse	C8/144B	1:200	Dako	Target Retrieval Solution pH9, Dako
CD56	Mouse	123C3	1:400	NeoMarkers	Target Retrieval Solution pH9, Dako
CD68	Mouse	KP1	1:100	Novus Bio	10 mM citrate buffer, pH6
CD33	Mouse	PWS-44	1:100	Novocastra	Target Retrieval Solution pH9, Dako
FOXP3	Rat	PCH101	1:20	Ebioscience	10 mM citrate buffer, pH6
CXCL9	Rabbit	--	1:100	Novus Bio	10 mM citrate buffer, pH6
CXCL10	Rabbit	--	1:100	Abcam	10 mM citrate buffer, pH6
CCL2	Mouse	23002	1:1000	R&D System	1 mM EDTA, pH8
CCL2	Rabbit	--	1:200	Abcam	10 mM citrate buffer, pH6
Ki67	Mouse	MIB-1	1:200	Dako	10 mM citrate buffer, pH6
ER	Mouse	EP1	1:200	Dako	10 mM citrate buffer, pH6
HER2	Rabbit	--	1:50	Dako	10 mM citrate buffer, pH6

Image acquisition and analyses were performed using a DM2000 optical microscope (Leica Microsystems GmbH, Wetzlar, Germany) and a DFC320 digital camera (Leica Mycrosystem GmbH). Slides stained with CD45, CD3, CD20, CD8, CD56 and CD68 were digitised by a slide scanner (ImageScope XT, Aperio), and the virtual slides were subsequently evaluated using the 'positive pixel count' algorithm of Aperio ImageScope. The positivity was calculated as the number of positive pixels/μm^2. Data were divided into two groups (positive and negative) using median value as cut-off.

Pathological assessment of stromal lymphocytic infiltration was carried out on the routinely-stained with Hematoxylin & Eosin slides, as described [Loi et al., 2013].

2.2.7 Immunofluorescence analyses

Immunofluorescence (IF) analyses were performed on FFPE tissues of the GHEA cohort to quantify the amount of HER2 protein. Slides were deparaffinised, serially rehydrated and, after antigen retrieval, tissues were incubated with blocking solution (Thermo Fisher

Scientific) and with anti-HER2 primary antibody as performed for IHC analysis (see paragraph 2.2.6). Nuclei were counterstained with DAPI (Thermo Fisher Scientific) and images acquired in the microscopy facility of our institute (Department of Experimental Oncology, Istituto Nazionale dei tumouri, Milan), with a Leica TCS SP8 X confocal laser scanning microscope (Leica Microsystems GmbH). The fluorochromes were excited by a continuous wave 405nm diode laser and a pulsed super continuum White Light Laser (470-670nm; 1nm tuning step size). In particular, AlexaFluor-546 was excited selecting 553 nm-laser line and detected from 557nm to 667 nm. Nine images were acquired for each slide using a HC PL APO CS2 40X/1.30 oil-immersion objective and a pinhole always set to 1 Airy unit. Data were analysed using Leica LAS X rel. 3.1 software (Leica Microsystems GmbH).

2.2.8 Flow citometry analyses

PBMCs isolated from patients of the Neo-INT cohort or healthy donors were analysed using MAbs to human antigens, including PE-anti-CD16 (3G8, BD Bioscience, San Jose, CA, USA), PECy5-anti-CD56 (B159, BD Bioscience), APC-eFluor780-anti-CD3 (SK7, eBioscence, San Diego, CA, USA), and APC-NKG2D (ON72, Beckman Coulter, Miami, FL, USA).

Direct IF on tissue-derived murine cells was perfomed using APCeFluor780-anti-CD45 (30-F11, eBioscience), PE-anti-CD11b (MI/70, BD Bioscience), PerCpCy5.5-anti-F4/80 (BM8, eBioscience), APC-anti-MHC-II (M5/114.15.2, Miltenyi Biotec, Bergisch Gladbach, Germany). Direct IF on human BC cell lines to evaluate PD-L1 expression was performed staining cells with PE-anti-PD-L1 mouse MAbs (MIH1, eBioscience). Samples were analysed by gating on live cells using the FACSCanto system (BD Bioscience) and FlowJo software (Tree Star Inc, San Carlos, CA, USA).

2.3 Molecular biology

2.3.1 Gene expression profile

GEPs were generated in collaboration with the Functional Genomic and Bioinformatic Facility (Department of Experimental Oncology, Istituto Nazionale dei tumouri, Milan). RNA was extracted from FFPE tissue slides (20 μm thick) of primary tumours using the miRNeasy FFPE kit (Qiagen, Valencia, CA) according to the manufacturer's protocol. RNA quality was checked by pre-analytical screening using qRT-PCR as described [Ravo et al., 2008]. Whole-Genome DASL (cDNA-mediated Annealing, Selection, Extension, and Ligation) assay and HumanHT12_v4 BeadChips (Illumina, Inc., San Diego, CA) were used according to Illumina protocol. The BeadChips cover more than 29,000 annotated genes derived from RefSeq (Build 36.2, Release 38). The Illumina BeadArray Reader was used for scanning the arrays. Image acquisition and recovery of primary data were performed using Illumina BeadScan software, after which the data were quantile-normalised using BeadStudio software.

After filtering, data matrix was generated for the GHEA cohort (53 samples) and two data matrices were generated for the TRUP cohort: one containing 24 primary tumours before any treatment (TRUP) and one containing 17 matched samples (before and after one cycle of trastuzumab treatment, TRUP_AB). The data for GHEA and TRUP cohorts were deposited at the Gene Expression Omnibus (GEO) repository (accession numbers GSE55348 and GSE62327, respectively).

2.3.2 nCounter assay

RNA obtained from tumour tissues of the GHEA cohort was used to perform a custom nCounter assay according to NanoString protocol (NanoString Technologies, Seattle, WA, USA). The hybridization reaction was prepared mixing reporter CodeSet, hybridization

buffer, 100 ng RNA, and Capture ProbeSet and run at 65°C for 18 hours. The nCounter Prep Station was used for post-hybridization processing to prepare nCounter cartridges, and the Digital analyser for data collection. nSolver™ Analysis Software was used for quality check, normalization and subsequent analyses.

2.3.3 FISH analysis

The status of *ERBB2* gene in HER2-positive BC cell lines was analysed using the PathVision HER2/neu DNA probe kit (Vysis, Abbot Molecular, Abbot Park, IL, USA) in collaboration with Dr. P. Gasparini (Tumour Genomics Unit, Departmemt of Experimental Oncology and Molecular Medicine, Fondazione IRCCS Istituto Nazionale dei tumuri). FISH analysis was performed in 100 nuclei and at least 10 metaphase spreads. Metaphase spreads from tumour cells were prepared using standard cytogenetic methodologies [Gasparini et al., 2010]. Slides were pre-treated with 2X SSC/0.5% NP40 at 37°C for 30 min and co-denatured at 70°C for 2 min and 37°C overnight using Hybrite kit (Vysis). HER2 amplification was determined based on the presence of clusters in at least 10% of analysed cells. FISH hybridised slides were analysed with an Olympus BX51 microscope coupled to a charge-coupled device camera COHU 4912 (Olympus, Milan, Italy). Captured images were analysed using Mac Probe software (PowerGene, Olympus).

2.3.4 RNA extraction and qRT-PCR

To evaluate HER2-addiction of tumour of the Neo-INT cohort, RNA was extracted from FFPE tissue slides (5 µm thick) using the miRNeasy FFPE kit (Qiagen) according to the manufacturer's protocol. cDNAs were reverse-transcribed from 0.3 µg of total RNA in a 20 µl volume with SuperScript III (Thermo Fisher Scientific) using random-hexamer primers. To evaluate NKG2D expression on circulating cells, total RNA from frozen buffy-coats of patients of the TRUP cohort before any treatment was extracted with Qiazol (Qiagen), according to the manufacturer‘s protocol. cDNAs were reverse-transcribed from 1 µg of

total RNA in a 20 µl volume with SuperScript III (Thermo Fisher Scientific) using random-hexamer primers. Experiments of BC cell lines used RNA extracted using Qiazol (Qiagen) according to the manufacturer‘s instructions. cDNAs were reversed transcribed from 1 µg of total RNA in a 20 µl volume using High capacity RNA to cDNA kit (Thermo Fisher Scientific). qRT-PCR was performed using SYBR Green dye or Taqman probe-based assays (see Table 12 for assay details) on the ABI Prism 7900HT sequence detection system (Applied Biosystems,Thermo Fisher Scientific). Relative abundances of transcripts were calculated by the comparative Ct method using *GAPDH* as reference gene. *NKG2D* expression levels were calculated using *CD16* as reference gene and RNA obtained from a healthy donor buffy-coat as reference sample.

Table 12. List of assays used in qRT-PCR experiments

Gene	Code or sequence
CD16	Hs.04334165_m1
GAPDH	Hs.02758991_g1
CCL2	Hs.00234140_m1
CCL5	Hs.00982282_m1
CXCL9	Hs.00171065_m1
CXCL10	Hs.01124251_g1
CXCL11	Hs.04187682_g1
ERBB2	Hs.01007077_m1
NKG2D	Hs.00183683_m1
PD-L1	Hs.01125301_m1
PD-L2	Hs.01057777_m1
GAPDH	5’-CATGGCCTCCAAGGAGTAAG-3’; 5’-GACTGAGTGTGGCAGGGAC-3’
IRF1	5’-AAAAGGAGCCAGATCCCAAGA-3’; 5’-CATCCGGTACACTCGCACAG-3’

2.4 In silico analyses

Bioinformatic analyses were performed using R [R Development Core Team, 2007], version 2.15, BioConductor [Gentleman et al., 2004], release 2.10, and BrB-ArrayTool developed by Dr. Richard Simon and the BRB-ArrayTools Development Team (v4.2.0, http://linus.nci.nih.gov/BRB-ArrayTools.html). Gene-set enrichment analyses were performed using GSEA v2.0.13 [Subramanian et al., 2005]. Genes represented by more than one probe were collapsed to the probe with the maximum value using the Collapse Dataset tool. Gene set permutation type was applied 1000 times and gene set enrichment was considered significant at $p<0.05$, FDR<10%.

2.4.1 Unsupervised subtype discovery

To identify BCs subgroup within the HER2-positive tumours, the consensus unsupervised method (as implemented in the R package ConsensusClusterPlus) [Wilkerson and Hayes, 2010] was used. Unsupervised tumour subtypes were identified using partitioning around centroid clustering, 1-Euclidian correlation as distance matrix and applying 1,000 re-sampling interactions. The existence of $2<k<7$ clusters was tested, as described [Monti et al., 2003]. The empirical cumulative distribution function (CDF) plots, that show consensus distributions for each k, were used to determine the number of clusters giving the maximum stability. According to Monti et al., [Monti et al., 2003], the choice of the number of clusters depends on the delta area plot and when the CDF area no longer increases. To estimate the accuracy of the classification, silhouette width values [Rousseeuw et al., 1987] were calculated (R-package: cluster) for all samples. To project and validate our classification to other external datasets, PAM [Pollack et al., 2002] was applied to develop a classifier. A subclass mapping algorithm [Hoshida et al., 2007] was used to evaluate similarities in the global GEP between the training and validation sets.

2.4.2 TRAR model development and performance

TRAR model was developed on the training GHEA53 set using a semi-standardised method involving principal component analysis [Bair and Tibshirani, 2004]. The significance of each gene entered into the model was measured based on a univariate Cox proportional hazards regression of survival time versus the gene log expression level. A 10-fold cross-validation method was applied: 10% of the cases were omitted and for the remaining cases, the genes correlated with DFS at $p<0.01$ were selected. Subsequently, principal component analysis was used to reduce the dimensionality of genes present in the model to capture most of their variability. The first two principal components PC1 and PC2 were used to develop a prognostic model in which a prognostic trastuzumab advantage risk (TRAR) score was calculated as: $TRAR= \alpha\ PC1+ \beta\ PC2$, where α and β are the regression coefficients of the two principal components fitted by the Cox proportional hazards model in 10-fold cross-validation. Samples were classified as high- or low-risk by a 10-fold cross-validation approach: based on the median index values obtained in the training set comprising 90% of the cases, the remaining 10% omitted test cases were classified. After reiteration of the entire procedure, omitting a different 10% of cases until each case was omitted once, all cases were stratified. Analysis and plotting were conducted using R package superpc (http://www-stat.stanford.edu/~tibs/superpc).

The prediction accuracy was evaluated through time-dependent Receiver Operator Characteristic (ROC) curves at maximum time points of follow-up using the SurvJamda R package [Yasrebi, 2011]. ROC curve assessment for censored survival data was performed using the non-parametric estimator based on nearest neighbour bivariate distribution [Heagerty et al., 2000]. Accuracy of the prediction was evaluated measuring the mean and the standard deviation of the Area under the ROC curves (AUC) after 10-fold cross-validation.

2.4.3 External datasets

HER2-positive patients of the following public datasets were analysed: i) Metabric [Curtis et al., 2012]; ii) GSE22358 [Gluck et al., 2012]; iii) GSE41656 [de Ronde et al., 2013]; iv) GSE50948 [Prat et al., 2014a]. Microarray data were processed starting from the authors' raw data; if raw data or processing methods were not available, the processed data were retrieved. From the Metabric dataset, 132 cases were selected from the dataset by IHC and HER2-gain obtained by CNV data through Affymetrix SNP 6.0 chip SNP6 (IHC 3+ and IHC 2+ with HER2_GAIN). Raw gene expression data profiled on HumanHT12_v3 BeadChips (Illumina) were retrieved from the EMBL-EBI repository (https://www.ebi.ac.uk/ega/datasets/) and were normalised (R-package: lumi) [Du et al., 2008]. Raw data for GSE22358 and GSE41656 were retrieved from the GEO repository (http://www.ncbi.nlm.nih.gov/gds/) and processed as described by the authors [Gluck et al., 2012;de Ronde et al., 2013]. Since processing method for GSE50948 samples were not available, processed data were retrieved from the GEO repository.

2.4.4 External signatures

Immune metagenes were determined based on the method of Rody et al [Rody et al., 2009]. The 569 Affymetrix ProbeSets were first mapped on the Illumina platform. Due to low number of genes on GHEA dataset, 3 (MHC-I, MHC-II and IgG metagenes) out of 7 immune metagenes were excluded. In TRUP_AB cohort IgG metagene was excluded for the same reason. Average expression of genes belonging to each metagene was calculated.

The HER2-derived prognostic predictor (HDPP) was determined in GHEA samples as described [Staaf et al., 2010]. Briefly, the genes of the HDPP signature were mapped on Illumina BeadChips; 83% of the genes were present. Samples were classified based on the

highest Pearson correlation to HDPP centroids. Only samples with correlation >0 were retained for survival analysis.

The research-based PAM50 subtype predictor was determined using the publicly available algorithm as described [Prat et al., 2014a].

2.5 In vivo experiments

Six- to 8-week-old FVB mice (Charles River, Calco, Italy) were maintained in laminar-flow rooms at constant temperature and humidity, with food and water given *ad libitum*. Experimental protocols used for animal studies were approved by the Ethics Committee for Animal Experimentation (OPBA) of Fondazione IRCCS Istituto Nazionale dei tumori of Milan in accordance with institutional guidelines. FVB mice were injected into the mammary fat pad with $1x10^6$ MI6 cells, a murine mammary breast carcinoma cell line derived from transgenic mice overexpressing the human d16HER2 isoform [Castagnoli et al., 2014].

To study the intratumour modulation of MHC-II, 5 mg/kg trastuzumab per mouse were administered intraperitoneally twice a week starting when tumours reached a median volume of 150 mm^3. Tumours were collected and analysed 1 week after the treatment start. To study the role of CCL2 in modulating the immune microenvironment, CCL2 blocking antibodies (InVivoMab, Bio X Cell, West Lebanon, NH, USA) were administered (200 μg/mouse) intraperitoneally when tumours reached a median volume of 100 mm^3 every two days. Tumours were collected from mice after 7 treatments. Single-cell suspensions were obtained from tumours after incubation for 1 h at 37 °C with 1 ml containing 300 units collagenase and 100 units hyaluronidase (StemCell Technologies, Grenoble, France) and cells analysed by flow cytometry.

2.6 Statistical analyses

Analyses were performed using GraphPad Prism 5 (GraphPad Software). Differences between groups were determined by two-tailed Student's *t*-test. Association among categorical variables was tested by Fisher's exact test. Two-sided $p < 0.05$ was considered statistically significant.

Survival functions were assessed using the Kaplan-Meier estimator, while log-rank test was used to compare survival distributions; DFS was defined as the time from start of trastuzumab treatment to the first event of local, regional or distant recurrence. Survival analysis was carried out using Cox proportional hazard regression models, and the effects of explanatory variables on event hazard were quantified as hazard ratios (HR) [Cox and Oakes, 1984].

CHAPTER 3: RESULTS

3.1 Identification of tissue markers to predict benefit from trastuzumab treatment

3.1.1 Identification of HER2-positive BC subtypes by unsupervised consensus clustering

To test whether whole transcriptome expression profiling of HER2-positive BCs can identify clinically significant subgroups of patients treated with adjuvant trastuzumab, we analysed the GEP of 53 tumours of the recently published multicenter Italian observational study GHEA cohort [Campiglio et al., 2013], which includes 243 HER2-positive BC patients treated with adjuvant chemotherapy plus trastuzumab between 2005 and 2009 in our Institute. Of all 32 relapsed tumours within the 4-year follow-up, 23 samples with good quality RNA were selected for this study and matched 1:1 (16 tumours) and 1:2 (7 tumours) with non-relapsed tumours for patient age, ER, lymph node involvement and tumour size (see Table 8 M&M) and analysed by whole transcriptome expression profile using an Illumina platform.

Putative subsets of patients within our cohort were identified by subtype tumour classification. Unsupervised clustering of gene expression data using the consensus clustering method identified four stable clusters with an average silhouette of 0.83 (Fig. 19). Due to the small sample size of cluster IV, the three samples of this cluster were excluded from subsequent subtyping analyses. Clinico-pathological characteristics of tumours in the three subsets, herein named HER2-I, HER2-II and HER2-III, were similar (Fig. 20A). Remarkably, the HER2-III subgroup, despite no differences in clinically evaluated HER2 and ER expression when compared with the other subgroups, presented significantly lower *ESR1* and higher *ERBB2* mRNA levels (Fig. 20B) and was associated with better DFS upon trastuzumab treatment than HER2-I and HER2-II tumours (Fig 20C).

Indeed, these latter tumours considered jointly presented a significantly higher risk of relapse (HR=14.3, 95% CI = 6.2-35.7, p=0.0001) than HER2-III carcinomas.

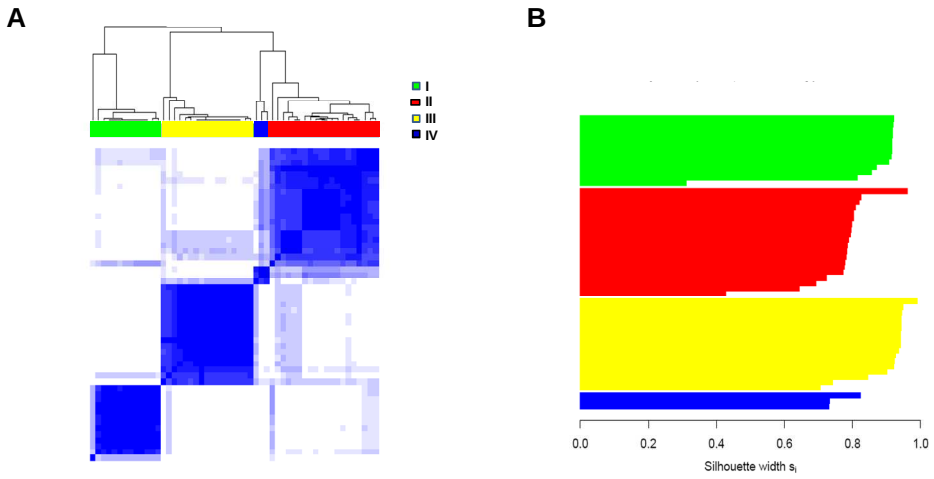

Figure 19. Cluster stability analyses
A) Colour-coded heat maps corresponding to consensus matrices M(^{4}). **B)** Cluster membership evaluated by silhouette widths.

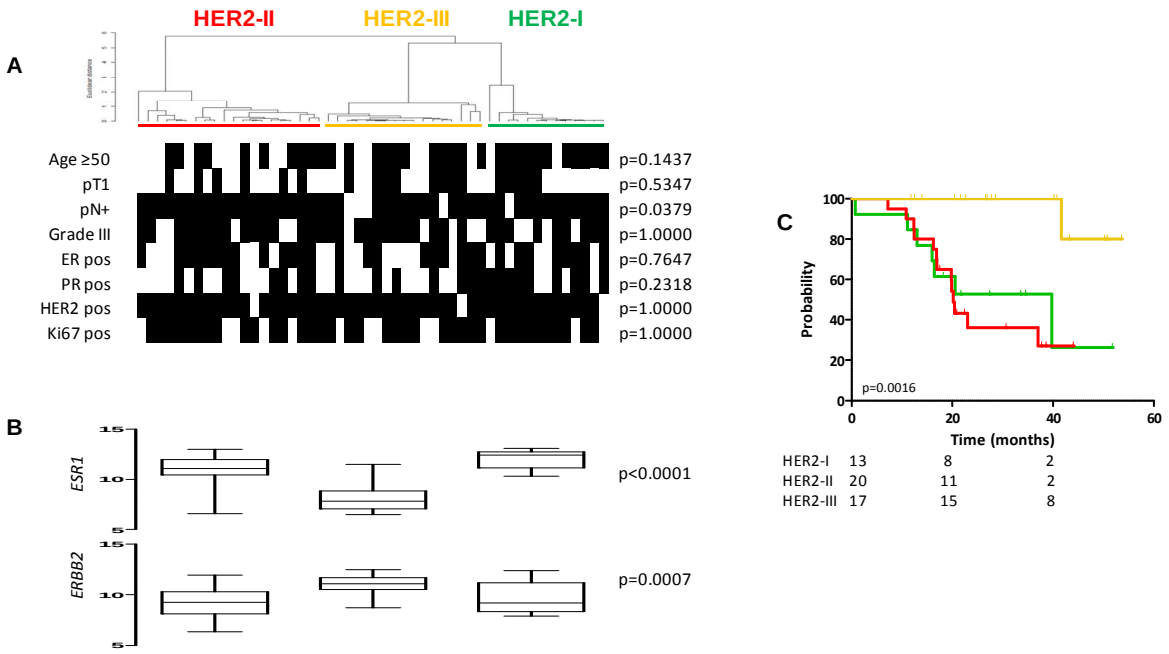

Figure 20. HER2-positive BC subtypes according to gene expression profile
A) Partition of tumours according to unsupervised consensus clustering. Clinico-pathological characteristics are shown. pN, lymph node; ER, estrogen receptor; PR, progesterone receptor. p-values by Fisher's exact test. **B)** *ERBB2* and *ESR1* expression according to partition. p-values by one-way ANOVA. **C)** DFS of tumours according to clustering partition. p-value by log-rank test.

Gene set enrichment analysis according to cluster partition revealed several gene sets that were differentially enriched in the different subgroups: tumours in the HER2-I subgroup showed up-regulation of the intrinsic luminal gene set; those in HER2-II were enriched for genes involved in metabolism (fatty acid metabolism, glycolysis and gluconeogenesis) and estrogen receptor signaling; and HER2-III was mainly characterised by overexpression of immune system-related genes (T and B cell activation, NK cell, Toll-like receptor signaling, IFN and tumour necrosis factor, and cytokines/chemokines) (Table 13). To validate our HER2 subtypes in other datasets of HER2-positive BCs, we developed a prediction algorithm based on PAM able to classify patients into these three clusters. Entry of 120 genes into the model yielded a cross-validation miss-classification rate of 2%. Figure 21A shows the heat map of the classifier genes, providing evidence that each subtype has a distinct expression pattern. Application of this subtype classifier to the Metabric [Curtis et al., 2012] and GSE41656 [de Ronde et al., 2013] datasets confirmed a good molecular correspondence ($p<0.05$) of our classification in these two external datasets (Fig. 21B and 21C, respectively) and the subpartition of HER2-positive BCs in these clusters.

Table 13. Pathways enriched in HER2 subtypes by GSEA analysis according to cluster partition

Pathway	ES	p-value	FDR
HER2-I			
PEROU INTRINSIC LUMINAL	0.69	<0.001	<0.001
HER2-II			
FATTY ACID METABOLISM_MSIGDB	0.47	<0.001	0.068
PEROU INTRINSIC BASAL	0.52	0.002	0.052
GLUCONEOGENESIS_MSIGDB	0.48	0.006	0.059
GLYCOLYSIS_MSIGDB	0.48	0.002	0.051
BC ESTROGEN SIGNALING_MSIGDB	0.42	0.002	0.068
GROWTH FACTOR	0.43	0.005	0.076
HYPOXIA SIGNALING PATHWAY	0.47	0.002	0.072
ELECTRON TRANSPORT_MSIGDB	0.44	0.006	0.079
PHENYLALANINE METABOLISM_MSIGDB	0.56	0.012	0.086
FOCAL ADHESION_KEGG	0.36	<0.001	0.086
GLYCEROLIPID METABOLISM_MSIGDB	0.46	0.015	0.078
HUMAN STEM CELLS 2	0.37	0.002	0.075
NOTCH SIGNALING PATHWAY	0.37	0.007	0.092
ELECTRON TRANSPORTER ACTIVITY_MSIGDB	0.37	0.009	0.088
HER2-III			
T-CELL AND B-CELL ACTIVATION	0.79	<0.001	<0.001
LYMPHOID CELLS	0.73	<0.001	<0.001
INFLAMMATION	0.67	<0.001	<0.001
INFLAMMATORY CYTOKINES & RECEPTORS	0.71	<0.001	<0.001
CHEMOKINE LIGAND RECEPTOR	0.68	<0.001	<0.001
NK CELL MEDIATED CYTOTOXICITY_KEGG	0.64	<0.001	<0.001
TH1-TH2-TH3	0.72	<0.001	<0.001
TCR SIGNALING PATHWAY_KEGG	0.64	<0.001	<0.001
ANTIGEN PROCESSING AND PRESENTATION_KEGG	0.69	<0.001	<0.001
CELL ADHESION MOLECULES (CAMS)_KEGG	0.61	<0.001	<0.001
INTERFERON	0.65	<0.001	<0.001
IMMUNE FUNCTION_MSIGDB	0.66	<0.001	<0.001
NK CELLS	0.68	<0.001	<0.001
CELL ADHESION_MSIGDB	0.58	<0.001	<0.001
TOLL-LIKE RECEPTOR SIGNALING PATHWAY_KEGG	0.56	<0.001	0.001
INFLAMMATORY RESPONSE PATHWAY_MSIGDB	0.68	<0.001	0.002
HUMAN STEM CELLS 3	0.64	<0.001	0.002
CELL SURFACE RECEPTOR SIGNAL TRANSDUCTION_MSIGDB	0.49	<0.001	0.002
TUMOUR NECROSIS FACTOR	0.53	<0.001	0.003
INTERLEUKINS AND RECEPTORS	0.57	<0.001	0.005
JAK-STAT SIGNALING PATHWAY	0.44	<0.001	0.012
TNF LIGANDS&RECEPTORS	0.58	0.017	0.031
G-PROTEIN COUPLED RECEPTOR II	0.46	0.004	0.043
NGLYCAN BIOSYNTHESIS_MSIGDB	0.57	0.034	0.045
STRESS GENOTOXIC SPECIFIC DN_MSIGDB	0.48	0.020	0.071
PEROU INTRINSIC BASAL	0.48	0.024	0.081
NFKB SIGNALING PATHWAY	0.39	0.010	0.081
CELL ADHESION MOLECULE ACTIVITY_MSIGDB	0.40	0.011	0.094

ES: enrichment score, FDR: false discovery rate

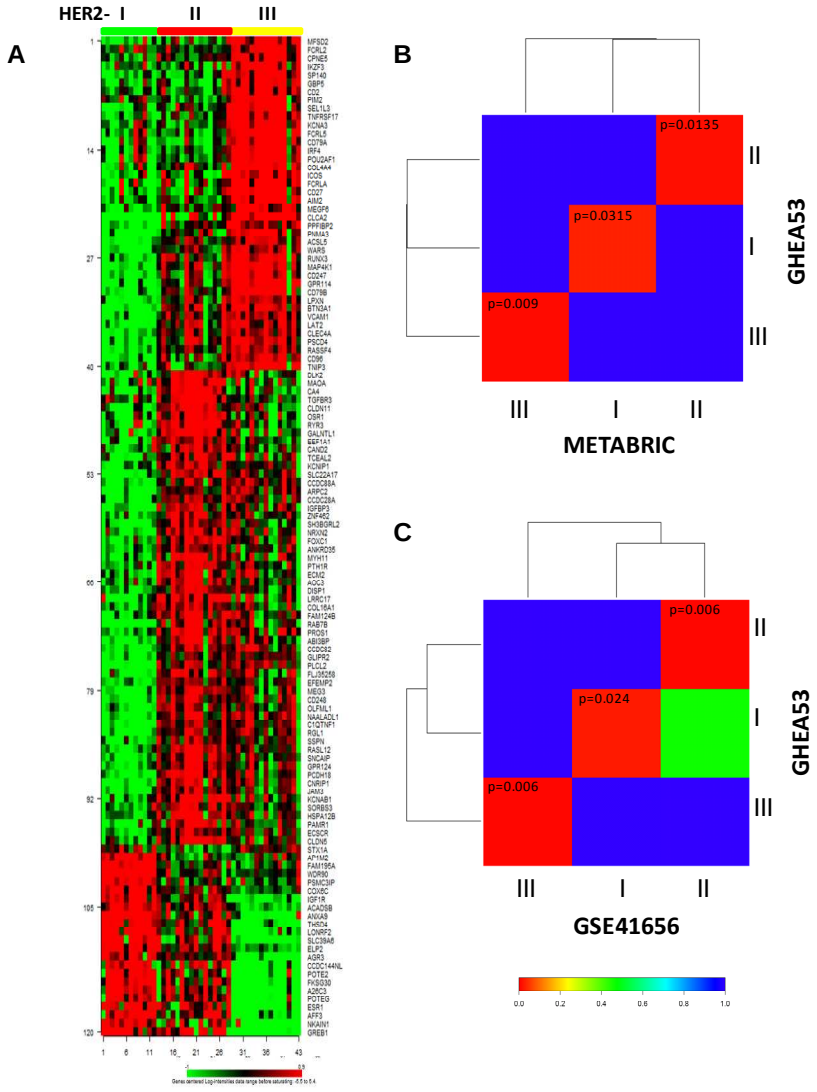

Figure 21. Molecular characteristics of BCs according to cluster partition
A) Expression profile of consensus clustering genes in BC according to cluster classification in the GHEA cohort. **B)** Cluster correlation plots between Metabric or **C)** GSE41656 and GHEA cohorts (HER2-I, HER2-II, HER2-III). Bonferroni-corrected p-values are reported.

3.1.2 TRAR model

Once ascertained the heterogeneity of HER2-positive BCs and its relation to patients' prognosis upon trastuzumab treatment, we aimed at creating an algoritm to stratify patients according to their benefit from trastuzumab treatment. A Cox's proportional hazard model was used to estimate the association between gene expression and DFS, and a multivariate permutation test was used to check the proportion of false discovery. 330 probes corresponding to 308 unique genes were significantly associated to DFS

(α<0.005; permutation test p<0.01). Using a semi-supervised principal component method [Bair and Tibshirani, 2004] by fitting Cox proportional hazard models we developed the TRAR model based on the expression of 41 genes (Table 14 and Fig. 22A).

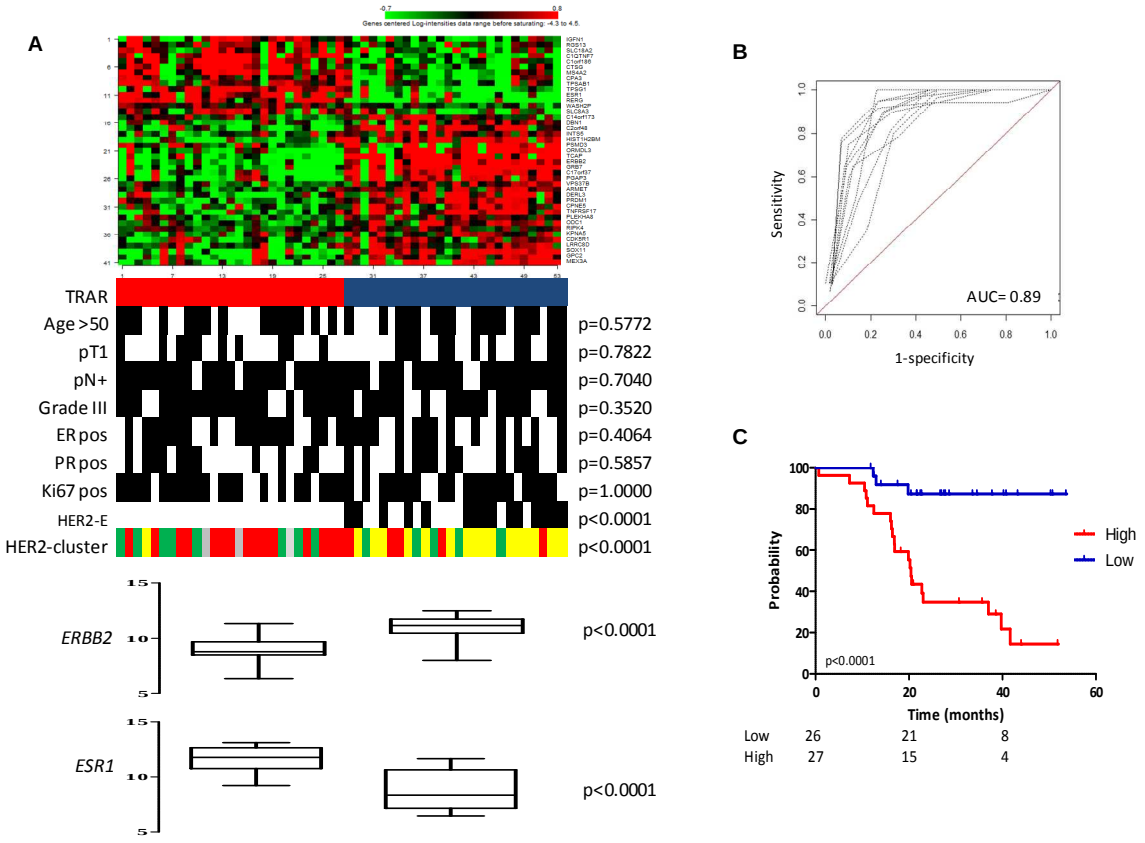

Figure 22. Development of TRAR model

A) Heatmap of 41-gene model expression and TRAR classification (red: TRAR-high; blue: TRAR-low). Clinico-pathological characteristics are shown. pN, ; ER, estrogen receptor; PR, progesterone receptor; HER2-E: HER2-enriched by PAM50 classification; HER2 cluster: HER2-I (green), HER2-II (red), HER2-III (yellow), HER2-IV (grey). p-values by Fisher's exact test. Lower panel: *ERBB2* and *ESR1* expression according to TRAR classes. p-values by one-way ANOVA. **B)** Performance of the classifier. ROC curves were based on TRAR-high and TRAR-low classes computed using the 41-gene model on 10-fold cross-validation. AUC: Area Under the ROC Curve. **C)** Association between TRAR-high (red) and -low (blue) patients with DFS. p-value by log-rank test. Modified from [Triulzi et al., 2015]

Table 14. List of 41 genes of the TRAR model. Adopted from [Triulzi et al., 2015]

Gene Symbol	Gene name
C14orf173	chromosome 14 open reading frame 173
C17orf37	chromosome 17 open reading frame 37
C1orf186*	chromosome 1 open reading frame 186
C1QTNF7	C1q and tumour necrosis factor related protein 7
C2orf48	chromosome 2 open reading frame 48
CDK5R1	cyclin-dependent kinase 5, regulatory subunit 1 (p35)
CPA3	carboxypeptidase A3 (mast cell)
CPNE5	copine V
CTSG	cathepsin G
DBN1	drebrin 1
DERL3	derlin 3
ERBB2*	v-erb-b2 erythroblastic leukemia viral oncogene homolog 2
ESR1*	estrogen receptor 1
GPC2*	glypican 2
GRB7*	growth factor receptor-bound protein 7
HIST1H2BM	histone cluster 1, H2bm
IGFN1	immunoglobulin-like and fibronectin type III domain containing 1
INTS5	integrator complex subunit 5
KPNA5	karyopherin alpha 5 (importin alpha 6)
LRRC8D	leucine rich repeat containing 8 family, member D
MANF	mesencephalic astrocyte-derived neurotrophic factor
MEX3A	mex-3 homolog A (C. elegans)
MS4A2	membrane-spanning 4-domains, subfamily A, member 2
ODC1*	ornithine decarboxylase 1
ORMDL3*	ORM1-like 3 (S. cerevisiae)
PGAP3	post-GPI attachment to proteins 3
PLEKHA8	pleckstrin homology domain containing, family A member 8
PRDM1	PR domain containing 1, with ZNF domain
PSMD3	proteasome 26S subunit, non-ATPase, 3
RERG*	RAS-like, estrogen-regulated, growth inhibitor
RGS13	regulator of G-protein signaling 13
RIPK4	receptor-interacting serine-threonine kinase 4
SLC18A2	solute carrier family 18 (vesicular monoamine), member 2
SLC8A3	solute carrier family 8 (sodium/calcium exchanger), member 3
SOX11	SRY (sex determining region Y)-box 11
TCAP	titin-cap (telethonin)
TNFRSF17	tumour necrosis factor receptor superfamily, member 17
TPSAB1	tryptase alpha/beta 1
TPSG1	tryptase gamma 1
VPS37B*	vacuolar protein sorting 37 homolog B (S. cerevisiae)
WASH2P	WAS protein family homolog 2 pseudogene

***TRAR core element

Based on a threshold defined by a 10-fold cross-validation method [De Cecco et al., 2014], samples were grouped as high (TRAR-high, n=27) or low (TRAR-low, n=26) risk of early relapse, as confirmed by survival analysis revealing an 8-fold higher risk of relapse in the high- versus low-risk group in this selected cohort (HR=8.0, 95% CI=3.5-18.2, p=0.0001, Fig. 22C). The classification was independent of clinico-pathological characteristics, with 16 out of 17 HER2-III tumours belonging to the TRAR-low group (Fig 22A). Evaluation of the in-sample prediction performance using time-dependent ROC curves showed that the average AUC over 10-fold cross-validation reached a value of 0.89 with an acceptable standard deviation (+/- 0.05) (Fig 22B), confirming the good performance of our model. During model permutation 9 genes of the 41 persisted in the model representing a core element of TRAR (Table 14). Six of these genes were associated with HER2 (*ERBB2*, *GRB7*, *ORMDL3)* or ER (*C1orf186*, *ESR1*, *RERG*). *ERBB2* and HER2-related genes were more highly expressed in TRAR-low than in TRAR-high patients, whereas the opposite was found for *ESR1* and ER-associated genes (Fig. 22A).

3.1.3 Comparison of TRAR to PAM50 classification

Based on the evident relevance of *ERBB2* and *ESR1* mRNA levels in discriminating TRAR-high and TRAR-low patients, we applied to GHEA dataset the PAM50 subtype predictor, which identifies the HER2-E subtype as the tumour group most responsive to trastuzumab [Prat et al., 2014a]. Kaplan-Meier analysis confirmed that in our cohort patients with HER2-E tumours had the best prognosis upon trastuzumab treatment compared to tumours belonging to the other subgroups together (*p*=0.0020, Fig. 23A). The PAM50 classification was significantly associated with TRAR (p<0.0001): all of HER2-E tumours were classified as TRAR-low, and 70% luminal A+B tumours as TRAR-high (Table 15). Note that not all TRAR-low tumours were classified as HER2-E (Fig. 22A and Table 15).

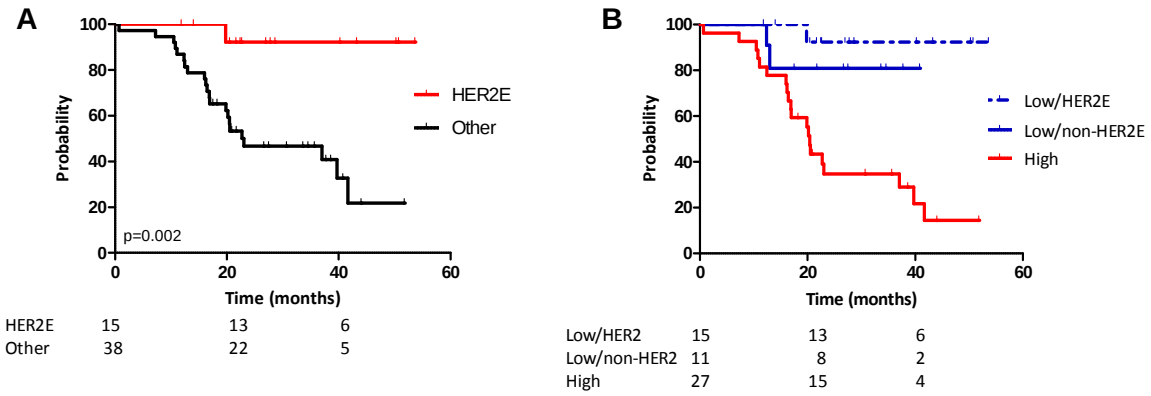

Figure 23. Prognostic value of PAM50 subtypes in the GHEA cohort
A) Association between HER2-E subtype (red) and other intrinsic subtypes (basal-like, luminal A and B, normal-like: black) with DFS in the GHEA dataset. p-value by log-rank test. **B)** Association between TRAR-high (red) and -low (HER2-E: blue; non-HER2-E dotted blue) patients with DFS. Modified from [Triulzi et al., 2015].

Table 15. Association between PAM50 and TRAR classifications

	HER2-E		Lum A		Lum B		Basal-like		Normal-like		
	N	**%**	**N**	**%**	**N**	**%**	**N**	**%**	**N**	**%**	**Ŧp-value**
Number of patients	15	-	9	-	14	-	4	-	11	-	
Age (mean±SD)	53±10		54±4		58±7		45±8		45±11		0.2220
Histologic grade											
II	4	27	3	33	3	21	2	50	2	18	0.7785
III	11	73	6	67	11	79	2	50	9	82	
Estrogen receptor											
positive	6	40	6	67	12	86	2	50	6	55	0.1252
negative	9	60	3	33	2	14	2	50	5	45	
TRAR											
high	0	0	8	89	8	57	2	50	9	82	<0.0001
low	15	100	1	11	6	43	2	50	2	18	

Ŧ p-value is calculated by Fisher exact test.

Since multivariate analysis is not applicable because of the co-linearity of the two variables, to compare the performance of the two signatures we applied Kaplan-Meier analysis separating TRAR-low tumours into HER2-E and non-HER2-E. The stratification indicated that both had similar recurrence probability and a significantly lower recurrence probability than TRAR-high tumours (TRAR-low/non-HER2-E vs TRAR-high: p=0.0312, TRAR-low/HER2-E vs TRAR-high: p=0.0003, Fig. 23B).

3.1.4 Prognostic significance of TRAR model

To test whether the TRAR model identifies patients with intrinsic poor prognosis independent of trastuzumab treatment, we analysed 132 HER2-positive BCs of the Metabric dataset treated with adjuvant chemotherapy alone. TRAR-high tumours did not show worse prognosis than TRAR-low tumours, but instead a borderline statistical significance toward better prognosis for TRAR-high versus TRAR-low tumours was found (HR=0.64; 95% CI: 0.38-1.08, p=0.0986; Fig. 24A). Notably, analysis of TRAR-low tumours partitioned according to PAM50 classifier indicated similar recurrence rates for both HER2-E and non-HER2-E tumours, when treated with chemotherapy alone (Fig. 24B). These results strongly suggested that TRAR discriminates HER2-positive BCs based on their benefit from trastuzumab treatment and not from chemotherapy.

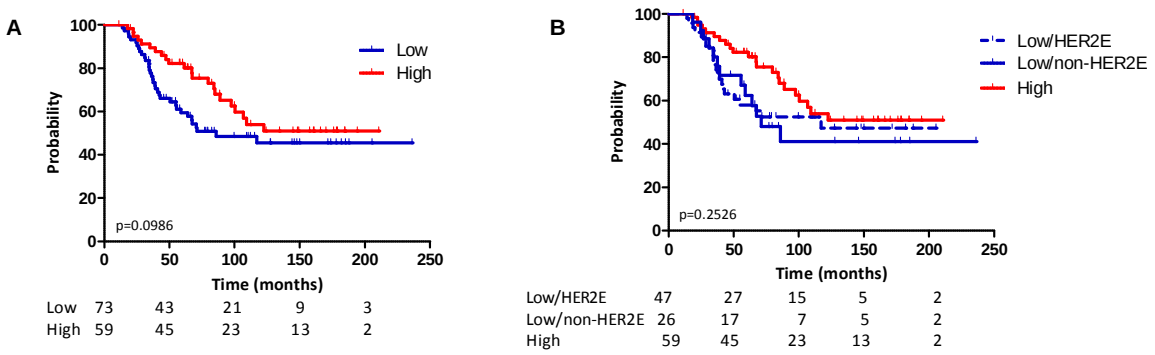

Figure 24. Prognostic significance of TRAR model
A-B) Association between TRAR-high (red) and TRAR-low (blue) (A) or TRAR-low/non-HER2-E (dotted blue) and TRAR-low/HER2-E (blue) (B) with overall survival in HER2-positive tumours of the Metabric dataset. p-values by log-rank test.

In accordance with results of the Metabric dataset, the classification of GHEA tumours by the HDPP, predictive of outcome in patients with HER2-positive tumours treated with chemotherapy alone [Staaf et al., 2010], showed a direct association between TRAR-low and HDPP-poor subsets. Indeed, according to the centroid classification used to determine HDPP class, the TRAR-low subset contained mainly HDPP-poor tumours (69% vs 26% in TRAR-high subset, p=0.0024), which showed a good outcome in our cohort of

trastuzumab-treated patients (HR=0.41, 95% CI: 0.17-0.98, p= 0.0370). Overall, these data indicate that TRAR-low tumours have features of bad prognosis if treated with chemotherapy alone and thus suggest that TRAR model is specific for the benefit from trastuzumab treatment.

3.1.5 Predictive significance of TRAR model

To test the predictive performance of the TRAR classifier in identifying BCs that respond to neo-adjuvant trastuzumab and to compare its performance to PAM50 classification, we performed the GEP of 24 core biopsies obtained from tumours retrieved from the TRUP window-of-opportunity trial [Koukourakis et al., 2014] before any treatment. Patients of this cohort received one cycle of trastuzumab followed by trastuzumab and docetaxel in neoadjuvant setting. Application of TRAR to this dataset showed that patients achieving a pCR to trastuzumab-based chemotherapy had significantly lower predictive indices than those with a residual disease (RD) (Fig. 25A). The TRAR classifier had good performance in identifying responders (AUC= 0.85, 95% CI: 0.69–1.00, p= 0.0133, Fig. 25B). When the cut-off obtained in the GHEA cohort was applied, TRAR classification was significantly associated with response (CR, p=0.0137) but not with other clinico-pathological characteristics (Fig. 25C). Also in this cohort of patients, TRAR correlated with PAM50 classification (Fig. 25C) and identified the 2 pCR with perfect accuracy in non-HER2-E tumours (p=0.0273), indicating its predictive superiority. Moreover, patients of the TRUP cohort that respond to one cycle of trastuzumab alone (i.e. with a reduction in the clinical volume) showed a trend toward lower predictive indices (p=0.0838) than those who progressed upon trastuzumab treatment (Fig. 25D) suggesting that TRAR-low tumours could forego chemotherapy treatment.

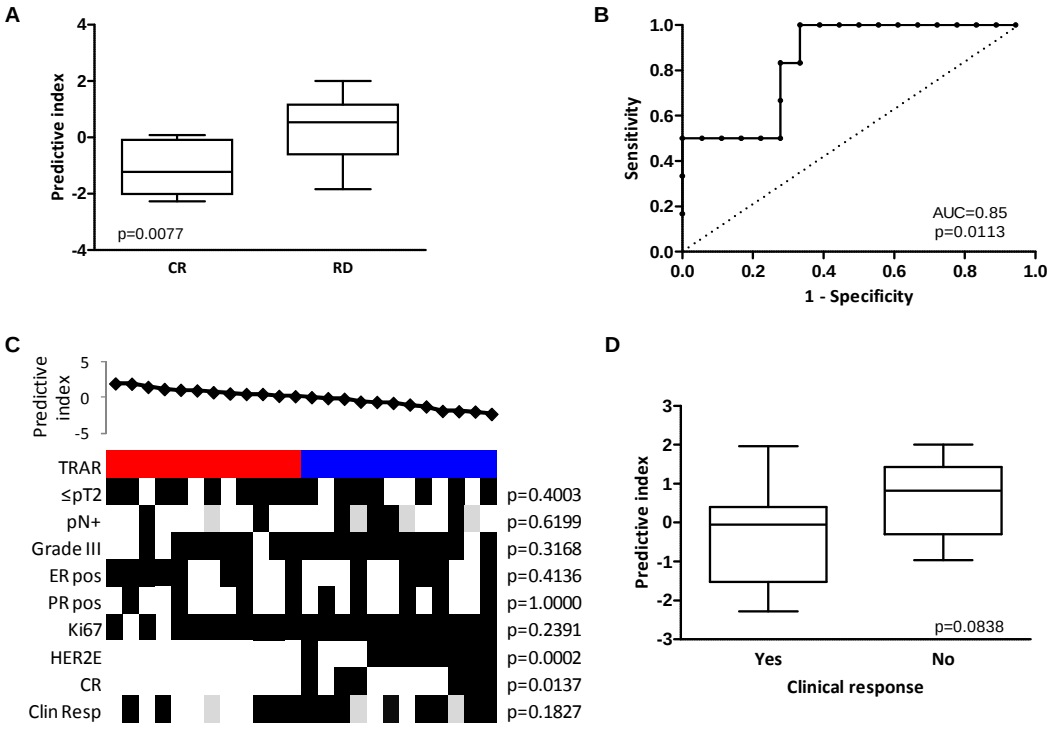

Figure 25. Predictive performance of TRAR model in a neoadjuvant treated cohort
A) Association between TRAR predictive indices and response to trastuzumab neo-adjuvant therapy in HER2-positive BCs of the TRUP cohort. CR: complete response, RD: residual disease. p-value by unpaired t-test. **B)** ROC curve of response prediction for the TRAR model. AUC: Area under the ROC curve. **C)** Association between TRAR predictive indices and clinico-pathological characteristics. TRAR classification (red: TRAR-high; blue: TRAR-low); pN: lymph node; ER: estrogen receptor; PR: progesterone receptor; HER2-E: HER2-enriched by PAM50 classification; CR: pathological complete response. Clin Resp: clinical response as described in (D). Grey boxes indicate missing data. p-values by Fisher's exact test. **D)** Association between TRAR predictive indices and clinical response to one cycle of trastuzumab alone. Tumours were considered responsive (Yes) when clinical dimensions were smaller after treatment than before and non-responsive (No) when the opposite occurred. p-value by unpaired t-test. Adopted from [Triulzi et al., 2015].

To validate the predictive performance of the classifier in identifying BCs that respond to neo-adjuvant trastuzumab, we applied TRAR to the only two available public datasets, GSE22358 and GSE50948. Patients achieving a complete response to trastuzumab-based chemotherapy showed significantly lower TRAR indices than those with residual disease (p=0.0057 and p=0.0126, respectively; Fig. 26). In both datasets, the classifier showed good performance in identifying responsive patients (GSE22358: AUC=0.81, 95% CI: 0.63–0.99, p=0.0057; GSE50948: AUC=0.66, 95% CI: 0.53-0.78, p=0.0180). Again, the TRAR and PAM50 classifications were associated, with a significantly lower expression of the TRAR

predictive indices in HER2-E than non-HER2-E tumours (Fig. 27). Moreover, TRAR also showed fair ability (even if not statistically significant) in identifying responsive tumours classified as non-HER2-E by PAM50 in these two datasets (GSE22358: AUC=0.73, 95% CI: 0.34-1.00, *p*=0.1918; GSE50948: AUC=0.71, 95% CI: 0.49-0.93, *p*=0.0591). In contrast, the TRAR predictive indices of HER2-positive BCs that respond or do not respond to neo-adjuvant chemotherapy alone did not differ significantly in the GSE50948 and GSE41656 datasets (Fig. 28), supporting its predictive power in trastuzumab treated patients.

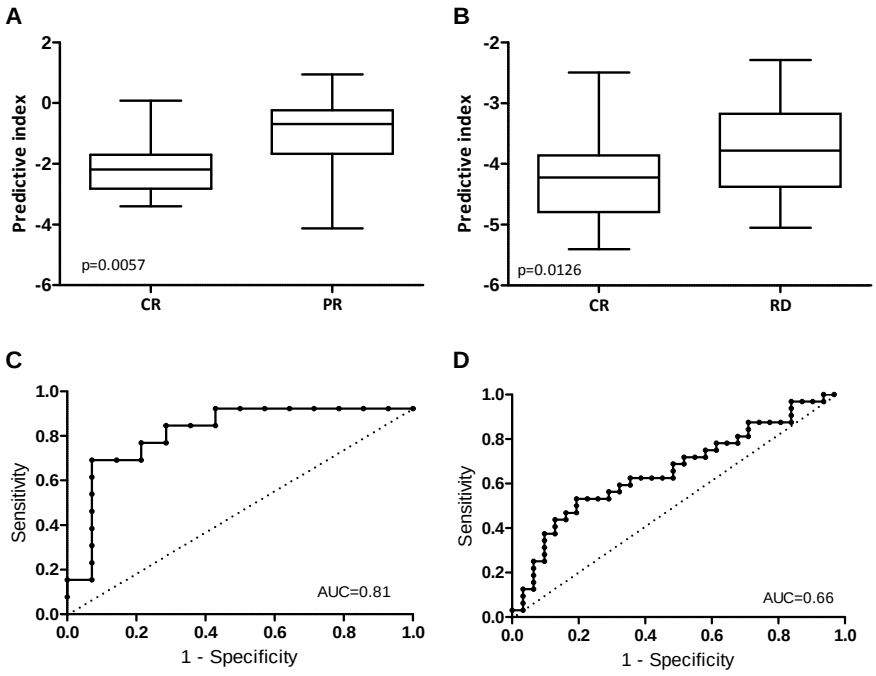

Figure 26. Validation of TRAR predictive significance in independent datasets
A,B) Association between TRAR indices and response to trastuzumab neo-adjuvant therapy in HER2-positive BCs of the GSE22358 (A) and GSE50948 (B) datasets. CR: complete or near to complete response, PR: partial response, RD: residual disease. p-values by unpaired t-test. **C,D)** ROC curve of response prediction for the TRAR model in GSE22358 (C) and GSE50948 (D) datasets. AUC: Area under the ROC curve. Adopted from [Triulzi et al., 2015].

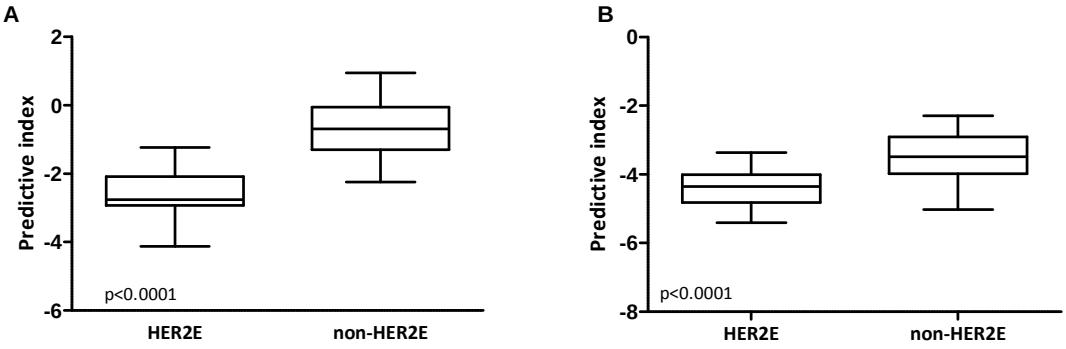

Figure 27. Association between TRAR and PAM50 in independent datasets
A,B) TRAR predictive indices of tumours classified as HER2-E and non-HER2-E in GSE22358 (A) and GSE41656 (B) datasets. p-values by unpaired t-test. Adopted from [Triulzi et al., 2015].

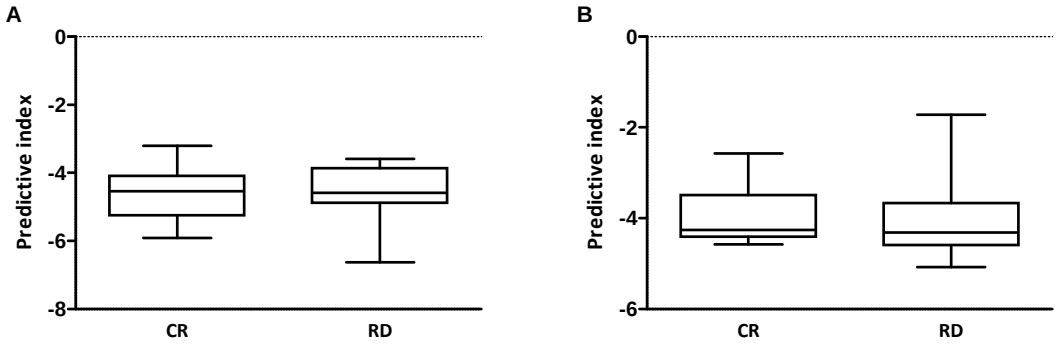

Figure 28. TRAR predictive performance in chemotherapy treated patients
A,B) Association between TRAR indices and response to neo-adjuvant chemotherapy alone in HER2-positive BCs of the GSE50948 (C) and GSE41656 (D) datasets. Adopted from [Triulzi et al., 2015].

To deeply analyse the ability of TRAR to identify patients who benefit from the addition of trastuzumab to chemotherapy we compared the areas under the ROC curves of TRAR in the chemotherapy and trastuzumab arms of the GSE50948 dataset, containing information from patients of the NOAH trial [Prat et al., 2014a]. As shown in Table 16 TRAR had a significantly (p=0.0363) higher performance in predicting response in the trastuzumab arm than in the chemotherapy arm, indicating that our model exhibits a different predictive value according to the addition of trastuzumab to chemotherapy.

Table 16. TRAR predictive performance in the two arms of the GSE50948 dataset

Arm	N°	AUC	SE	95% CI	
Chemotherapy	51	0.4352	0.0846	0.26935	0.60110
Trastuzumab	63	0.6643	0.0694	0.52829	0.80034
Ho: area (0) = area(1)		chi2(1)=4.38	p=0.0363		

3.1.6 Development of n-Counter assay for TRAR evaluation

In order to develop an assay that calculates TRAR indices without performing whole genome expression analysis of tumours and usable in clinical setting, we approached Nanostring nCounter technology which delivers direct, multiplexed measurements of gene expression through digital readouts of the abundance of mRNA transcripts. We simultaneously measured the expression levels of 33 out of 41 TRAR genes and of 15 endogenous control (housekeeping) genes in a single hybridization reaction using an nCounter CodeSet. Each assay also included 6 positive and 8 negative quality controls for normalization purposes. The housekeeping gene list contained 4 genes (*ACTB*, *GUSB*, *LDHA* and *TUBB*) from the nCounter Human Reference Panel gene list and 11 genes selected according to their expression in the GHEA dataset. In details, we selected genes with low variability among samples [i.e. with interquartile range (IQR) belonging to the the lowest quartile of the IQR distribution of all genes] and with expression comparable to high (*DDT*, *LCAT*, *NONO* and *RPL13A*), intermediate (*ARL6IP6*, *TAF6*, *TBC1D25* and *TUG1*) and low (*PPIH*, *TOB2* and *USP43*) expressing genes.

Due to RNA availability, 46 out of 53 samples of the GHEA cohort were profiled and 42 cases passed the quality check. Expression of TRAR genes was independently normalised to the geometric mean of the housekeeping genes in each sample and then the TRAR scores were calculated. As shown in Figure 29, resulting TRAR scores were highly correlated with those originally evaluated by whole GEP, supporting this technology as a possible tool to compute this predictive score.

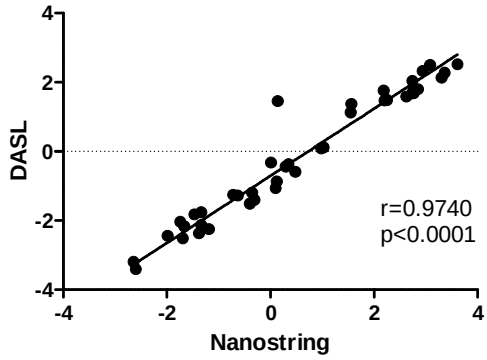

Figure 29. Correlation between TRAR score as evaluated by DASL and Nanostring technologies
Pearson's coefficient (r) and relative p-value are shown

All these data together indicated that HER2-positive tumours are quite heterogeneous from a biological point of view and such heterogeneity contains information about trastuzumab efficacy. Indeed, patients with HER2-III tumours have bad prognosis if treated with chemotherapy alone but are those that benefit the most from trastuzumab treatment. TRAR model identifies these tumours with good performance, even better than PAM50 classifier. Validation of its predictiveness in a new cohort of HER2-positive BCs and the identification of a cut-off for the n-Counter assay to identify TRAR-low tumours are the next steps in the evaluation of its clinical utility.

3.2. Identification of circulating markers to predict benefit from trastuzumab treatment.

3.2.1 NKG2D expression on NK cells and its correlation with trastuzumab response

To find a possible circulating predictive biomarker of trastuzumab response, we investigated the phenotype of circulating NK cell in patients (Neo-INT cohort) with HER2-positive BCs before neoadjuvant chemotherapy and trastuzumab in correlation with response to treatment. We focused on NK cells on the basis of their relevant role in inducing trastuzumab-mediated ADCC, a described mechanism of trastuzumab cytotoxic action when administered as monotherapy in clinical samples [Gennari et al., 2004;Varchetta et al., 2007;Beano et al., 2008]. Two out of 9 patients of the analysed cohort reached the pCR and *ERBB2* expression analysis in the tumour core biopsies supported their addiction to the HER2 oncogene. Indeed these tumours had the highest *ERBB2* expression levels (p=0.0297, Fig. 30A). Flow cytometry analysis of the NK proportion and phenotype in PBMCs obtained from patients cohort showed that the expression of NKG2D receptor on NK cells, and not of other natural cytotoxicity receptors involved in human NK activity (i.e., NKp30, NKp44 and NKp46), was associated with response to trastuzumab treatment. Indeed, the two patients that reached the pCR were those with the highest NKG2D expression (p=0.0142, Fig. 30B).

These data were confirmed in 18 samples of the TRUP cohort. In fact, analysis by qRT-PCR using RNA obtained from the buffy-coat of collected blood confirmed association between HER2-addiction and circulating NKG2D expression: HER2-E as well as TRAR-low tumours (data not shown) expressed significantly higher levels of circulating NKG2D (Fig. 30C). Moreover, we confirmed with borderline statistical significance that patients who

reached a pCR after neoadjuvant treatment with trastuzumab-based chemotherapy had higher basal NKG2D expression on circulating NK cells than partial responders did (Fig. 30D, p=0.0806).

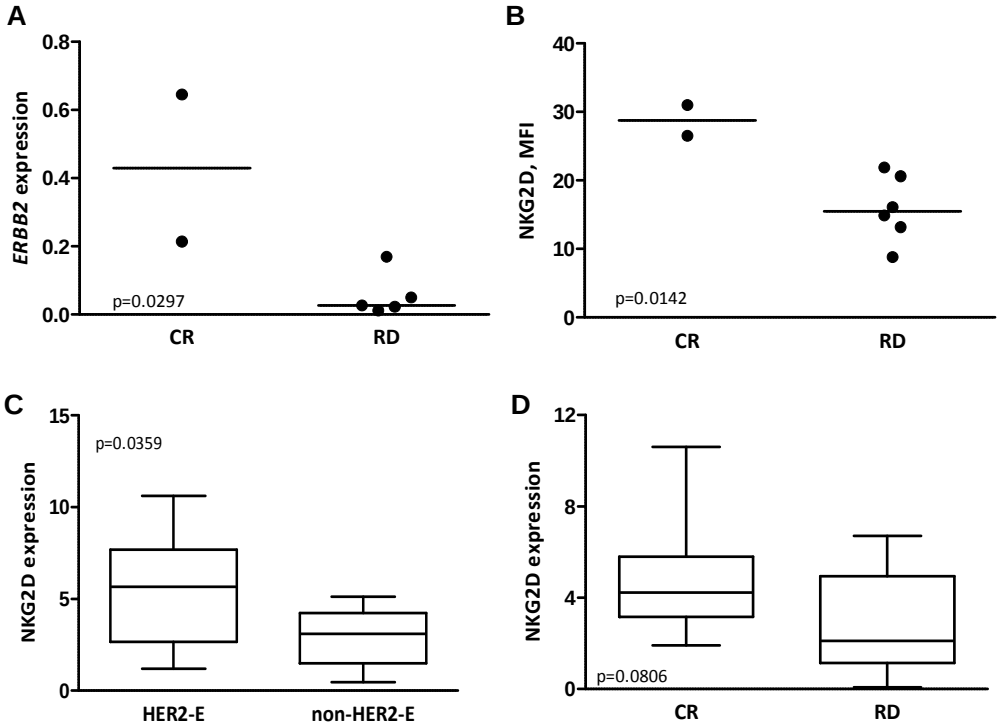

Figure 30. NKG2D expression on circulating NK cells and response to trastuzumab
A) *ERBB2* expression as evaluated by qRT-PCR using RNA obtained from BC core-biopsies of the Neo-INT cohort. *GAPDH* was used as reference. **B)** NKG2D median expression on NK cells (CD3-CD56+) from HER2-positive BC patients (Neo-INT cohort), as evaluated by flow-cytometry. **C-D)** NKG2D expression as evaluated by qRT-PCR on RNA obtained from the blood buffy-coat of 18 HER2-positive BC patients of the TRUP cohort before any treatment according to PAM50 classification (C) and response to treatment (D). CR: complete response; RD: residual disease. p-values by unpaired t-test. Modified from [Di Modica et al., 2016].

3.2.2 Modulation of NK receptors by chemotherapy

Since trastuzumab is used in the clinical setting in combination with chemotherapy, we evaluated the effect of chemotherapy on the expression of NKG2D exploiting the collection of PBMCs from patients of the Neo-INT cohort after treatment with 4 cycles of taxane-based chemotherapy before receiving trastuzumab based therapy. Analysis of NK cell phenotype before (pre) and after (post) the first treatment cycle showed that chemotherapy significantly increased NKG2D expression on NK cells (Fig. 31A) even if it

slightly impaired NK cell proportions (Fig. 31B), in particular CD16+ NK cells (Fig. 31C). On the contrary, other natural cytotoxicity receptors involved in human NK activity (i.e., NKp30, NKp44 and NKp46) were not modified by treatment. These data indicate that chemotherapy can modify NK phenotype/activity and thus trastuzumab activity.

Then we investigated whether NKG2D expression is associated with NK cell function by using PBMCs obtained from healthy donors treated with plasma obtained from patients, because we found that these plasma are able to recapitulate NKG2D expression on NK cells obtained from healthy donors. Indeed, accordingly to NKG2D expression in patients before and after treatment with chemotherapy, NK cells treated with post-treatment plasma expressed higher levels of this receptor than those treated with plasma collected before treatment (Fig. 31D).

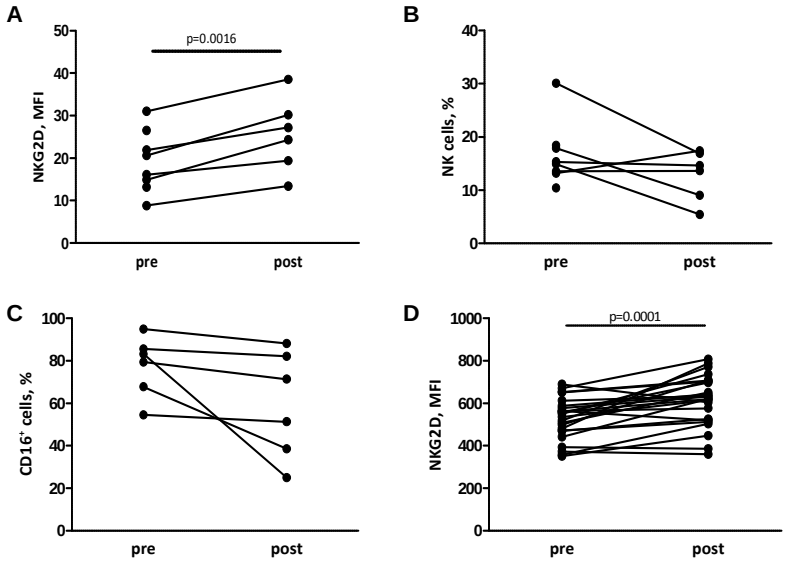

Figure 31. NKG2D expression modulation by chemotherapy
A-C) NKG2D expression (A), the percentage of NK cells, identified as CD3- CD56+ (B),and their proportion of CD16+ (C) as analysed by flow cytometry before (pre) any treatment and after the first chemotherapy cycle (post). **D)** NKG2D expression on NK cells (CD3-, CD56+, CD16+) of PBMC from independent healthy donors treated *in vitro* with pre- and post-treatment plasma derived from patients. p-values by paired t-test. Adopted from [Di Modica et al., 2016]

We observed that treatment of PBMCs from donors with pre-treatment plasma from different patients (P1-P5) modulate their ADCC ability (Fig. 32A), and the mean cytotoxic

activity of the effector cells correlated with NKG2D expression on NK cells (r=0.86, p=0.06). These results suggested that NK cells from patients with HER2-addicted tumours (P1) are more prone to make ADCC than others. Interestingly, the lower the PBMC lytic activity induced by pre-treatment plasma, the higher the fold-increase in PBMC ADCC activity induced by post-treatment versus pre-treatment plasma (Fig. 32A). Indeed, treatment of PBMC from healthy donors with post-treatment plasma from patient P1, the one with the highest expression of NKG2D on NK cells and so the highest ADCC activity before treatment, did not induce a significant increase but on the contrary a significant reduction in trastuzumab-mediated ADCC compared to pre-treatment plasma (Fig. 32B). By contrast, post-treatment plasma derived from patient P5 induced an increment in NKG2D expression and consequently in ADCC compared to the corresponding pre-treatment plasma (Fig. 32B), which had the lowest basal ADCC activity (Fig. 32A). These data suggest that the benefit of chemotherapy in improving trastuzumab-mediated ADCC occurs mainly in patients with low basal cytotoxic activity of immune effector cells, and that addition of chemotherapy to antibody administration may not be so relevant in improving trastuzumab activity in patients with elevated basal lytic activity of effector cells. Consistent with this view, NKG2D basal expression in the TRUP cohort before any treatment was higher in tumours that benefitted from one cycle of trastuzumab alone than in non-responsive tumours (p=0.0249, Fig. 32C).

These data, even if based on small cohorts of patients, showed that HER2-addicted tumours have a typical circulating NK profile that is predictive of trastuzumab based-therapy response. Chemotherapy treatment modifies the patients' NK profile, increasing the expression of NKG2D on NK cells and their ability in inducing trastuzumab-mediated ADCC, mainly in those patients with a low basal activity of NK cells. Thus, these data

suggest that patients with HER-addicted tumours, having a high circulating NK basal activation state, could forego chemotherapy treatment.

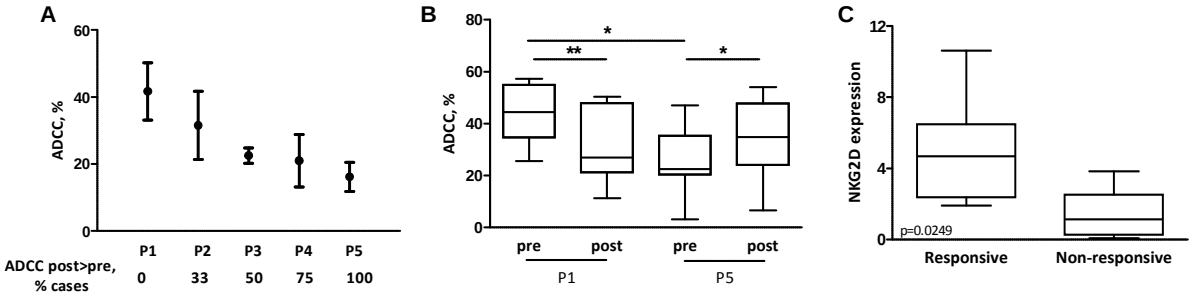

Figure 32. ADCC activity of NK cells according to NKG2D expression

A) Trastuzumab-mediated lysis of ^{51}Cr-labeled BT474 cells induced by healthy donor PBMCs (n=4) treated with plasma obtained from 5 patients (P1-P5) before chemotherapy administration. Data are mean and range. ADCC post>pre refers to the percentage of times that PBMC treated with post-treatment plasma induced greater trastuzumab-mediated ADCC of BT474 cells than when treated with the pre-treatment plasma. **B)** ADCC of BT474 cells induced by PBMC obtained from healthy donors treated with pre- and post-treatment plasma of patients P1 and P5 (n=7). *p<0.05, **p<0.01 by paired t-test. **C)** NKG2D expression, as evaluated by qRT-PCR using RNA obtained from the blood buffy-coat of 18 HER2-positive BC patients of the TRUP cohort before any treatment, according to response to one cycle of trastuzumab alone. p-value by unpaired t-test. Adopted from [Di Modica et al., 2016].

3.3. The response to trastuzumab monotherapy

3.3.1 Tumour biological features associated to trastuzumab cytotoxic and cytostatic activity

Based on above described results showing that TRAR-low tumours and patients with high NKG2D expression on NK cells benefit from one cycle of trastuzumab monotherapy, we exploited the GEP of the TRUP cohort to investigate molecular features associated with trastuzumab activity in the clinical setting. Indeed, trastuzumab mechanisms of action are still not completely clear and what is known today mainly derived from experiments performed *in vitro* and in animal models.

Response to trastuzumab in patients of the TRUP cohort was registered by clinicians as modification in tumour dimensions (response C) induced by trastuzumab treatment. Reduction in tumour volume logically reflects the cytotoxic activity of trastuzumab and those patients who experienced a reduction of at least 20% in tumour volume were scored as responders. Moreover, the Ki67 positivity, as evaluated by IHC in core biopsies obtained before and after treatment with trastuzumab, was used to score the 'response K', that reflects the cytostatic activity of trastuzumab. Patients were considered K-responders if the number of Ki67 positive cells in the post-treatment biopsy was reduced by at least 50% compared to pre-treatment biopsy. Figure 33A shows the distribution of C- and K-responders in the analysed TRUP cohort. Note that not all tumours that experienced a clinical response also achieved a strong reduction in Ki67 positivity, while in the majority (86%) of tumours in which trastuzumab was not cytotoxic (C-), it was not cytostatic too (K-).

Gene set enrichment analyses were performed according to response C and response K (Fig. 33). Comparison-i (C+ *vs* C-) showed a positive and negative enrichment in pathways

related respectively to the immune cells and to the citric acid cycle (TCA), in tumours that achieved a response C (C+) (Table 17 and Fig. 33B). K-responders' (K+) tumours, compared to non responders (K-), were positively enriched in pathways related to extracellular matrix (ECM) organization and RTK signaling pathways, and negatively enriched in TCA and proliferation (comparison-ii, Table 17 and Fig. 33B). As expected, according to pathways found in comparison-i, pathways related to immune system and TCA were found significantly enriched when comparing C+ and C- tumours within K- tumours (comparison-iii) and in the comparison between C+K+ vs C-K- tumours (comparison-v, Fig. 33B and Table 17). Comparison-iv (i.e: C+K+ vs C+K-) output the same clusters of pathways of comparison-ii and immune pathways (Fig. 33B and Table 17), indicating that enrichment in immune genes within C responders is higher in tumours with also a strong cytostatic response to trastuzumab than K- tumours and pointing out big differences between C+K+ and C+K- tumours (Fig. 34). From these data we can infer that C+K+ tumours are those most enriched in immune genes and less enriched in TCA-related and proliferation-related genes.

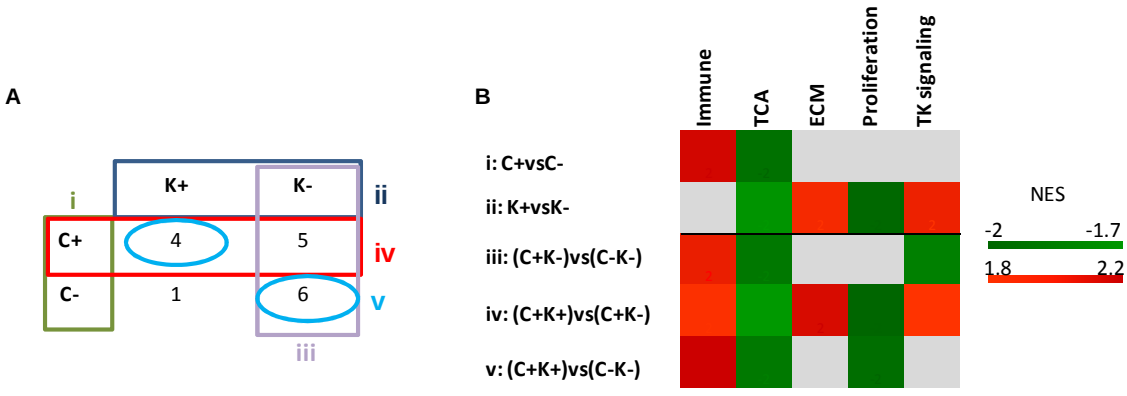

Figure 33. GSEA analyses of tumours according to response to one cycle of trastuzumab
A) Scheme of comparisons performed in TRUP dataset by GSEA and the number of tumours in each group. C+: responders (i.e. patients who experienced a reduction of at least 20% in tumour volume); C-: non responders. K+: responders (i.e. patients who experienced a reduction of at least 50% in the number of Ki67 positive cells in their tumours after treatment with trastuzumab); K-: non responders. **B)** Averaged normalised enrichment score (NES) of pathways belonging to each cluster resulted to be significantly (FDR<10%) enriched in each comparison. Grey squares indicate no enrichment.

Table 17. List of pathways enriched in comparisons i-v

Pathway	i	ii	iii	iv	v
REACTOME_PD-1_SIGNALING	2.26	ns	1.91	2.03	2.19
REACTOME_INTERFERON_ALPHA_BETA_SIGNALING	2.19	ns	2.01	ns	ns
REACTOME_PHOSPHORYLATION_OF_CD3_AND_TCR_ZETA_CHAINS	1.98	ns	ns	1.93	ns
REACTOME_IL3/5_AND_GMCSF_SIGNALING	ns	ns	ns	1.80	ns
REACTOME_IL_RECEPTOR_SHC_SIGNALING	ns	ns	ns	1.79	ns
REACTOME_IL2_SIGNALING	ns	ns	ns	1.71	ns
REACTOME_TCR_SIGNALING	ns	ns	ns	1.68	ns
REACTOME_PYRUVATE_METABOLISM	-1.95	ns	-1.91	ns	-1.91
REACTOME_TCA_CYCLE_AND_RESPIRATORY_ELECTRON_TRANSPORT	ns	-1.72	ns	-1.65	ns
REACTOME_RESPIRATORY_ELECTRON_TRANSPORT	ns	-1.82	ns	-1.84	ns
REACTOME_COLLAGEN_FORMATION	ns	1.82	ns	2.16	ns
REACTOME_INTEGRIN_CELL_SURFACE_INTERACTIONS	ns	ns	ns	2.15	ns
REACTOME_EXTRACELLULAR_MATRIX_ORGANIZATION	ns	ns	ns	2.08	ns
REACTOME_NCAM1_INTERACTIONS	ns	1.93	ns	2.03	ns
REACTOME_DNA_REPLICATION	ns	-1.96	ns	-2.09	ns
REACTOME_MITOTIC_M_M_G1_PHASES	ns	-1.97	ns	-2.05	ns
REACTOME_TELOMERE_MAINTENANCE	ns	-1.99	ns	-1.95	-1.83
REACTOME_CHROMOSOME_MAINTENANCE	ns	-1.88	ns	-1.89	ns
REACTOME_DEPOSITION_OF_NEW_CENPA_CONTAINING_NUCLEOSOMES_AT_THE_CENTROMERE	ns	-2.21	ns	-2.09	-2.10
REACTOME_SIGNALLING_TO_ERKS	ns	1.98	ns	1.66	ns
REACTOME_SIGNALING_BY_PDGF	ns	1.89	ns	2.17	ns
REACTOME_PI3K_CASCADE	ns	ns	-1.94	1.68	ns
REACTOME_DOWNSTREAM_SIGNALING_OF_ACTIVATED_FGFR	ns	ns	-1.81	1.67	ns
REACTOME_GENERATION_OF_SECOND_MESSENGER_MOLECULES	ns	ns	ns	1.84	ns

Colours identified clusters (pink: immune, blue: TCA, yellow: ECM, grey: proliferation, green TK signaling). NES for each pathway is shown. ns: not significant

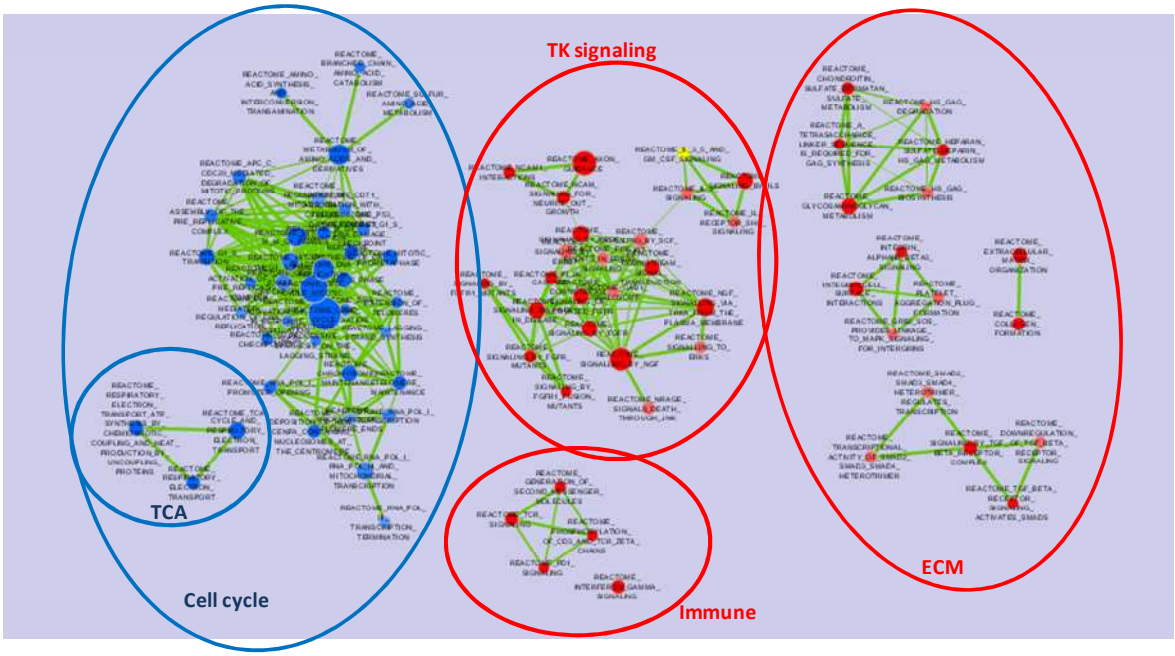

Figure 34. Enrichment map of the differentially enriched pathways in C+K+ vs C+K-
Shown are pathways (Reactome pathways) significantly (FDR<10%) enriched in the comparison between C+K+ and C+K- tumours by GSEA analysis and organized by Cytoscape software. Major clusters were manually labeled. Each pathway is visualised as a circle and colour coded according to positive or negative enrichment in C+K+ tumours (red: positive enrichment, blue: negative

enrichment). The size of each circle reflects the number of genes included in the pathway. Green edges represent gene overlap between pathways.

The positive enrichment of immune pathways and the negative enrichment of TCA cycle genes in responsive tumours (C+K+) supported a relationship between these two clusters. Indeed, cancer cells that primarily rely on glycolysis rather than on oxidative phosphorylation for energy production, a mechanism known as the Warburg effect, released in the TME high amount of lactate that has several immune-modulatory properties, creating a pro-tumour microenvironment [Becker et al., 2013]. The inverse association between enrichment in cell cycle-related pathways and response to trastuzumab monotherapy is in accordance with a negative association between ki67 expression and response to 3 cycles of trastuzumab monotherapy found in human setting [Mohsin et al., 2005].

3.3.2 Identifying responders to trastuzumab monotherapy

Based on the described relevant role of the immune system in trastuzumab cytotoxic activity [Kroemer et al., 2015], the above described association between NKG2D expression and response to trastuzumab as well as the enrichment of immune genes in responders to trastuzumab alone, we applied immune metagenes described by Rody *et al*. [Rody et al., 2009] to the TRUP dataset to test their predictive performance in identifying responders to trastuzumab monotherapy. Among the applied 6 metagenes (MHC-I, MHC-II, HCK, LCK, IFN, STAT1), C+K+ tumours expressed higher levels of MHC-II metagene (p=0.0696) than other tumours (Fig. 35). Even if not statistically significant, lymphocyte-specific kinase (LCK) and hematopoietic cell kinase (HCK) metagenes showed the same trend of MHC-II, in accordance to a strict correlation among the expression of these metagenes (r=0.76 p=0.0002 and r=0.71 p=0.017, respectively), supporting the role

of immune genes/cells in the activity of trastuzumab monotherapy.

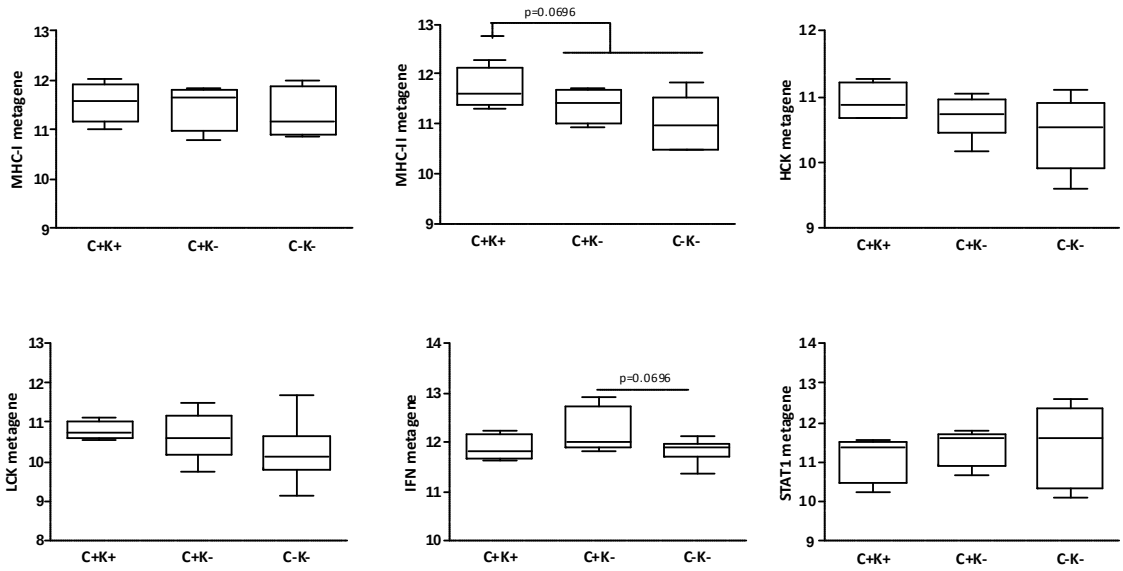

Figure 35. Association between immune metagene expression and response to trastuzumab

Expression of Rody metagenes [Rody et al., 2009] is shown according to tumour partition based on C and K responses. HCK: hematopoietic cell kinase; LCK: lymphocyte-specific kinase; MHC: major histocompatibility complex. p-values by unpaired t-test.

Notably C+K+ tumours that responded to one cycle of trastuzumab alone, also reached pCR at a higher rate than other tumours (p=0.0534). Indeed, 75% (3/4) of C+K+ patients reached a CR at surgery vs 0% (0/5) of C+K- and 29% (2/7) of C-K- patients. Analyses of matched pre- and post-treatment biopsies of TRUP_AB cohort were used to identify modifications induced by trastuzumab in clinical samples. Comparison of matched pre- and post-treatment biopsies, independently from response to trastuzumab, showed a positive enrichment in a cluster of pathways related to APC and metabolism, and a negative enrichment in a cluster of cell cycle-related pathways in biopsies obtained after trastuzumab treatment. Positive and negative enrichment of APC- and cell cycle-related pathways, respectively, was validated in the GSE76360 dataset containing GEP of tumour biopsies derived from 50 patients before and 14 days after treatment with one cycle of trastuzumab alone. These data sustained a modification of infiltrating immune cells induced by trastuzumab as suggested [Shi et al., 2015; Arnould et al., 2006] and a

reduction in cell-cycle genes in all tumours treated with trastuzumab. Accordingly tumors derived from injection of MI6 cells in FVB mice and treated with one cycle of trastuzumab (1 week treatment), have higher infiltration in their TME of MHC-II and CD11b positive immune cells than untreated tumors (Fig. 36), supporting a recruitment of myeloid cells in general and of APCs by trastuzumab.

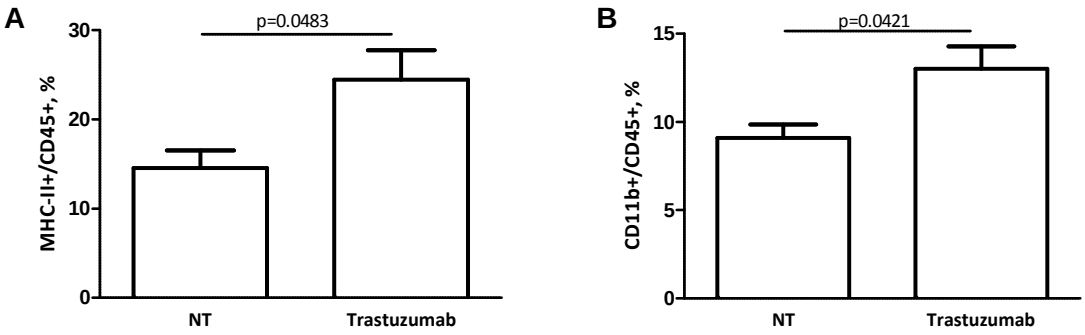

Figure 36. Modulation of APC by trastuzumab in murine xenografts
A-B) Frequency of the MHC-II (A) and CD11b (B) positive cells from the live CD45+ cells infiltrating MI6 tumours treated or not (NT) with trastuzumab as analyzed byu flow cytometry analyses. p-values by unpaired t-test.

Application of Rody metagenes to tumours of TRUP_AB cohort showed a significant inverse correlation between expression of each MHC-II, LCK and HCK metagene in pre-treatment biopsies and their fold change induced by trastuzumab (MHC-II: r=-0.63 p=0.0067; LCK: r=-0.58 p=0.0140; HCK: r=-0.60 p=0.0104): the higher their expression before treatment the lower their modulation after treatment. These data supported a modification in immune cell infiltration in tumours with the lowest expression of these metagenes. Notably, tumours of the TRUP cohort with the highest increment in the expression of these metagenes after trastuzumab treatment belong to patients who responded to trastuzumab based therapy (trastuzumab plus docetaxel, clinical response > 75%, Fig. 37). The fold increase in these tumours was significantly higher than in low-responders and in C+K+ tumours, in which trastuzumab did not induce a significant modification in the immune profile. The inverse correlation between immune metagene

upmodulations by trastuzumab and their basal expression was validated in samples of the GSE76360 dataset (MHC-II: r=-0.54 p<0.0001; LCK: r=-0.55 p<0.0001; HCK: r=-0.48 p=0.0004), even if the association with response was not feasible due to unavailability of data regarding treatment responses.

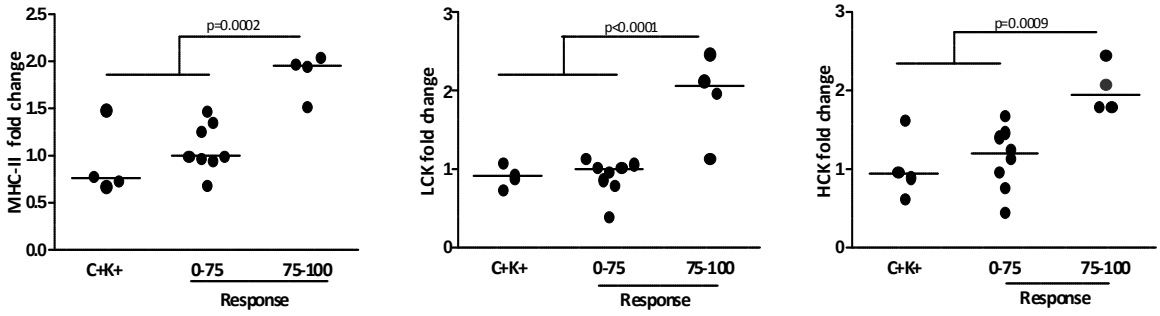

Figure 37. Modification of immune metagene expression by trastuzumab treatment
Shown are fold change in the expression of immune metagenes in post-treatment vs pre-treatment biopsies according to response to trastuzumab-based chemotherapy as evaluated at surgery. Fold change in C+K+ tumours was also shown. p-values by unpaired t-test.

These data, even if based on a small cohort of tumours, showed that immune genes are strongly associated to cytotoxic activity of trastuzumab. Accordingly, tumours that have a high basal expression of immune genes are those that benefit the most from trastuzumab monotherapy. Moreover, in some cases trastuzumab treatment can induce upmodulation of such immune genes favouring their response to treatment. We are aware that these data need a validation in another cohort, but application of these metagenes to cohort of patients treated with anti-HER2-antibodies alone, as in one of the arms of the NeoSphere or the ongoing phase II PAMELA trials, would validate whether MHC-II expressing tumours could avoid chemotherapy and reach pCR with anti-HER2 drugs alone.

3.4 How HER2 oncogene affects the tumour immune milieu and trastuzumab activity

3.4.1 Biological pathways enriched in TRAR-low tumours

Exploiting the whole-transcriptome profile of the GHEA cohort, we investigated the biological features of TRAR-low and TRAR-high tumours. Enrichment analysis according to TRAR model identified several gene sets differentially and significantly enriched in the TRAR-low subgroup, characterised by overexpression of several immune system-related genes and proliferation-associated pathways (Fig. 38A and Table 18).

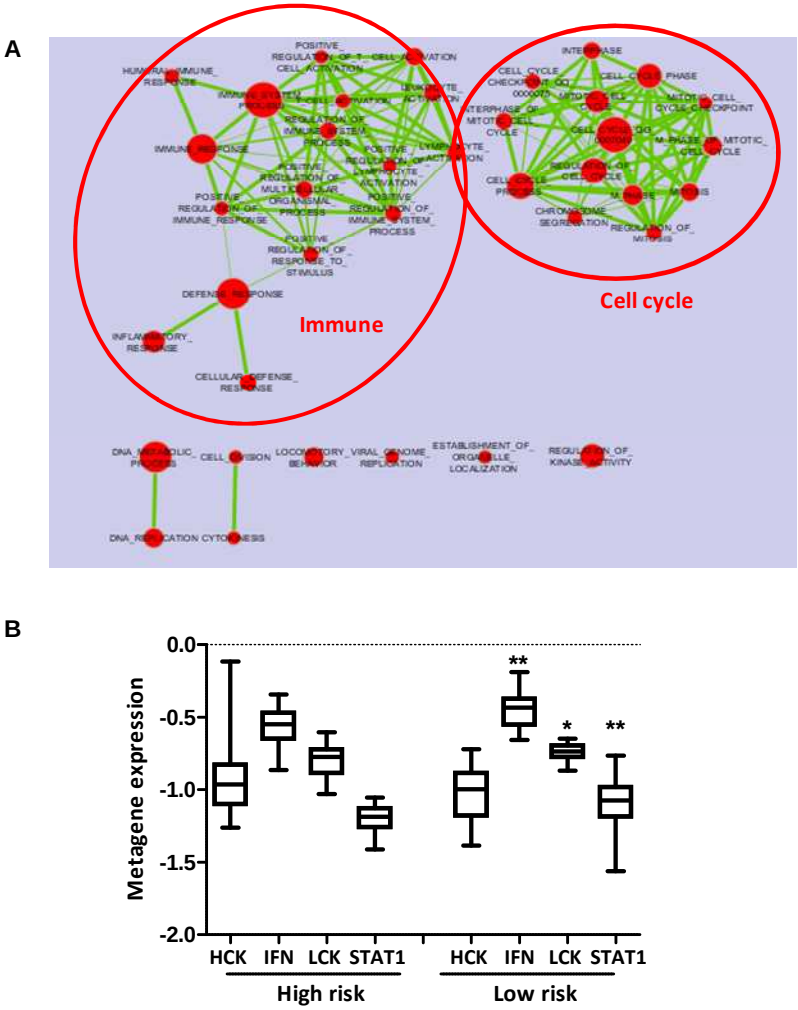

Figure 38. Immune metagene expression according to TRAR classification
A) Enrichment Map of pathways (Gene Ontology Biological Processes) significantly enriched (p< 0.005, FDR<0.1) in TRAR-low compared to TRAR-high tumours by GSEA analysis. **B)** Association between immune metagene expression (HCK: hematopoietic cell kinase, IFN: interferon, LCK: lymphocyte-specific kinase metagenes) and TRAR subtypes. * p<0.05, ** p<0.01 by unpaired t-test. Adopted from [Triulzi et al., 2015]

Table 18. Pathways enriched in tumours according to TRAR classification by GSEA analysis. Adopted from [Triulzi et al., 2015]

Pathway	ES	p-value	FDR
TRAR-low vs TRAR-high			
M PHASE	0.64	<0.0001	<0.0001
M PHASE OF MITOTIC CELL CYCLE	0.67	<0.0001	<0.0001
MITOSIS	0.66	<0.0001	<0.0001
IMMUNE RESPONSE	0.56	<0.0001	<0.0001
CELL CYCLE PROCESS	0.56	<0.0001	<0.0001
CELL CYCLE PHASE	0.56	<0.0001	<0.0001
IMMUNE SYSTEM PROCESS	0.52	<0.0001	<0.0001
REGULATION OF MITOSIS	0.70	<0.0001	<0.0001
MITOTIC CELL CYCLE	0.56	<0.0001	<0.0001
POSITIVE REGULATION OF IMMUNE SYSTEM PROCESS	0.67	<0.0001	0.0003
CHROMOSOME SEGREGATION	0.68	<0.0001	0.0009
POSITIVE REGULATION OF MULTICELLULAR ORGANISMAL	0.60	<0.0001	0.0011
LYMPHOCYTE ACTIVATION	0.58	<0.0001	0.0012
CELL DIVISION	0.75	<0.0001	0.0015
REGULATION OF IMMUNE SYSTEM PROCESS	0.58	<0.0001	0.0014
CELL CYCLE GO 0007049	0.46	<0.0001	0.0017
LEUKOCYTE ACTIVATION	0.56	<0.0001	0.0035
CELL ACTIVATION	0.55	<0.0001	0.0033
DEFENSE RESPONSE	0.46	<0.0001	0.0041
T CELL ACTIVATION	0.61	<0.0001	0.0040
POSITIVE REGULATION OF IMMUNE RESPONSE	0.68	<0.0001	0.0048
POSITIVE REGULATION OF LYMPHOCYTE ACTIVATION	0.70	<0.0001	0.0046
POSITIVE REGULATION OF T CELL ACTIVATION	0.72	<0.0001	0.0049
CELLULAR DEFENSE RESPONSE	0.58	<0.0001	0.0052
INFLAMMATORY RESPONSE	0.50	<0.0001	0.0054
CYTOKINESIS	0.74	0.0038	0.0054
SISTER CHROMATID SEGREGATION	0.73	0.0058	0.0083
VIRAL GENOME REPLICATION	0.68	<0.0001	0.0098
CELL CYCLE CHECKPOINT	0.54	<0.0001	0.0115
ESTABLISHMENT OF ORGANELLE LOCALIZATION	0.72	0.0021	0.0121
POSITIVE REGULATION OF RESPONSE TO STIMULUS	0.56	0.0019	0.0244
LOCOMOTORY BEHAVIOUR	0.48	<0.0001	0.0281
VIRAL INFECTIOUS CYCLE	0.58	0.0076	0.0287
HUMORAL IMMUNE RESPONSE	0.61	0.0038	0.0322
MITOTIC CELL CYCLE CHECKPOINT	0.61	0.0019	0.0387
ORGANELLE LOCALIZATION	0.60	0.0081	0.0478
DNA RECOMBINATION	0.52	0.0059	0.0471
BIOGENIC AMINE METABOLIC PROCESS	0.66	0.0203	0.0459
CYTOKINE AND CHEMOKINE MEDIATED SIGNALING PATHWAY	0.64	0.0100	0.0505
RESPONSE TO VIRUS	0.52	0.0058	0.0508
REGULATION OF LYMPHOCYTE ACTIVATION	0.55	0.0096	0.0498
DNA REPLICATION	0.44	0.0019	0.0492
VIRAL REPRODUCTION	0.54	0.0080	0.0517
INTERPHASE OF MITOTIC CELL CYCLE	0.48	<0.0001	0.0546
REGULATION OF CELL CYCLE	0.40	<0.0001	0.0557
INTERPHASE	0.46	0.0039	0.0561
VIRAL REPRODUCTIVE PROCESS	0.55	0.0073	0.0579
RESPONSE TO OTHER ORGANISM	0.46	0.0057	0.0665
REGULATION OF T CELL ACTIVATION	0.57	0.0181	0.0666
REGULATION OF IMMUNE RESPONSE	0.55	0.0225	0.0712
DNA METABOLIC PROCESS	0.37	<0.0001	0.0731
NEGATIVE REGULATION OF DNA METABOLIC PROCESS	0.60	0.0290	0.0991
POSITIVE REGULATION OF TRANSLATION	0.54	0.0233	0.0992
REGULATION OF CYCLIN DEPENDENT PROTEIN KINASE ACTIVITY	0.48	0.0100	0.0975
REGULATION OF KINASE ACTIVITY	0.39	<0.0001	0.0950
DNA INTEGRITY CHECKPOINT	0.54	0.0187	0.0947

Further examination of immune infiltration subtypes using immune metagenes [Rody et al., 2009] in the GHEA cohort showed that, compared to TRAR-high tumours, TRAR-low tumours expressed significantly higher levels of LCK metagene, a surrogate marker of T cells, and STAT1 and IFN metagenes that are associated with IFN signal transduction (Fig. 38B).

3.4.2 Immune cell infiltration of HER2-positive BC according to TRAR classification

To investigate whether enrichment in immune genes in TRAR-low tumours derived from immune cell infiltration, the amount and features of tumour-infiltrating cells were analyzed in FFPE tumour slides. Pathological assessment indicated no differences in the total amount of stromal immune cells, analysed as described [Salgado et al., 2015b], in tumours according to TRAR classification, and IHC characterisation of immune infiltrates revealed similar percentages of CD45+ cells in the two groups (Table 19).

Table 19. Association between immune infiltrates and TRAR. Modified from [Triulzi et al., 2015]

Variable	TRAR-high n/tot (%)	TRAR-low n/tot (%)	ǂp-value
CD45 Positive*	11/27 (41)	14/26 (54)	0.4142
CD20 Positive*	11/26 (42)	12/20 (60)	0.3726
CD3 Positive*	8/25 (32)	16/22 (73)	0.0084
CD8 Positive*	7/27 (26)	16/24 (67)	0.0050
CD68 Positive*	6/26 (23)	10/20 (50)	0.0701

ǂ p-values are calculated by Fisher exact test.

*Stained slides were digitised by a slide scanner (ImageScope XT, Aperio), and the virtual slides were subsequently evaluated using the 'positive pixel count' algorithm of Aperio ImageScope v11.2.0.7580. The percentage of positive stromal cells was calculated as the number of positive pixels/μm^2. Data were divided into two groups (positive and negative) using median value as cut-off.

No or very low numbers (< 5 cells) of NK cells were found in all tumours independently from TRAR classification and CD20 positivity was similar in the two subgroups. A trend

toward a higher infiltration of CD68+ cells (p=0.0701) in TRAR-low tumours was found. Moreover, TRAR-low tumours showed significantly higher T cell infiltration (p=0.0084) than did TRAR-high tumours (Table 19 and Fig. 39). Further classification of T cells showed that CD8 positivity was higher in TRAR-low than in TRAR-high cases (Table 19).

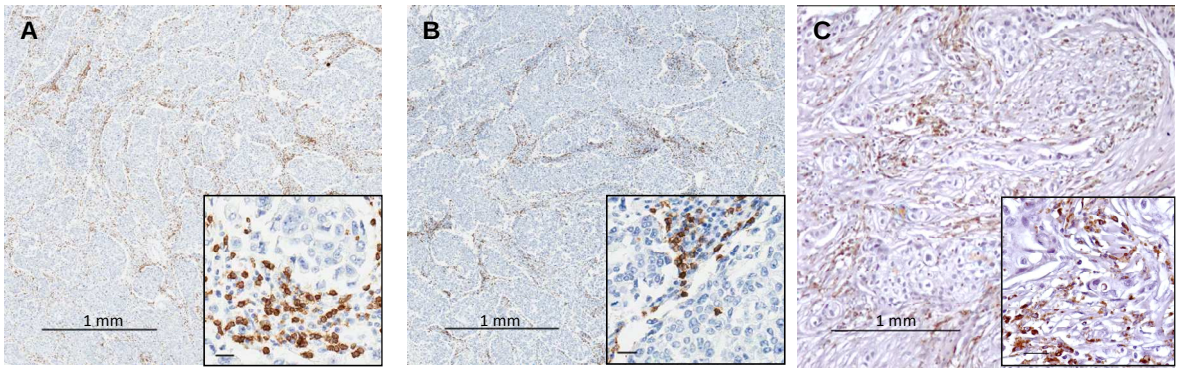

Figure 39. Immunohistochemical evaluation of immune cells in tissues of GHEA cohort A-C) Representative images of CD3 (A) CD8 (B) and CD68 (C) positive tumours. Scale bars in zoomed images, 20 µm. Modified from [Triulzi et al., 2015]

3.4.3 Chemokine expression in GHEA BCs according to TRAR classification

Based on the enrichment of immune genes, of chemokine and cytokine ligand and receptor pathways (Table 18) and immune cells in TRAR-low tumours we hypothesized that HER2 oncogene activation in these tumours is directly responsible for the expression of chemokines and the recruitment of immune cells in the TME. In accordance with our hypothesis average expression of all chemokines in the GHEA dataset was significantly highly expressed in TRAR-low than TRAR-high tumours (Fig. 40A), and some of them were found to be significantly differentially expressed between the two risk groups by supervised analysis (Fig. 40B). TRAR-low tumours showed significantly higher levels of CC subfamily chemokines (CCL2, CCL5, CCL8, CCL11 and CCL22), mainly involved in the recruitment of monocytes to the site of inflammation, and of CXC subfamily chemokines (CXCL9, 10, 11 and 13) that induce the migration mainly of T cells and B cells [Franciszkiewicz et al., 2012].

A

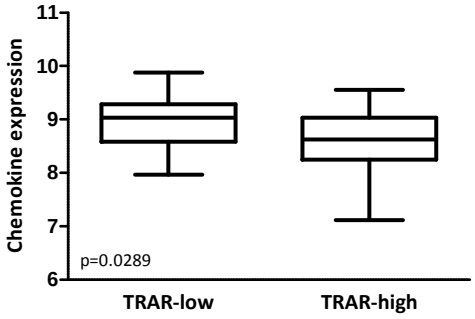

B

Gene Symbol	TRAR-low	TRAR-high	Fold change	p-value
CXCL9	7.2423	5.4487	3.4669	5.960E-08
CXCL10	11.1510	9.4645	3.2187	6.807E-08
CXCL11	8.9895	7.8383	2.2210	9.652E-03
CXCL13	7.9653	6.4817	2.7965	8.195E-04
CCL2	11.3688	10.9942	1.2965	4.893E-02
CCL5	12.0987	11.3665	1.6611	2.105E-03
CCL8	9.5710	8.9753	1.5112	3.181E-02
CCL11	7.1760	6.5191	1.5766	1.213E-02
CCL22	7.7761	7.1081	1.5889	2.995E-02

Figure 40. Chemokine expression according to TRAR classification
A) Average expression of chemokine genes in GHEA tumours. p-value by unpaired t-test. **B)** Chemokine genes significantly and differentially expressed in TRAR-low *vs* TRAR-high tumours. For each gene the mean expression (Log2) in each group, the fold difference between the two groups and the relative p-value obtained by unpaired t-test were reported.

Based on the higher infiltration of T cells in TRAR-low than in TRAR-high tumours, and on the fact that CXCLs are the top differentially expressed chemokines between the two risk groups, we investigated the expression of CXCL9 and CXCL10, as representative of CXCL chemokines, in GHEA tumours by IHC. Both chemokines were mainly expressed by tumour cells, but CXCL10 positivity in some cases was found only in stromal cells of the TME (Fig. 41). In accordance to GEP analysis, CXCL10 was more expressed in TRAR-low (Fig. 41B, positivity in cancer or stromal cells vs negative tumours) than in TRAR-high tumours. Moreover, the majority of TRAR-low tumours expressed CXCL9 compared to almost half of TRAR-high tumours (96% vs 59%, Fig. 41A), supporting the involvement of tumour cells in the production of these molecules and in the recruitment of immune cells in the TME.

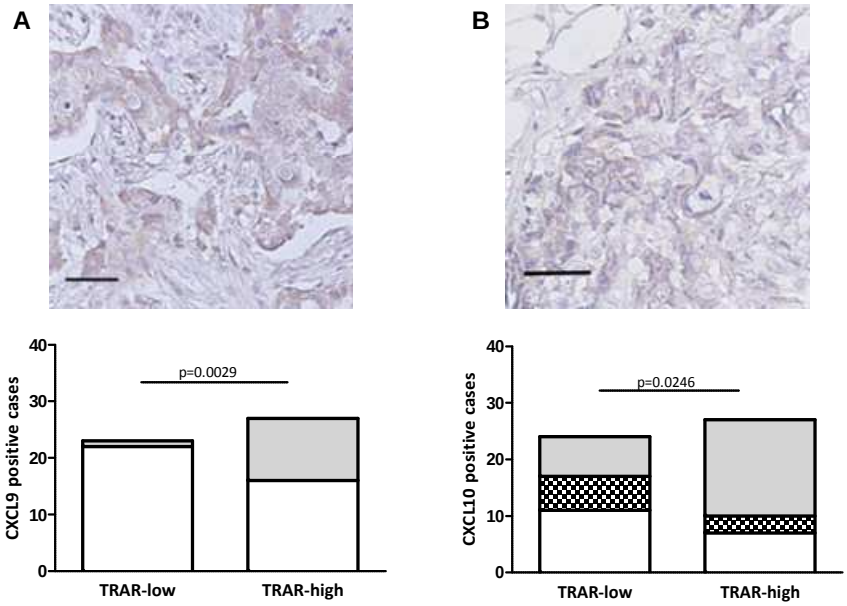

Figure 41. Immunohistochemical evaluation of CXCLs in tissues of GHEA cohort
A) CXCL9, **B)** CXCL10 representative images of positive tumours. Positive tumors contain at least 5% of positive cells. Scale bars, 50µm. Lower panel showed the number of positive cases (grey boxes: positivity in tumour cells; black and white boxes: positivity in stromal cells) and negative cases (white boxes) according to TRAR classification. p-values by Fisher's test.

3.4.4 CXCLs modulation by HER2 signals

In order to understand whether in HER2-positive BC cells expression of CXCL chemokines is regulated directly from HER2 signals other than by IFN-γ-induced pSTAT1 [Viola et al., 2012;Saha et al., 2010], as observed in BT474 (Fig. 42), HER2-positive cells were treated with trastuzumab and EGF/HRG in order to block and activate the receptor respectively, and then analysed by qRT-PCR. Treatment of HER2-addicted BC cells with EGF or HRG for 6 hours did not induce a significant modulation of CXCL9, CXCL10 and CXCL11 expression (Fig. 43A and 43B). Accordingly, their expression was not significantly modulated by inhibition of HER2 signals through trastuzumab treatment (Fig. 43C). These data indicate that CXCLs expression in tumour cells does not directly derive from HER2 signals.

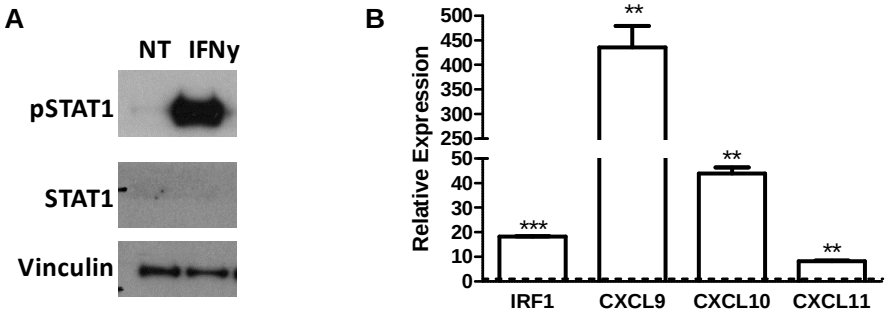

Figure 42. Modulation of CXCL chemokines by IFN-γ
A) Control of IFN-γ treatment (100 ng/ml) efficacy on STAT1 phosphorylation in BT474 as evaluated by WB. Vinculin was used as protein loading control. **B)** Chemokine mRNA expression modulation by 6 h IFN-γ treatment as evaluated by qRT-PCR. IRF1 was used as positive control of IFN-γ activity. Data are expressed as fold to untreated cells. ** p<0.01, *** p<0.0001 by unpaired t-test

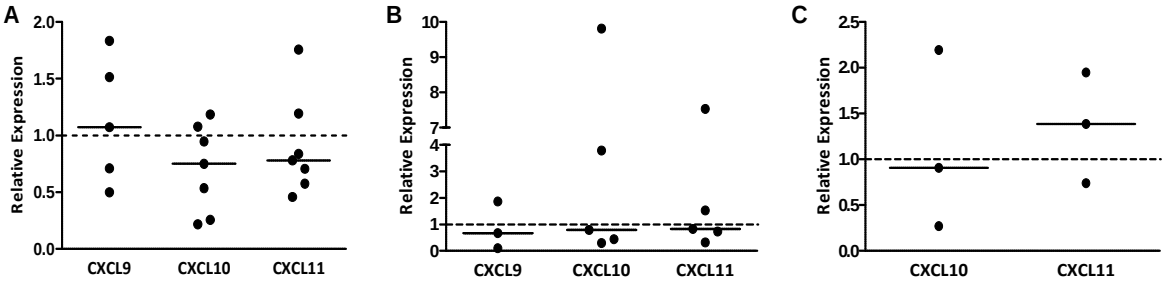

Figure 43. Chemokine expression upon HER2 modulation in HER2-positive BC cells
A-C) Chemokine mRNA expression in cells as evaluated by qRT-PCR after 6 h-treatment with 20 ng/ml EGF (A), HRG (B) and 10 μg/ml trastuzumab (C). Data are expressed as fold to untreated cells and are referred to independent experiments in BT474, ZR75.30 and SKBR3.

3.4.5 CCL2 modulation by HER2 signals

Among the CCL chemokines found to be significantly upmodulated in TRAR-low compared to TRAR-high tumours, we posed our attention on CCL2 and CCL5 as representative of CCL chemokine family. Evaluation of their expression in HER2-addicted cells after treatment with EGF/HRG or trastuzumab showed that only CCL2 was always upmodulated by HER2 stimuli and downmodulated by trastuzumab, while CCL5 modulation was more variable (Fig. 44). Further investigation of CCL2 modulation in BT474 and SKBR3 showed that CCL2 modulation by HER2 stimuli, that induced activation of canonical AKT and ERK pathways downstream HER2 (Fig. 45A), occured both at mRNA

(Fig. 45B) and at protein level in both cell lines, as analysed by ELISA assay 24 hours after treatment (Fig. 45C). The highest induction of CCL2 production occurred in SKBR3 treated with EGF (Fig. 45C).

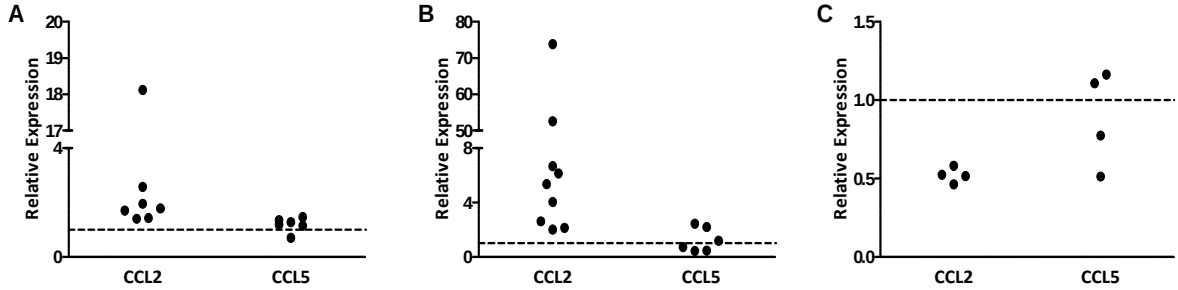

Figure 44. CCL chemokine expression upon HER2 modulation in HER2-positive BC cells
A-C) CCL2 and CCL5 mRNA expression in cells as evaluated by qRT-PCR after 6 h-treatment with 20 ng/ml EGF (A), HRG (B) and 10 µg/ml trastuzumab (C). Data are expressed as fold to untreated cells (dotted line) and are referred to independent experiments in BT474, ZR75.30 and SKBR3.

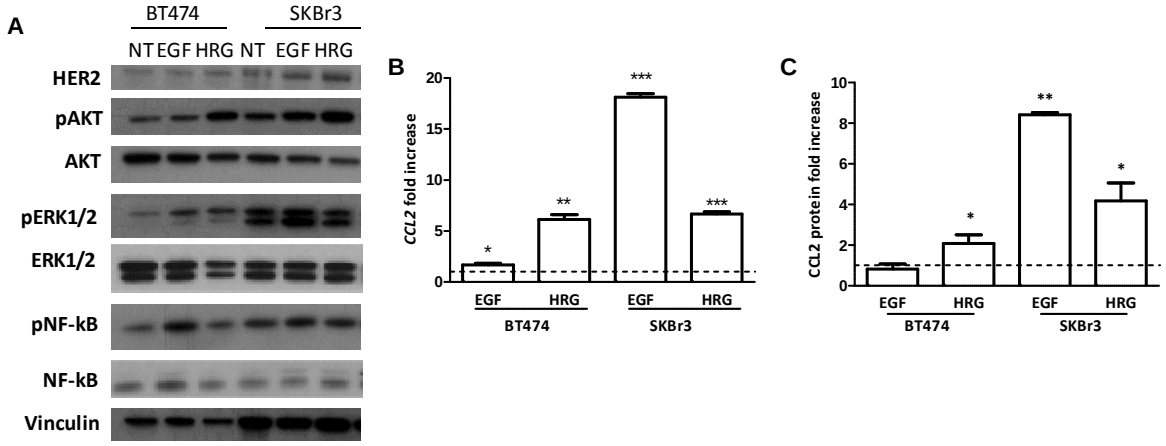

Figure 45. CCL2 expression modulation by HER2 signals
A) WB analysis of HER2 downstream signals in BT474 and SKBR3 cells treated or not with 20 ng/ml EGF or HRG for 6 hours. Vinculin was used as protein loading control. **B)** CCL2 mRNA quantification by qRT-PCR in BT474 and SKBR3 cells treated as in A. Shown are the mean and SD of fold increases in treated versus untreated cells (dotted line). Data are referred to one representative of three experiment. **C)** CCL2 protein quantification by ELISA in supernatant of BT474 and SKBR3 cells treated with 20 ng/ml EGF or HRG for 24 hours. Shown are the mean and SD of fold increases in treated versus untreated cells (dotted line). Data are referred to one representative of two experiment. * $p<0.05$, ** $p<0.01$, *** $p<0.001$ by unpaired t-test.

To test whether CCL2 is modulated by HER2 also *in vivo*, we exploited the availability of murine tumours derived from transgenic mice expressing the d16HER2 isoform of the human HER2 oncogene [Castagnoli et al., 2014]. These tumours had heterogeneous HER2 expression with a strong positivity in cells at the margins of the tumour nodules and loss

of the oncoprotein in their centre (Fig. 46A). Evaluation of CCL2 positivity by IHC in these tumours showed a quite perfect overlapping in HER2 and CCL2 positive cells, again supporting the dependence of this chemokine from HER2. To support CCL2 modulation by HER2 signaling also in human samples, CCL2 expression was analysed *in silico* in tumour biopsies obtained from patients of the 03-311 trial [Varadan et al., 2016], who where treated with one cycle of trastuzumab alone. Its expression was found significantly reduced in post-treatment compared to pre-treatment biopsies. The reduction was of about 40% (±18%) in 70% of cases (Fig. 46B). Evaluation of CCL2 expression in FFPE specimens of the GHEA cohort confirmed its higher expression in TRAR-low than in TRAR-high tumours and its production by tumour cells (Fig. 47), thus supporting a direct connection between HER2 activity and CCL2 expression also in human tumours.

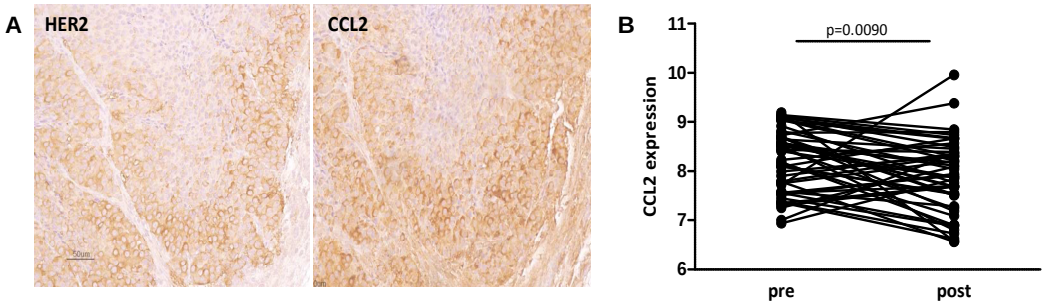

Figure 46. CCL2 modulation by HER2 *in vivo*
A) HER2 and CCL2 expression in tumours derived from d16HER2 transgenic mice as evaluated by IHC. **B)** CCL2 expression in 50 HER2-positive BC biopsies belonging to the GSE70360 dataset [Varadan et al., 2016] obtained before (pre) and after (post) treatment with one cycle of trastuzumab alone. p-value by paired t-test.

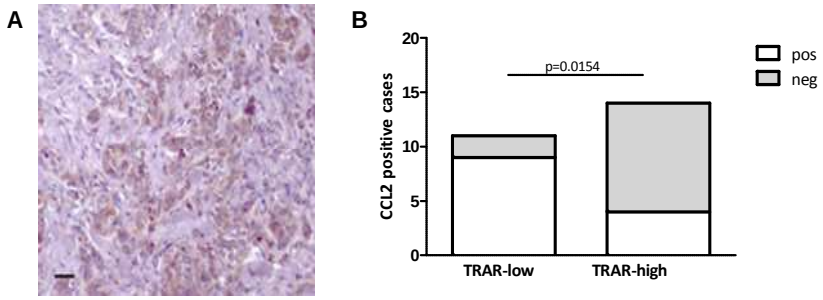

Figure 47. Immunohistochemical evaluation of CCL2 in tissues of GHEA cohort

A) CCL2 representative image of positive tumour. Scale bars, 100 µm. **B)** Association between CCL2 expression and TRAR classification. Positive tumours (pos) contain at least 5% of positive tumour cells. p-value by Fisher's test.

Once demonstrated the direct involvement of HER2 in regulating CCL2 expression, HER2-addicted cell lines were treated with MEK (MEKi, UO126) and PI3K (PI3Ki, LY294002) inhibitors and analysed for CCL2 expression to identify the signaling cascade responsible for its transcription. As shown in figure 48B, treatment with MEKi for 6 hours did not induce a significant reduction in CCL2 expression in all cell lines as did PI3Ki. The reduction in CCL2 expression by PI3Ki, and not by MEKi, was observed in SKBR3 also at protein level, as analysed by ELISA assay after 24 hours (Fig. 48C), suggesting the involvement of PI3K/AKT pathway in its transcriptional modulation. We then analysed the ability of PI3Ki to block the increase of CCL2 induced by EGF/HRG: CCL2 upmodulation by EGF or HRG was dramatically reduced by PI3Ki, as analysed by ELISA assay after 24 hours (Fig. 48D and 48E, respectively), indicating PI3K/AKT pathway as involved in the regulation of its expression downstream HER2. Based on the observed activation of NF-kB transcriptional factor downstream PI3K/AKT pathway (Fig. 48A), the same experiment was performed in the presence of NF-kB inhibitor for 24 hours (NF-kBi, BAY 11-7082). In both SKBR3 and BT474 cell lines, NF-kBi blocked the upmodulation of CCL2 induced by EGF/HRG, indicating this molecule as the transcriptional factor of CCL2 downstream HER2 (Fig. 48F).

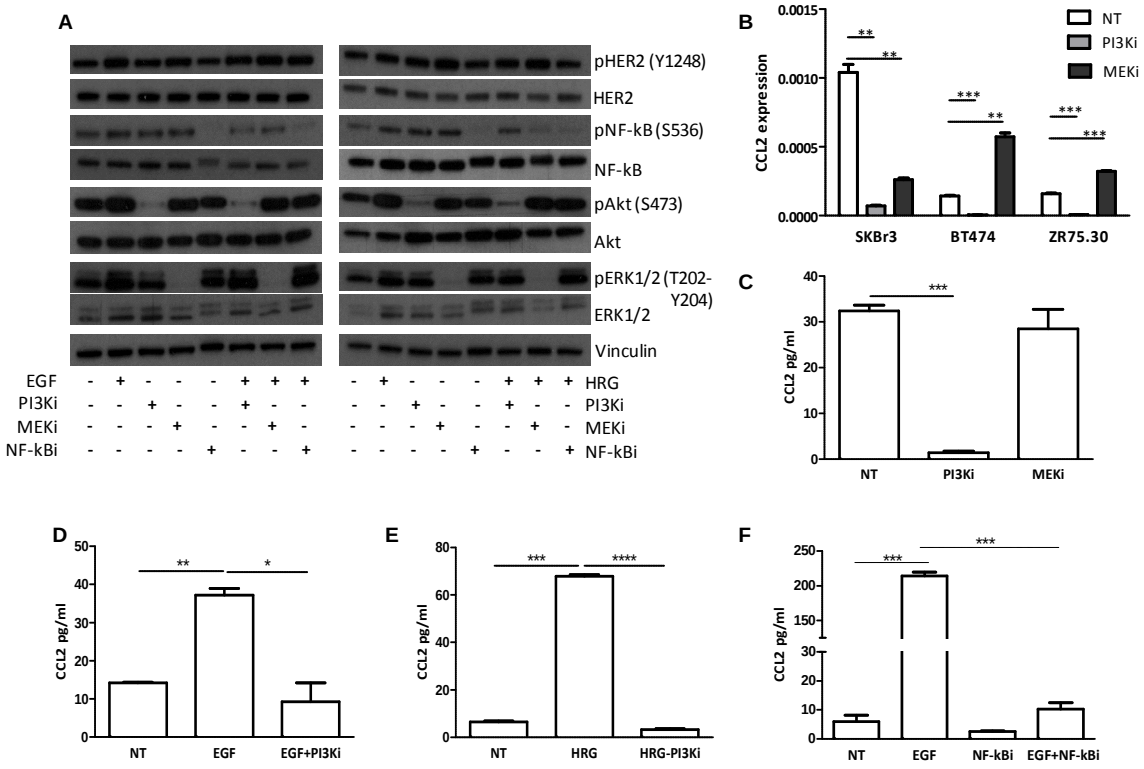

Figure 48. CCL2 modulation in BC cells upon inhibition of HER2 signaling
A) WB analysis of signals downstream HER2 in SKBR3 cells treated or not with 20 ng/ml EGF/HRG and/or 10 µM inhibitors for 5 minutes. **B)** CCL2 mRNA quantification by qRT-PCR in BT474, SKBR3 and ZR75.30 cells treated or not with PI3Ki (LY94002) or MEKi (UO126) for 6 hours. **C)** CCL2 protein quantification by ELISA in SKBR3 cells treated or not with inhibitor as in B. **D-E)** CCL2 protein quantification in supernatant of SKBR3 treated with EGF (D) or HRG (E) and/or with PI3Ki for 24 hours. **F)** CCL2 protein quantification in SKBR3 cells treated or not with EGF and/or NF-kBi (BAY 11-7082) for 24 hours. Data are mean ± SD and referred to one representative of two experiments. * p<0.05, ** p<0.01, *** p<0.001 by unpaired t-test.

3.4.6 Mechanisms of immune evasion of TRAR-low tumours.

Based on data indicating that TRAR-low tumours have higher number of CD8+ cells in their microenvironment than TRAR-high tumours, it is likely that a mechanism of immune suppression/evasion is elicited by tumour cells to preserve their growth. We first analysed the presence of immune suppressive cells, like Tregs and MDSCs, within the TME. IHC evaluation of FOXP3+ and CD33+ cells in FFPE sections of HER2-positive BCs of the GHEA cohort showed a similar amount of infiltrating Treg and MDSC cells independently of TRAR classification (Fig. 49A and 49B, respectively).

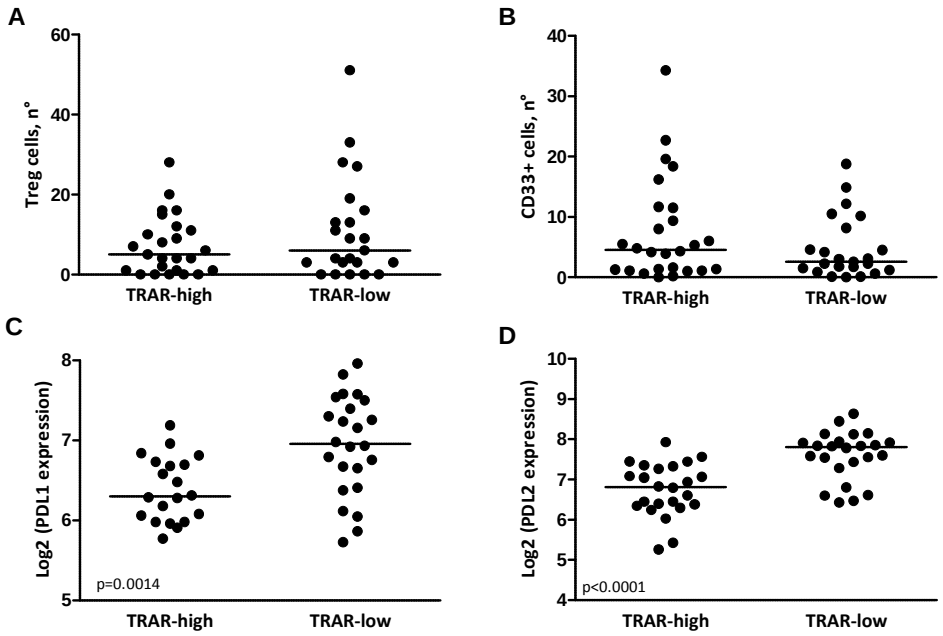

Figure 49. Mechanisms of immune evasion of TRAR-low tumours

A-B) IHC evaluation of FOXP3+ (A) and CD33+ cells (B) in tissues of the GHEA cohort. Shown are the average number of positive cells in three-fields (A) and the total amount of positive cells per µm2 of tissue (B). **C-D**) PD-L1 (C) and PD-L2 (D) expression according to TRAR classification. p-values by unpaired t-test.

Based on these data, and on the emerging data showing that PD-L1 expression by tumour cells could block lymphocytes activity [Pardoll, 2012], we analysed PD-L1 and PD-L2 expression according to TRAR classification. As shown in figure 49C and 49D, these ligands were significantly higher expressed in TRAR-low than in TRAR-high tumours suggesting their involvement in tumour immune evasion. We then investigated whether HER2 itself in addition to regulating CCL2 expression and thus immune cell recruitment in the TME could also regulate the expression of PD-1 ligands to control recruited immune cells. Evaluation of PD-L1 and PD-L2 expression in BC cell lines by qRT-PCR showed that, while PD-L2 was not quantifiable in all cell lines except for HCC1954 cells, PD-L1 was detectable in all cell lines and HCC1954 cells were the most positive (Fig. 50A). Accordingly, only HCC1954 cells basally expressed PD-L1 on the cell membrane, as analysed by flow cytometry, while PD-L1 expression was inducible in almost all cell lines

by IFN-γ stimulation (Fig. 50B), described to be the main regulator of its expression [Pardoll, 2012]

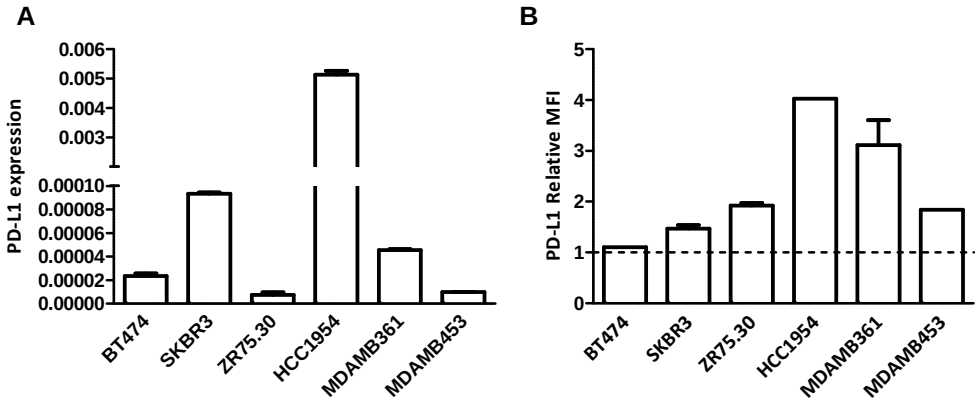

Figure 50. PD-L1 expression in BC cell lines
A) PD-L1 mRNA expression in BC cells. Data are referred to one representative of two experiments and are expressed as mean ± SD. **B)** PD-L1 relative median fluorescence intensities (MFI) in BC cells treated with 100 ng/ml IFN-γ for 24 hours. Shown are the mean and SD of fold increases in treated versus untreated cells (dotted line) of two independent experiments.

To investigate the possible modulation of PD-1 ligands by HER2 oncogene, we used HCC1954 cells as a model of PD-L1 positivity. Treatment with lapatinib, described to shut down HER2 signaling, significantly reduced the expression of ligands both at mRNA (Fig. 51A) and at protein levels (Fig. 52A). On the contrary, EGF treatment induced an upmodulation of both ligands (Fig. 51A and 52), that HRG did not do because these cells expressed very low levels of HER3, the receptor for HRG. Also in SKBR3, EGF and HRG treatment significantly increased PD-1 ligand expression at mRNA level (Fig. 52B), supporting the regulation of these molecules by HER2 activity. Analyses of HCC1954 and SKBR3 cells treated or not with inhibitor of HER2 downstream signals, showed that upmodulation of PD-L1 upon EGF treatment was reversed mainly by treatment with MEKi (Fig. 53).

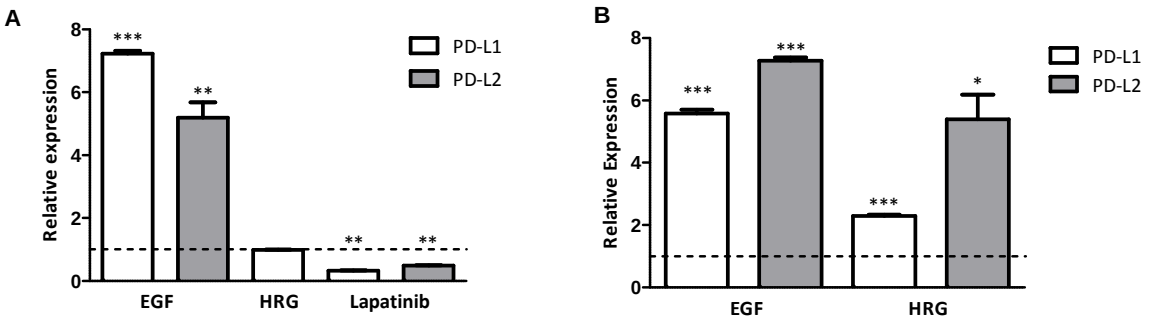

Figure 51. Modulation of PD-1 ligand expression by HER2

A) PD-L1 and PD-L2 mRNA expression in HCC1954 cells treated with 20 ng/ml EGF or HRG for 6 hours and 0.3 µM lapatinib for 24 hours. **B)** PD-L1 and PD-L2 mRNA expression in SKBR3 cells after treatment with 20 ng/ml EGF or HRG for 6 hours. Data are mean ± SD of fold increase in treated *vs* untreated cells (dotted lines) and are representative of two experiments. * p<0.05, ** p<0.01, *** p<0.001 by unpaired t-test.

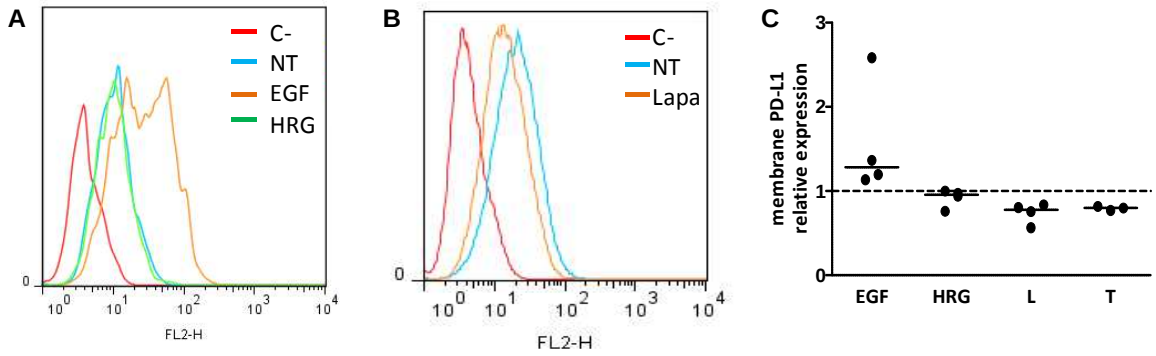

Figure 52. Membrane-associated PD-L1 expression modulation by HER2

A-B) Representative analysis of membrane-associated PD-L1 expression in HCC1954 cells treated or not with 20 ng/ml EGF or HRG for 6 h (A) and with 0.3 µM lapatinib (L) for 24 h (B). **C)** Relative quantification of membrane-associated PD-L1 expression in treated versus untreated (dotted line) HCC1954 cells. T: trastuzumab. Cells were treated as in A with 10 µg/ml for 24h. Each dot represents an independent experiment.

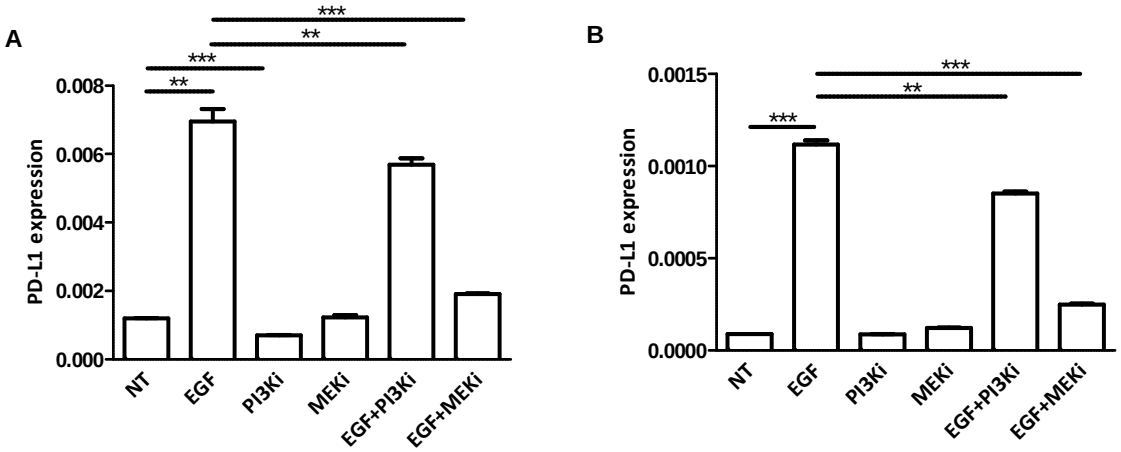

Figure 53. Modulation of PD-L1 expression upon HER2 signaling inhibition

A-B) Relative PD-L1 in HCC1954 (A) and SKBR3 (B) mRNA quantification by qRT-PCR in cells treated with 20 ng/ml EGF and/or with 10 µM PI3Ki (LY294002) or MEKi (UO126) for 6 hours. Data are mean ±SD and are representive of two experiments.** p<0.01, *** p<0.001 by unpaired t-test.

Overall, these data showed that TRAR-low tumours are highly infiltrated by immune cells and express higher amount of chemokines involved in their recruitment. Moreover, we demonstrated that activated HER2 oncogene concomitantly induces the expression of CCL2 and PD-L1/PD-L2 potentially regulating both infiltration of pro-trastuzumab immune cells and their suppression. The next step is to demonstrate the relevance of CCL2 expression by tumour cells in the recruitment of pro-trastuzumab immune cells and in its therapeutic efficacy. Preliminary analysis in HER2-positive murine tumour xenografts treated or not with anti-CCL2 Abs showed a reduced amount of F480+ macrophages and CD3+ T cells in a-CCL2 treated mice compared to untreated tumours (Fig. 54). NK cells were not modulated by a-CCL2 treatment. These data support a role for CCL2 in the recruitment of both innate and adaptive immune cells and suggest its involvement in trastuzumab activity. Evaluation of trastuzumab efficacy of murine tumours treated or not with a-CCL2 will prove the relevance of the demonstrated relation between HER2 activity and CCL2 expression in trastuzumab response of TRAR-low patients.

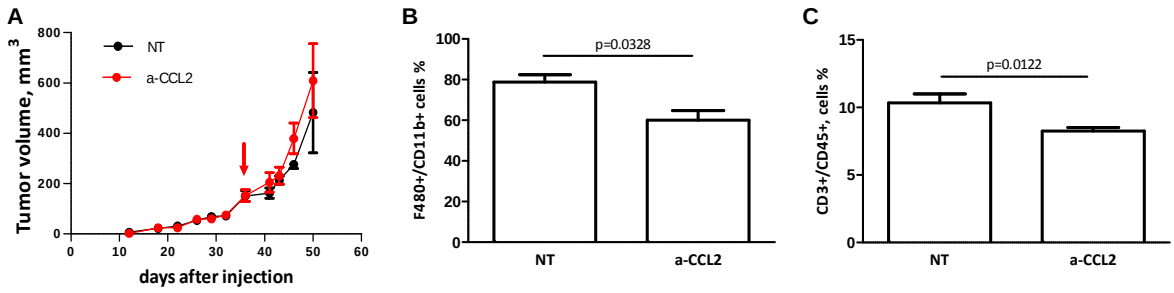

Figure 54. Tumour immune infiltration upon inhibition of CCL2 expression
A) Growth of d16HER2-positive murine tumours in FVB mice. Red arrow indicates the start of treatments with a-CCL2 Abs. **B)** Frequency of F480 positive cells from the live CD11b+ cells infiltrating d16HER2-positive murine tumours treated or not (NT) with anti-CCL2 Abs as analyzed by flow cytometry analyses. CD11b+ cells were gated from CD45+ cells. **C)** Frequency of CD3 positive cells from the live CD45+ cells. p-values by unpaired t-test.

3.5 Relationship between ERBB2 mRNA levels and tumour dependence on HER2

3.5.1 Association between HER2 expression and HER2-addiction in human specimens

Based on the high heterogeneity of *ERBB2* expression within HER2-positive tumours belonging to TRAR-high and -low subsets, we evaluated its expression in GHEA and TRUP cohorts by qRT-PCR to validate it. As shown in Figure 55, a highly significant correlation was found between *ERBB2* expression levels by gene expression and qRT-PCR in both datasets, validating the *ERBB2* mRNA heterogeneous expression in HER2-positive BCs that received trastuzumab treatment.

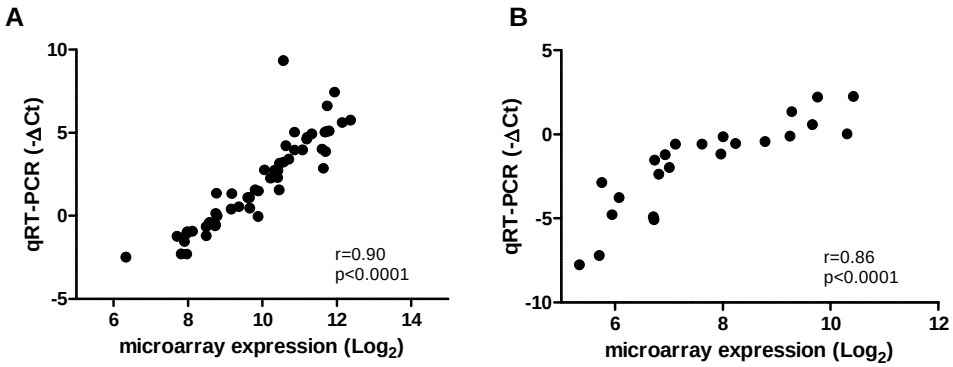

Figure 55. *ERBB2* gene expression validation in GHEA and TRUP cohorts
A-B) Correlation between *ERBB2* mRNA expression levels as evaluated by qRT-PCR (normalised upon *ACTB*) and microarray data in the GHEA (A) and TRUP (B) cohorts. Pearson's coefficient (r) and relative p-values are shown

We first examined whether this heterogeneity in *ERBB2* mRNA expression levels reflects differences in protein expression using quantitative IF analysis in tumours of GHEA cohort. To avoid fluorescence signal saturation in tumours with the highest HER2 expression, images of all samples were acquired using the microscope setting parameters of the most positive tumour and protein expression was scored as the mean fluorescence intensity (IF-score) in nine fields of each tumour slide analysed with a 40x objective. The

HER2 IF-score ranged from 35 to 133 showing a high heterogeneity also in HER2 protein amount in these tumours. Figure 56A shows representative images of tumours with HER2 IF-score in each terzile of the distribution (3+, 4+, 5+). Analysis of correlation between HER2 IF-score and mRNA levels showed a non-significant very low correlation between these two parameters (Fig. 56B). Accordingly, HER2 protein expression levels did not correlate with DFS in these tumours (Fig. 57A) and did not associate with HER2-E subset (Fig. 57C), as did *ERBB2* mRNA levels (HR=5.67, 95% CI=2.48-12.96, p<0.0001, Fig. 57B and Fig. 57D). These data suggested that *ERBB2* mRNA levels better mirror tumour addiction to HER2 oncoprotein than HER2 protein.

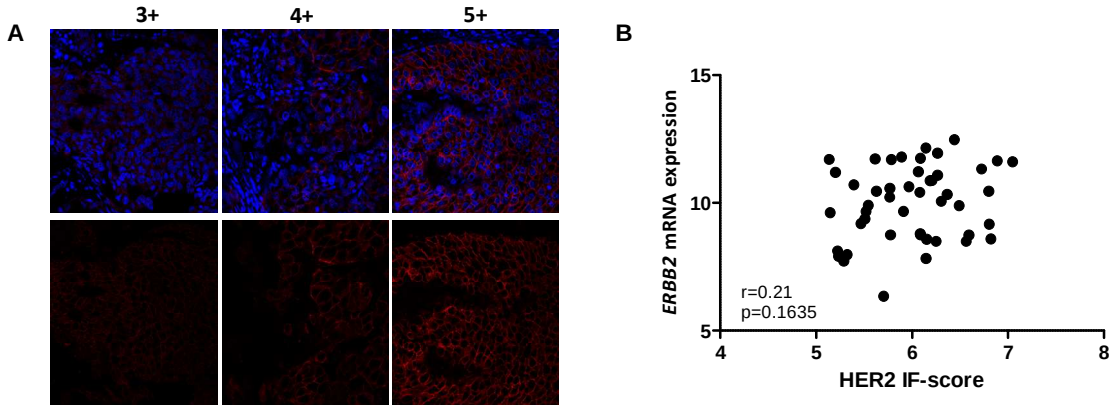

Figure 56. Immunofluorescence analysis of HER2 protein expression in GHEA BCs
A) Representative images of HER2 positivity (red) by IF are shown. Images were analysed using the same setting parameters. Tumours were scored as 3+ (1st tertile), 4+ (2nd tertile) and 5+ (3rd tertile) according to mean fluorescence intensities of positive pixels. Nuclei were stained with Dapi (blue). **B)** Association between *ERBB2* mRNA expression levels (log2) with protein levels according to HER2 IF-score (log2). Pearson's coefficient and relative p-value are shown.

We then investigate whether *ERBB2* mRNA levels just reflected *ERBB2* gene amplification levels, considering data regarding *ERBB2*/CEP17 ratio obtained by FISH analysis. Correlation analyses showed a significantly weak correlation between *ERBB2* gene amplification and *ERBB2* mRNA levels (r=0.38, p=0.0455), indicating a dependence of *ERBB2* mRNA to its genetic amplification. However, a strong correlation between *ERBB2* amplification and HER2 IF-score (r=0.68, p<0.0001) was found, suggesting a complex regulation of HER2 transcription and translation.

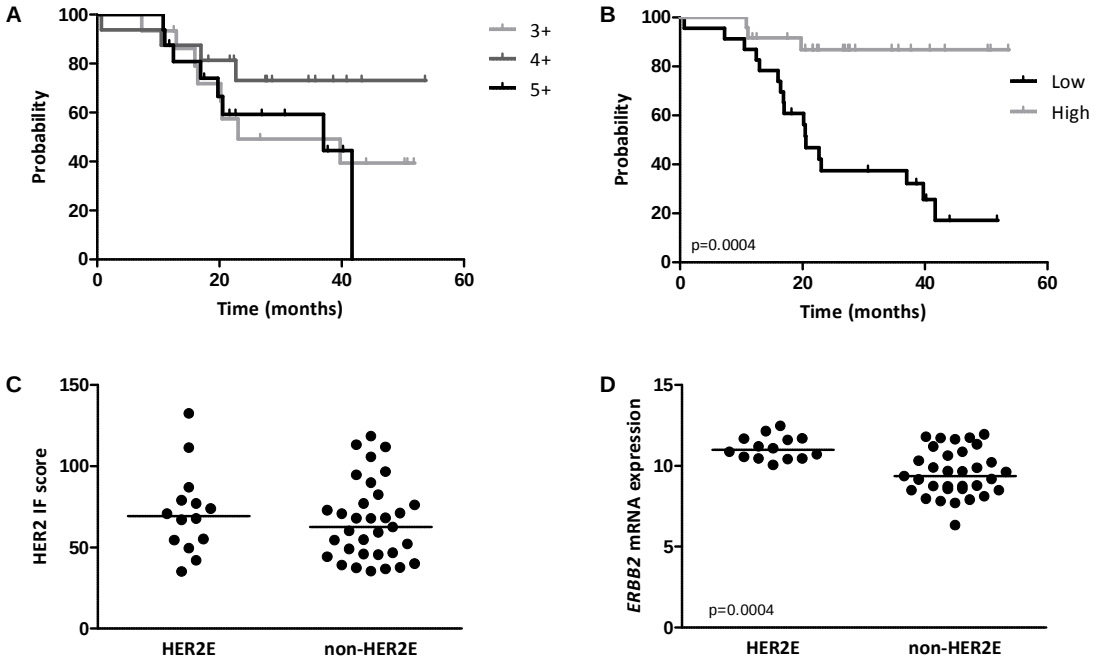

Figure 57. Differences between *ERBB2* mRNA and HER2 protein prognostic ability
A-B) Kaplan-Meier analysis of patients of the GHEA cohort classified by HER2 IF-score (A) and *ERBB2* mRNA levels (B). The *ERBB2* median expression value was used as cut-off to define the High and Low groups. p-value by log-rank test. **C-D)** Association between PAM50 classification and HER2 protein according to IF-score (C) and *ERBB2* mRNA levels (D). p-value by unpaired t-test.

3.5.2 Characterisation of HER2-positive BC cell lines

To understand why ERBB2 mRNA expression better mirrors tumour addiction to HER2 than protein levels, we analysed 6 HER2-amplified BC cell lines described to be addicted or not to HER2 oncogene *in vitro* [Shiu et al., 2014]. We firstly verified the HER2-dependance of cell lines available in our labouratory, assessing their response to lapatinib treatment as performed by Shiu et al [Shiu et al., 2014]. We confirmed BT474, SKBR3 and ZR75.30 as HER2-addicted, MDAMB361 and MDAMB453 as non-HER2-addicted, whereas HCC1954 showed an intermediate phenotype (Fig. 58A). HER2-addicted BC cell lines expressed higher levels of *ERBB2* mRNA (Fig. 58B), higher levels of HER2 on the cell membrane (Fig. 58C), higher amount of activated HER2 (Fig. 58D) and lower amount of HER2-heterodimers (lower HER1 and HER3 linked to activated HER2) (p=0.0354, Fig. 58D) than non-addicted cells (MDAMB361 and MDAMB453). The higher amount of

homodimers we found in HER2-addicted cells than non-addicted is concordant with the evaluation in the same BC cell lines by VeraTag assay described in the paper by Ghosh *et al* [Ghosh et al., 2011]. HCC1954 had *ERBB2* mRNA level, HER2 protein and its activation status similar to HER2-addicted cells (Fig. 58), thus we hereafter consider it as HER2-addicted too.

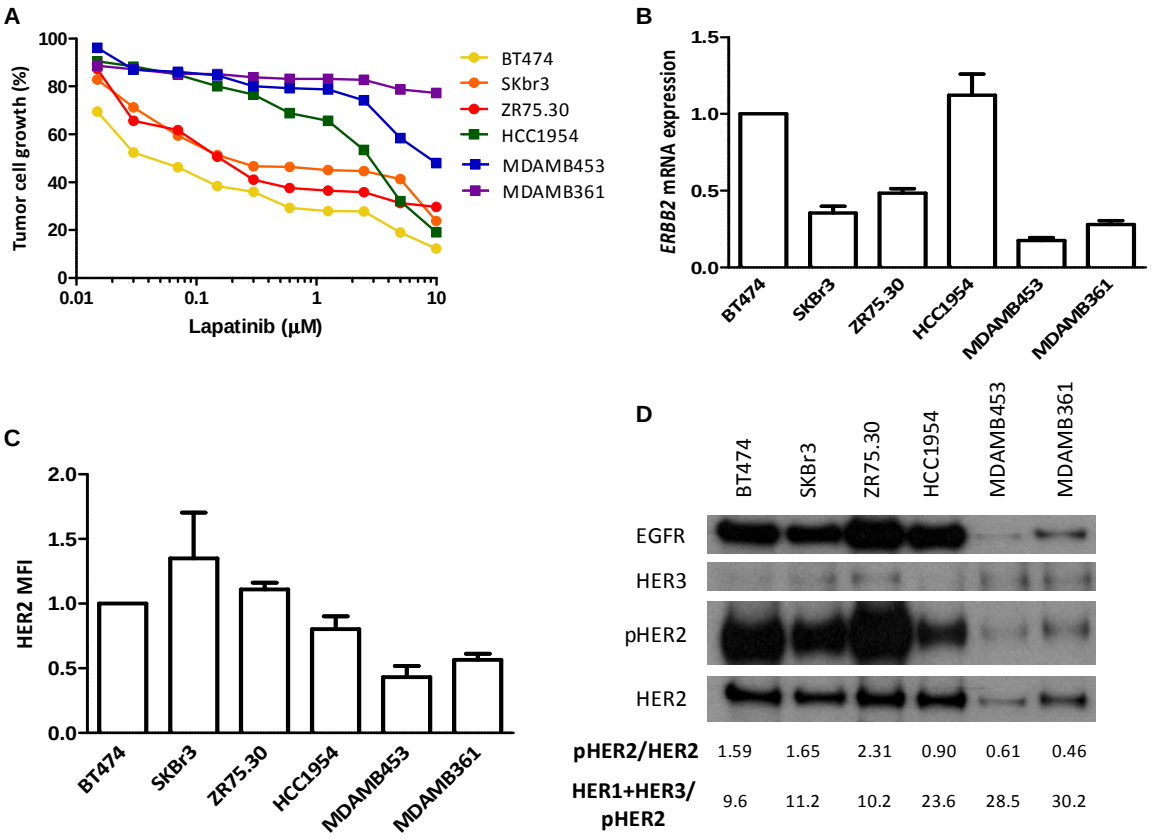

Figure 58. Characterisation of HER2-positive BC cell lines
A) Lapatinib dose response curves for HER2-positive BC cell lines. Data are normalised on untreated cells and are representative of two independent experiments. **B)** *ERBB2* mRNA levels as evaluated by qRT-PCR. Data are mean ± SD of three independent experiments and are ratio to BT474 *ERBB2* expression levels. **C)** Membrane-associated HER2 as evaluated by flow-cytometry analysis. Data are mean± SD of two independent experiments and are ratio to BT474 HER2 protein levels. **D)** Western blot analysis of HER2-positive BC cell extracts after immunoprecipitation with anti-HER2 antibodies. Images are representative of one of two independent experiments. Ratios were calculated on band quantification by Quantity One (Bio-Rad, Hercules, CA).

In accordance with these data, HER2-addicted BC cell lines showed a higher *ERBB2* gene amplification rate than non-addicted (BT474: 6.8, SKBR3: 7.1, ZR75.30: 7.9, HCC1954: 6.7, MDAMB453: 5.2, MDAMB361: 5.3). Amplification ratio was correlated

with HER2 protein amount [HER2 median fluorescent intensity (MFI)], as analysed by flow cytometry, but not with the mRNA amount (Table 20) in two independent experiments, supporting data observed in human samples. Notably, while *ERBB2* mRNA did not correlate with HER2 protein amount (r=0.19, p=0.7245) a trend toward significant correlation (r=0.7521, p=0.0846) was found between *ERBB2* mRNA and HER2 activation status (pHER2/HER2), as analysed by WB, suggesting that also in human samples HER2 transcription could reflects HER2 activation status.

Table 20. Correlation between *ERBB2* amplification and its mRNA and protein amount

	HER2 mRNA exp1	**HER2 mRNA exp2**	**HER2 MFI exp1**	**HER2 MFI exp2**
Pearson r	0.47	0.32	0.79	0.77
p-value	0.3475	0.5366	0.0587	0.0717

MFI: median fluorescence intensity

To investigate whether *ERBB2* mRNA levels reflected sensitivity of BC cells to trastuzumab activity, trastuzumab-mediated ADCC assay was performed *in vitro* with HER2-positive BC cell lines as target and peripheral blood mononuclear cells (PBMC), obtained from independent healthy donors, as effector cells. A trend toward higher sensitivity of HER2-addicted cells (BT474 and SKBR3) than non-addicted (MDAMB361 and MDAMB453) to trastuzumab-mediated ADCC was observed (p=0.1073, Fig. 59A). Notably, *ERBB2* expression correlated with trastuzumab-mediated ADCC (r=0.96, p=0.038), whereas no correlation was found between ADCC and membrane-associated HER2, as assessed by flow cytometry (Fig. 59B), indicating that also in BC cell lines *ERBB2* mRNA levels mirror dependence to the oncogene and predict response to trastuzumab.

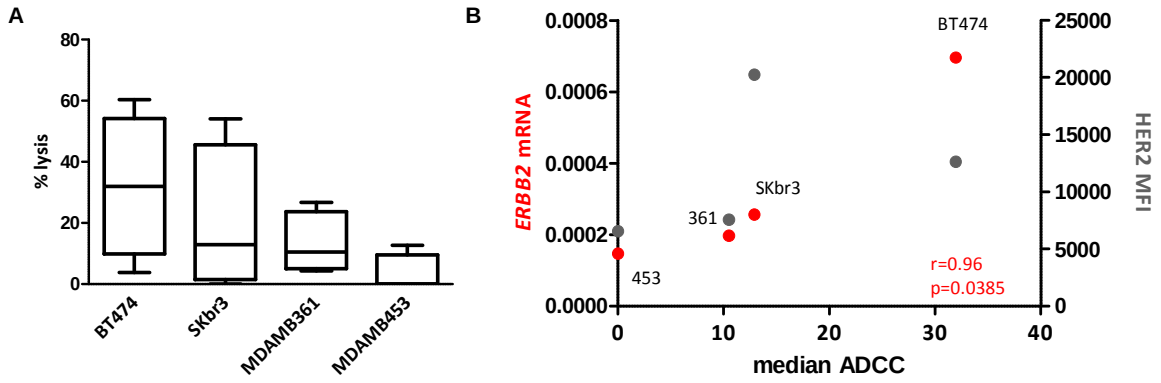

Figure 59. Correlation between HER2 expression and trastuzumab-mediated ADCC
A) ^{51}Cr labeled BC cell lines were cultured for 4 hours with PBMCs isolated from healthy donors' blood in medium containing trastuzumab (4 µg/ml). Shown are percentages of lysis of target cells at 50 effector/ 1 target cells ratio of PBMCs from independent donors (n=6). **B)** Correlation between median ADCC and *ERBB2* mRNA (left axis) and protein expression levels (right axis) as assessed by qRT-PCR and flow citometry respectively. Pearson's coefficient and relative p-value are shown.

3.5.3 Regulation of ERBB2 transcription by oncogene downstream signals

Based on above described results and on the higher described activation of HER2 downstream signaling pathway in HER2-E tumours [Cancer Genome Atlas Network, 2012], we investigated *in vitro* whether *ERBB2* mRNA transcription could depend on HER2 signals. HER2-positive BC cells were treated with lapatinib or EGF/HRG to block and activate the receptor, respectively, and analysed for HER2 protein content and activation by WB and for *ERBB2* levels by qRT-PCR. Contrary to expectations, lapatinib treatment, that blocked HER2 protein on the cell membrane and switched off its downstream signals (Fig. 60A), induced a significant increase in *ERBB2* transcription in almost all cell lines (Fig. 60B). Moreover, stimulation of HER2 downstream signals by 20 ng/ml EGF/HRG treatment for 6 h (Fig. 60C) induced a reduction in *ERBB2* mRNA levels both in BT474 and in MDAMB361 cells, representative of HER2-addicted and non-addicted cells, respectively (Fig. 60D).

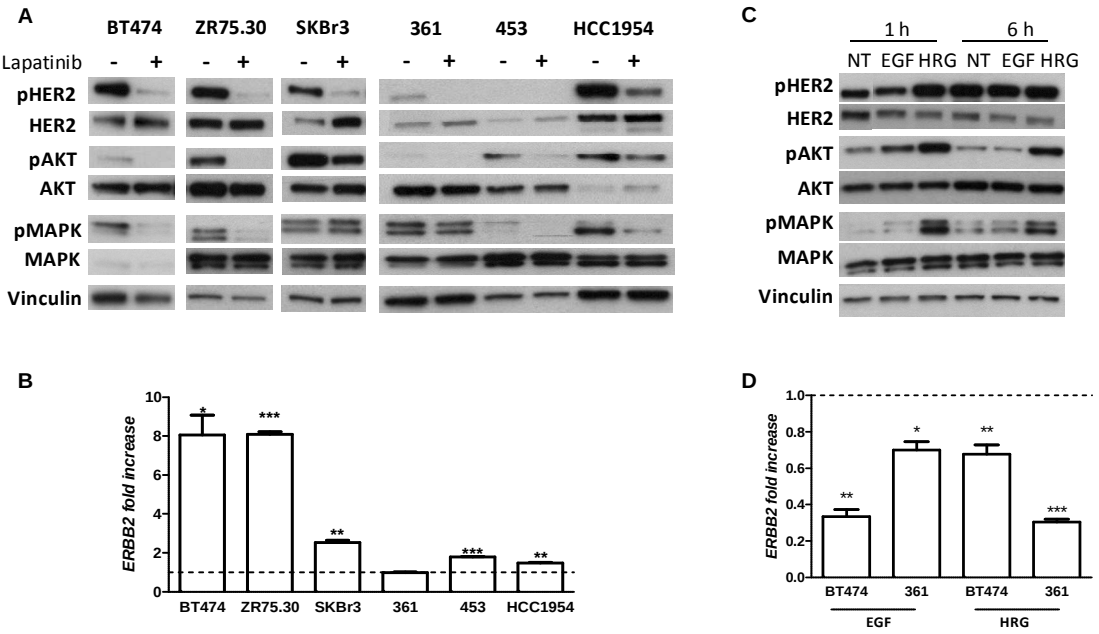

Figure 60. *ERBB2* expression modulation in HER2-positive BC cell lines
A-C) WB analysis of signaling molecules downstream HER2 receptor upon treatment with 0.3 μM lapatinib for 24 h in HER2-positive BC cells (A) or with 20 ng/ml EGF/HRG for 1 h and 6 h (C) in BT474 cells. Vinculin is used as protein loading control. **B-D)** *ERBB2* mRNA expression in cells treated as in A and C, respectively. Shown are the mean and SD of fold increases in treated versus untreated cells (dotted lines). *p<0.05, **p<0.01, ***p<0.001 by unpaired t-test. Data are representative of two independent experiments.

These data indicated that *in vitro ERBB2* mRNA levels are regulated by HER2 downstream signals, but contrary to expectation HER2 activation and inhibition reduced and augment, respectively its transcription within BC cell lines. AKT activation could be responsible for *ERBB2* modulation, as recently proposed [Awasthi and Hamburger, 2014]. In accordance with this paper, we found that AKT phosphorilation by EGF/HRG treatment repressed, while its shutdown caused by lapatinib, induced *ERBB2* transcription. Of note, AKT regulation of *ERBB2* levels could not explain differences in *ERBB2* mRNA levels observed in human HER2-positive BC according to TRAR or PAM50 classifications. It is likely that HER2, described to be tightly regulated by several transcriptional factors in HER2-negative tumours [Birnbaum et al., 2009], is subjected to regulation by other factors (like ER) relevant for trastuzumab activity. In support of this hypothesis, that will be the topic of future studies, GHEA tumours with high ER activity are the ones with lower

ERBB2 transcription levels and a highly significant correlation (r=0.71, p=0.0046) was found between *ERBB2* mRNA and its amplification levels in ER-negative tumours.

CHAPTER 4: DISCUSSION

Expression of HER2, determined by IHC or FISH is insufficient for selection of patients who will benefit from trastuzumab. Both our unsupervised and semi-supervised analyses of whole-transcriptome expression profiles of 53 BCs identified tumours with significantly different clinical outcomes upon adjuvant trastuzumab-based therapy. Indeed, unsupervised consensus clustering defined three main tumour subgroups, with tumours in the HER2-III subgroup showing considerably better clinical outcome than the HER2-I or HER-II subgroups despite similar clinico-pathological characteristics in all three groups. Most remarkably, HER2-III tumours were almost all classified as low-risk using the TRAR model, strongly suggesting that the particular tumour molecular portrait associated with trastuzumab benefit defines a biologically homogeneous subgroup of HER2-positive patients.

Unlike previous works [Perez et al., 2014; Pogue-Geile et al., 2013], to create the TRAR model we did not base our gene selection on an empirical or biological approach, but instead we applied a pre-developed semi-supervised learning method [Bair and Tibshirani, 2004] to our dataset. The ability of TRAR model to specifically identify tumours that respond to trastuzumab-containing therapy, but not to chemotherapy alone, indicates that the molecular characteristics detected are specific in predicting benefit from HER2-targeted therapy. Indeed, TRAR-low BCs did not show better prognosis when treated with chemotherapy alone. Consistent with these findings, HDPP, which is predictive of outcome in HER2-positive patients treated with chemotherapy alone [Staaf et al., 2010], was inversely associated with TRAR classification in trastuzumab-treated patients. Moreover, the response predictive value of our molecular signature in patients treated with neoadjuvant trastuzumab indicates that the molecular portrait is strictly related to trastuzumab sensitivity rather than to low aggressiveness of the tumour.

Our analyses pointed to the relevance of simultaneous high *ERBB2* and low *ESR1* levels in dictating trastuzumab efficacy, as demonstrated by the association of these characteristics with cluster HER2-III as well as with TRAR-low cases. Thus, among the ~20,000 genes analysed for expression levels, *ERBB2* and *ESR1* mRNA levels are those crucial in mirroring HER2 activity and, in turn, addiction of tumour cells to the oncogene and tumour susceptibility to anti-HER2 therapy. The association of TRAR-low tumour subset with the HER2-E intrinsic profile further supports the notion that tumours with the highest activation of HER2 signal are those most sensitive to trastuzumab action. Additionally, our analysis revealed the existence of a TRAR-low subset of tumours not strictly dependent on HER2 signals (non-HER2-E) that takes advantage of trastuzumab-containing treatment, suggesting that TRAR predicts trastuzumab benefit better than does PAM50. TRAR-high tumours might instead grow through signals derived from other receptors (e.g., ER, IGF1R), with consequent low benefit from anti-HER2 therapy. The observation that low expression of *ESR1* is associated with good benefit from trastuzumab is consistent with several lines of evidence suggesting that ER signaling is a mediator of trastuzumab resistance [Nahta and O'regan, 2012]. Remarkably, our molecular classifications were not distinguishable based on ER/PR IHC status, indicating that clinical evaluation of hormone receptors does not strictly correlate with their action in tumour progression. The same was true for *ERBB2* that showed high heterogeneity in its mRNA and protein levels in HER2-positive BCs of GHEA cohort. While *ERBB2* mRNA levels were predictive of trastuzumab benefit, as suggested by its presence in other predictive signatures [Pogue-Geile et al., 2013; Roepman et al., 2009; Park et al., 2014], HER2 protein amount did not associate with trastuzumab benefit. The same was found in the FinHer trial where HER2 expression, evaluated by the quantitative assay HERmark, was highly heterogeneous and was not significantly associated with outcome of patients

treated with trastuzumab [Joensuu et al., 2011]. Our *in vitro* analyses of *ERBB2* mRNA modulation by HER2 signaling did not help in understanding the reason behind its heterogeneity in human samples. Indeed, *ERBB2* modulation *in vitro* was found strictly dependent on and inversely associated with AKT activation status, as recently suggested [Awasthi and Hamburger, 2014]. Taking into consideration that in TCGA dataset HER2-E tumours have both high expression of *ERBB2* and high activation of PI3K/AKT pathway [Cancer Genome Atlas Network, 2012], it is likely that *ERBB2* mRNA expression levels in human samples are tightly regulated by factors, relevant in trastuzumab activity, other than AKT. Based on the relation between ER expression and trastuzumab inefficacy [Triulzi et al, 2016], its activity as direct regulator of *ERBB2* transcription [Giuliano et al., 2013] and as inhibitor of NF-kB transcription factor [Biswas et al., 2004], it is conceivable that ER is the player in *ERBB2* mRNA regulation. Further studies are needed to demonstrate the role of ER, but the lack of correlation between *ERBB2* mRNA levels and its amplification ratio (FISH ratio) only in ER positive tumours strongly sustained its involvement, reccomanding a dual (ER and HER2) block treatment in triple positive tumours (HER2-, ER- and PR-positive). In this context, clinical trials concomitantly blocking HER2 and ER activity to prevent the shift between these two oncogenic signaling pathways have been already performed [Jones, 2003]. However, in these trials the activity of the dual blockade has been compared with that of endocrine therapy alone rather than of trastuzumab alone. Thus, new studies are warranted to confirm or discard ER involvement.

In order to identify the biological characteristics of HER2-positive BCs according to their susceptibility to trastuzumab we exploited the whole-transcriptome profile of tumours of GHEA cohort: pathway analysis revealed that the HER2-III cluster as well as TRAR-low subset is enriched in expression of immune-associated pathways, pointing to the

existence in the same tumours of both HER2 dependency and immune infiltration. In this context, we found that tumours of patients who benefit from trastuzumab have significantly higher CD8+ T cells in their microenvironment, pointing for the first time in clinical samples to the relevance of these cells for trastuzumab activity, so far described only in preclinical models [Stagg et al., 2011; Park et al., 2010]. The association of CD8+ T cells and trastuzumab benefit is consistent with the predictive ability of pre-existing CD8+ T cells in the TME for a variety of therapies, like immunotherapies (IL2 therapies, checkpoint inhibitors and therapeutic cancer vaccines), chemotherapy and radiotherapy [Peske et al., 2015]. Notably, the association between HER2-dependence and a peculiar immune phenotype, found in the TME, was found also in the circulation. Indeed, patients of the Neo-INT and TRUP cohort with tumours highly dependent on HER2 signals expressed high levels of NKG2D on their circulating NK cells. Moreover, high NKG2D expression on NK cells was found associated with a high trastuzumab-mediated ADCC *in vitro* supporting their high activation. Accordingly, NKG2D receptor was demonstrated to be highly implicated in ADCC, inducing NK activation and degranulation rather than adhesion to tumour cells [Deguine et al., 2012]. The relevance of circulating NKG2D-positive NK cells as indicators of antibody therapy success is strengthened by results of Fisher and coworkers [Fischer et al., 2006], who showed that circulating NK cells able to mediate ADCC specifically express NKG2D, but not NKp30 or NKp46 activating receptors. Moreover, the involvement of the NKG2D signals in increasing trastuzumab-mediated ADCC is in agreement with the increased activity of an anti-HER2-NKG2D ligand fusion protein targeting HER2 tumours and triggering lymphocytes that express the NKG2D receptor compared to anti-HER2 antibody alone in preclinical models [Cho et al., 2010]. These data, rather than supporting the exploration of the predictive performance of NKG2D expression on circulating NK cells and/or tumour associated CD8+ T cells in

identifying patients who will benefit from trastuzumab, suggest that in TRAR-low patients trastuzumab may elicit the recruitment of circulating NK cells prone to efficiently mediate ADCC and the anti-tumour activity of immune cells already present in the TME. This is in agreement with observations in tumours of other histotypes (i.e., gastrointestinal stromal tumour, BRAF-driven melanoma, T-cell acute lymphoblastic lymphoma and pro-B-cell leukemia) treated with inhibitors of their driver oncogenes [Balachandran et al., 2011; Knight et al., 2013; Rakhra et al., 2010].

From a clinical point of view, comparison in an independent large cohort of patients of the predictive performance of tumour dependence on HER2 signal and immune features (number of TIL, number of CD8+ T cells or NKG2D expression) alone or combined, as in TRAR model, will allow the determination of the best method to identify tumours most sensitive to anti-HER2 drugs. Moreover, it is critical to understand whether in these patients trastuzumab alone is sufficient to create an immune microenvironment favourable to its activity, or whether chemotherapy, reported to induce immune system activation [Zitvogel et al., 2008], is always necessary to generate a host anti-tumour immune response favouring trastuzumab activity. Indeed, chemotherapy can trigger a Th1 anticancer immune response, boost an already ongoing CTL response and generate it *de novo* [Laoui et al., 2013]. Indeed, TIL-negative BCs can become positive upon treatment with paclitaxel chemotherapy or adryamicin and lapatinib [Laoui et al., 2013]. Accordingly, chemotherapy treatment in INT-Neo cohort induced an increment in NK activation through upmodulation of NKG2D expression, even if it caused a reduction in in the number of peripheral blood NK cell, as expected [Mozaffari et al., 2007]. This up-modulation supports the relevance of chemotherapy in improving the ability of trastuzumab to trigger host immune effectors against tumour cells. Moreover, it could explain the reported synergy between trastuzumab and docetaxel in HER2-positive BC

patients and in nude mice bearing HER2-positive tumours and treated with the two drugs in combination [Petrelli et al., 2011; Pegram et al., 2004]. Although based on a small subset of patients, our data suggest that the benefit of taxanes in improving trastuzumab-mediated ADCC occurs mainly in patients with low basal cytotoxic activity of their immune effector cells and with potentially low responsiveness to trastuzumab-mediated ADCC. Indeed, the meager enhancement of NKG2D after chemotherapy recorded in women with elevated basal NKG2D expression does not appear to support the relevance of chemotherapy in improving trastuzumab activity in patients with basal high lytic activity of effector cells. This is consistent with the association between low expression of TRAR indices (TRAR-low) and high expression of NKG2D in patients of the TRUP cohort that respond to one cycle of trastuzumab alone.

Notably, in analyses of the TRUP_AB cohort we found that also trastuzumab alone is able to modulate the TME-associated immune contexture and again this modification is not a common feature of all tumours. Indeed, the increment in MHC-II, LCK and HCK metagene expression after trastuzumab treatment was inversely correlated with their pre-treatment expression, suggesting that tumours with low infiltration of immune cells in their TME could respond to treatment if trastuzumab succeeds in modyfing the TME. Since such patients as well as those with TRAR-low tumours or high NKG2D expression on NK cells before any treatment are also those who reached a pCR, it remains to be determined whether trastuzumab alone might be sufficient for a pCR in such patients, as suggested by our results, or whether the addition of chemotherapy is always necessary to generate a long-lasting response. To this end, evaluation of such features on tumours from patients of Neosphere or PAMELA trials, who received only HER2-targeted therapies, would clarify this issue.

Based on the introduction of pertuzumab in combination with trastuzumab in the clinical practice in neoadjuvant setting and its plausible introduction also in the adjuvant setting, it would be relevant to understand whether patients with TRAR-low tumours need the addition of another HER2-targeted agent or whether trastuzumab alone is sufficient to induce clinical benefit. In this context analyses of Neosphere trial, comparing the percentage of pCR according to terzile partition of immune signature expression, showed that the addition of pertuzumab to trastuzumab increase the number of pCR compared to trastuzumab alone only in patients belonging to the lowest tertile (i.e with low expression of immune genes) [Bianchini et al., 2015], suggesting that these patients would benefit from the HER2-double blockage while those with high expression of immune genes would not need the addition of this costly drug.

From a biological perspective, the presence of both tumour addiction to HER2 signals and immune infiltration in TRAR-low tumours, and the association of both features to response to trastuzumab monotherapy in the TRUP_AB cohort strongly support a direct connection between these two features, with HER2 directly shaping the tumour immune infiltration and thus potentially explaining the ability of either features to predict disease outcome in trastuzumab-treated patients. This speculation is also supported by the fact that immune microenvironment of the primary tumour is predictive of trastuzumab benefit both in neoadjuvant and in adjuvant setting, when the primary tumour has been surgically removed and therapy is directed against micrometastatic tumour foci. The high production of chemokines commonly associated with T-cell trafficking, including CXCR3 ligands (CXCL9, CXCL10, and CXCL11), by TRAR-low tumour cells supports a direct recruitment of immune cells in the TME by tumour cells, anywhere they are in the body. CXCR3-ligands is the major chemokine axis enabling TIL entry into tumours [Peske et al., 2015], and was associated with TIL infiltration in several tumour models [Sharma et al.,

2015]. However, our preclinical data support a role for the HER2 oncogene only in the regulation of CCL2 chemokine, the main mediator of monocyte recruitment. Accordingly, TRAR-low tumours compared to TRAR-high were found more infiltrated by macrophages, and CCL2 depletion by antibodies treatment in preclinical models reduced F4/80 positive cells in the tumour site. The demonstrated NF-kB involvement in the regulation of CCL2 in HER2-positive BC cells is in line with the therapeutic activity of trastuzumab mainly in ER negative tumours. Indeed, NF-kB activation in BCs was found negatively associated with ER positivity [Biswas et al., 2004]. In details, among HER2-positive tumours, only BCs strictly dependent on HER2 (ER-negative) showed activation of this pathway, while ER-positive tumours were nearly all NF-kB negative, in accordance with the inhibitory crosstalk between NF-kB and ER signaling [Biswas et al., 2004]. Moreover, in the TCGA dataset HER2-E tumours, that are mainly ER-negative, have high activation of PI3K/AKT pathway [Cancer Genome Atlas Network, 2012], the upstream regulator of NF-kB, supporting CCL2 regulation by HER2 also in human samples. Thus, HER2 amplification and signaling in ER-negative tumours could generate an inflammatory environment as was described for other oncogenes like RET/PTC in thyroid cancer [Borrello et al., 2005], RAF in melanoma and MYC in pancreatic tumours [Mantovani et al., 2008]. In these inflamed and aggressive tumours, the NF-kB transcription factor acts as mediator of TME modifications that in turn exert many tumour promoting effects, inducing tumour proliferation, survival, angiogenesis and metastasis [Mantovani et al., 2008; Brady et al., 2016]. Moreover, growth factor such as EGF/HRG secreted by TAM [Brady et al., 2016] could boost HER2 signaling and CCL2 production amplifying the modification of the overall composition of the TME. T cells infiltration in the TME could be directly regulated by CCL2, as supported by our *in vivo* data, or derive from the development of the cancer immunity cycle triggered by macrophage ability to engulf and present antigens using MHC

molecules. IFN-γ rich TME, described to be crucial for Th1 immunity and trastuzumab response [Nocera et al., 2016], could be the inducer of CXCL expression in tumour cells of TRAR-low tumours. Infiltration of tumours by T cells could instead be associated with tumour antigenicity derived by a high mutational burden, as demonstrated in melanoma and lung cancer patients who respond to immune-checkpoint inhibitor [Van Allen et al., 2015; McGranahan et al., 2016; Snyder et al., 2014]. The low mutational burden of BCs compared to melanoma [Schumacher and Schreiber, 2015], and the lack of association between trastuzumab activity and neoantigen expression in tumours of the FinHer trial [Loi *et al*, 2014a], requests further analyses to understand whether immunogenicity could explain tumour infiltration by adaptive immune cells.

Irrespectively of the recruiting mechanism, TRAR-low tumours contains a high number of T cells likely to be specific for tumour-associated antigens, as indicated by clonal analyses and tetramer staining of CD8+ T cells isolated from human tumours [Whiteside, 2008]. Moreover, the high expression of CXCR3 ligands by tumour cells together with enrichment in CXCR3 receptor supports the presence in the TME of anti-tumour effector cells. The concomitant high expression of PD-1 ligands in these tumours could be one of the mechanisms exploited by tumours cells to evade the immune control. Differently from melanoma patients, where PD-L1 expression was described to be a negative feedback mechanism that followed CD8+ T cell infiltration and to depend on their presence [Spranger et al., 2013; Taube et al., 2012], the modulation of PD-1 ligands by HER2 signals we demonstrated in BC cell lines, suggests that in BCs this immunosuppressive pathway could be also directly orchestrated by cancer cells. Evaluation of PD-L1 expression in human BCs in situ in relation to TIL infiltration and localization will reveal whether an adaptive mechanism or a constitutive oncogene-driven PD-L1 expression occurs in HER2-addicted tumours. This regulation presumes that activity

of trastuzumab in therapy-responsive tumours derives from antibody ability in relieving suppression of recruited antitumour effector immunity. This speculation also implies that combination of trastuzumab with immune checkpoint inhibitors would not be necessary in TRAR-low tumours, while it could represent a valuable strategy for non responsive tumours.

All these data strongly suggest that the baseline immunologic status of tumours is crucial for trastuzumab activity and provide suggestions for novel immune-modulating treatment strategies to improve immune activation and response to trastuzumab, especially in patients who do not benefit from this treatment.

CHAPTER 5: CONCLUSIONS AND FUTURE PERSPECTIVES

In conclusion, we here identified differences in the whole-transcriptome of primary HER2-positive BC predictive of trastuzumab benefit. We developed TRAR-model able to identify patients who reach a pCR and with good DFS when treated with trastuzumab in neoadjuvant and adjuvant settings, respectively. From the whole-gene expression profile and clinico-pathological characterization of HER2-positive BC we understood that tumors responsive to trastuzumab (TRAR-low) are those both with tumor dependence on HER2 signals and high infiltration of immune cells, particularly macrophages and CD8+ T cells. Unresponsive tumors, instead, do not strictly depend on HER2 for growth but exploit additional growth factor receptors (RTK) and ER, and show less immune cell infiltration. Moreover, through *in vitro* and *in vivo* analyses we found that activated HER2 oncogene directly regulates infiltration of immune cells in TME and their suppression by concomitantly inducing expression of CCL2 and PD-1 ligands (Fig. 61A).

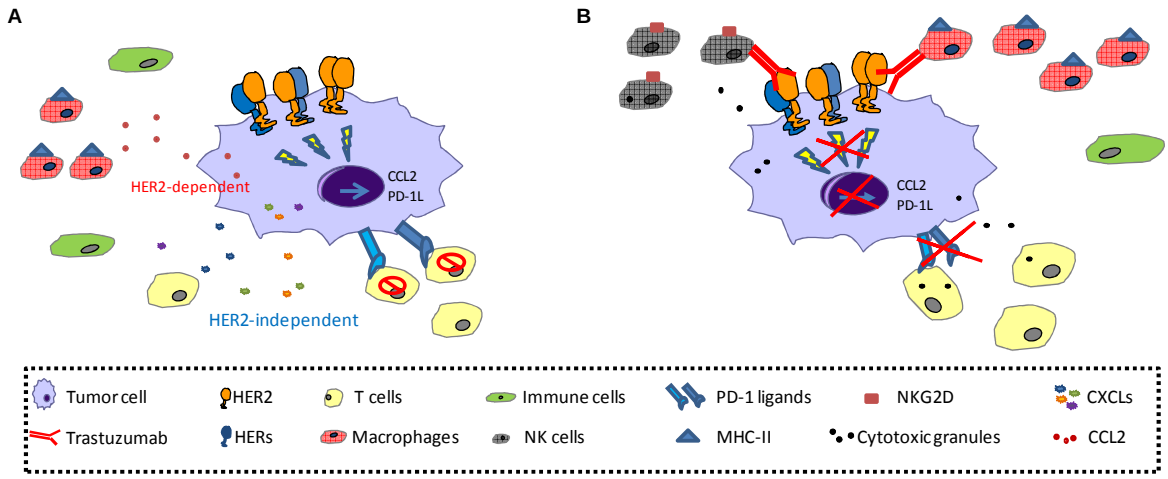

Figure 61. Schematic representation of TRAR-low BC features relevant for trastuzumab activity

A) Tumours responsive to trastuzumab have high HER2 signals, high expression of chemokines and high infiltration of immune cells, particularly macrophages and CD8+ T cells. CTL are likely to express PD-1 and to be inhibited by oncogene-induced expression of PD-1 ligands (PD-1L). **B)** Trastuzumab in these tumours both recruits NK cells and macrophages through its Fc and block HER2 signals causing the reactivation of CTL by suppressing PD-1L.

Thus, it is likely that trastuzumab efficacy in these tumors derives from its ability in recruiting highly activated NKG2D expressing NK cells, and macrophages and in relieving suppression of pre-existing antitumor effector cells (Fig. 61B).

The ongoing evaluation of TRAR scores in tumors of the NeoALTTO trial, will allow the validation in a big clinical trial of TRAR predictive power and the comparison with other predictive markers like PAM50. Moreover, this analysis will allow the definition of the predictive ability of TRAR also in the HER2 double blockade setting, since patients in one arm of NeoALTTO trial received trastuzumab in combination with lapatinib. In addition, the profiling of NeoALTTO biopsies obtained after a window of treatment with HER2-targeted therapy alone will allow the validation of features found modulated by trastuzumab, we detected in TRUP study, and their relevance in predicting trastuzumab clinical effectiveness.

The proof of the direct role of ER in blocking the dependence of tumours from the HER2 oncogene and the recruitment of pro-trastuzumab immune cells will encourage designing new clinical trial comparing the HER2/ER double blockade efficacy to that of HER2 targeted therapy alone in luminal B tumours. It is likely that also the timing of the double blockade should be evaluated: turning a luminal B tumour into HER2-E with a forefront inhibition of ER will make the tumour highly dependent on HER2 and highly infiltrated by immune cells, features relevant for the activity of the following treatment with trastuzumab.

From the other side, since the baseline immunologic status of tumours was found to be crucial for trastuzumab activity it is warranted to understand how to improve immune activation especially in patients who do not benefit from this treatment. In this context, the understanding of the mechanism through which NKG2D levels on NK cells are increased, the reason why trastuzumab recruits MHC-II positive cells only in some

tumours and the direct role of CCL2 in trastuzumab therapeutic efficacy, promise to help in improving trastuzumab activity through immunotherapy combinations in those patients who do not respond to treatment.

CHAPTER 6: REFERENCES

Alajati A, Sausgruber N, Aceto N, Duss S, Sarret S, Voshol H, Bonenfant D, tires-Alj M (2013) Mammary tumor formation and metastasis evoked by a HER2 splice variant. *Cancer Res* 73: 5320-5327 doi: 10.1158/0008-5472.CAN-12-3186.

Anido J, Scaltriti M, Bech Serra JJ, Santiago JB, Todo FR, Baselga J, Arribas J (2006) Biosynthesis of tumorigenic HER2 C-terminal fragments by alternative initiation of translation. *EMBO J* 25: 3234-3244

Arnould L, Gelly M, Penault-Llorca F, Benoit L, Bonnetain F, Migeon C, Cabaret V, Fermeaux V, Bertheau P, Garnier J, Jeannin JF, Coudert B (2006) Trastuzumab-based treatment of HER2-positive breast cancer: an antibody-dependent cellular cytotoxicity mechanism? *Br J Cancer* 94: 259-267

Arribas J, Borroto A (2002) Protein ectodomain shedding. *Chem Rev* 102: 4627-4638

Awasthi S, Hamburger AW (2014) Heregulin negatively regulates transcription of ErbB2/3 receptors via an AKT-mediated pathway. *J Cell Physiol* 229: 1831-1841

Bair E, Tibshirani R (2004) Semi-supervised methods to predict patient survival from gene expression data. *PLoS Biol* 2: E108

Balachandran VP, Cavnar MJ, Zeng S, Bamboat ZM, Ocuin LM, Obaid H, Sorenson EC, Popow R, Ariyan C, Rossi F, Besmer P, Guo T, Antonescu CR, Taguchi T, Yuan J, Wolchok JD, Allison JP, Dematteo RP (2011) Imatinib potentiates antitumor T cell responses in gastrointestinal stromal tumor through the inhibition of Ido. *Nat Med* 17: 1094-1100

Baselga J, Bradbury I, Eidtmann H, Di CS, De Azambuja E, Aura C, Gomez H, Dinh P, Fauria K, van D, V, Aktan G, Goldhirsch A, Chang TW, Horvath Z, Coccia-Portugal M, Domont J, Tseng LM, Kunz G, Sohn JH, Semiglazov V, Lerzo G, Palacova M, Probachai V, Pusztai L, Untch M, Gelber RD, Piccart-Gebhart M (2012) Lapatinib with trastuzumab for HER2-positive early breast cancer (NeoALTTO): a randomised, open-label, multicentre, phase 3 trial. *Lancet* 379: 633-640

Beano A, Signorino E, Evangelista A, Brusa D, Mistrangelo M, Polimeni MA, Spadi R, Donadio M, Ciuffreda L, Matera L (2008) Correlation between NK function and response to trastuzumab in metastatic breast cancer patients. *J Transl Med* 6:25.: 25

Becker JC, Andersen MH, Schrama D, Thor SP (2013) Immune-suppressive properties of the tumor microenvironment. *Cancer Immunol Immunother* 62: 1137-1148

Bellora F, Castriconi R, Dondero A, Carrega P, Mantovani A, Ferlazzo G, Moretta A, Bottino C (2014) Human NK cells and NK receptors. *Immunol Lett* 161: 168-173

Berns K, Horlings HM, Hennessy BT, Madiredjo M, Hijmans EM, Beelen K, Linn SC, Gonzalez-Angulo AM, Stemke-Hale K, Hauptmann M, Beijersbergen RL, Mills GB, van d, V, Bernards R (2007) A functional genetic approach identifies the PI3K pathway as a major determinant of trastuzumab resistance in breast cancer. *Cancer Cell* 12: 395-402

Bertelsen V, Stang E (2014) The Mysterious Ways of ErbB2/HER2 Trafficking. *Membranes (Basel)* 4: 424-446

Bianchini G, Gianni L (2014) The immune system and response to HER2-targeted treatment in breast cancer. *Lancet Oncol* 15: e58-e68 doi: 10.1016/S1470-2045(13)70477-7.

Bianchini G, Pusztai L, Pienkowski T, Im YH, Bianchi GV, Tseng LM, Liu MC, Lluch A, Galeota E, Magazzu D, de la Haba-Rodriguez J, Oh DY, Poirier B, Pedrini JL, Semiglazov V, Valagussa P, Gianni L (2015) Immune modulation of pathologic complete response after neoadjuvant HER2-directed therapies in the NeoSphere trial. *Ann Oncol* 26(12): 2429-2436 doi: 10.1093/annonc/mdv395.

Birnbaum D, Sircoulomb F, Imbert J (2009) A reason why the ERBB2 gene is amplified and not mutated in breast cancer. *Cancer Cell Int* 9: 5-9

Biswas DK, Shi Q, Baily S, Strickland I, Ghosh S, Pardee AB, Iglehart JD (2004) NF-kappa B activation in human breast cancer specimens and its role in cell proliferation and apoptosis. *Proc Natl Acad Sci U S A* 101: 10137-10142

Boone JJ, Bhosle J, Tilby MJ, Hartley JA, Hochhauser D (2009) Involvement of the HER2 pathway in repair of DNA damage produced by chemotherapeutic agents. *Mol Cancer Ther* 8: 3015-3023

Borrello MG, Alberti L, Fischer A, Degl'Innocenti D, Ferrario C, Gariboldi M, Marchesi F, Allavena P, Greco A, Collini P, Pilotti S, Cassinelli G, Bressan P, Fugazzola L, Mantovani A, Pierotti MA (2005) Induction of a proinflammatory program in normal human thyrocytes by the RET/PTC1 oncogene. *Proc Natl Acad Sci U S A* 102: 14825-14830

Brady NJ, Chuntova P, Schwertfeger KL (2016) Macrophages: Regulators of the Inflammatory Microenvironment during Mammary Gland Development and Breast Cancer. *Mediators Inflamm* 2016:4549676. doi: 10.1155/2016/4549676. Epub;%2016 Jan 17.: 4549676

Brenton JD, Carey LA, Ahmed AA, Caldas C (2005) Molecular classification and molecular forecasting of breast cancer: ready for clinical application? *J Clin Oncol* 23: 7350-7360

Burgess AW, Cho HS, Eigenbrot C, Ferguson KM, Garrett TP, Leahy DJ, Lemmon MA, Sliwkowski MX, Ward CW, Yokoyama S (2003) An open-and-shut case? Recent insights into the activation of EGF/ErbB receptors. *Mol Cell* 12: 541-552

Burkholder B, Huang RY, Burgess R, Luo S, Jones VS, Zhang W, Lv ZQ, Gao CY, Wang BL, Zhang YM, Huang RP (2014) Tumor-induced perturbations of cytokines and immune cell networks. *Biochim Biophys Acta* 1845: 182-201

Burstein HJ, Harris LN, Gelman R, Lester SC, Nunes RA, Kaelin CM, Parker LM, Ellisen LW, Kuter I, Gadd MA, Christian RL, Kennedy PR, Borges VF, Bunnell CA, Younger J, Smith BL, Winer EP (2003) Preoperative therapy with trastuzumab and paclitaxel followed by sequential adjuvant doxorubicin/cyclophosphamide for HER2 overexpressing stage II or III breast cancer: a pilot study. *J Clin Oncol* 21: 46-53

Buzdar AU, Valero V, Ibrahim NK, Francis D, Broglio KR, Theriault RL, Pusztai L, Green MC, Singletary SE, Hunt KK, Sahin AA, Esteva F, Symmans WF, Ewer MS, Buchholz TA, Hortobagyi GN (2007) Neoadjuvant therapy with paclitaxel followed by 5-fluorouracil,

epirubicin, and cyclophosphamide chemotherapy and concurrent trastuzumab in human epidermal growth factor receptor 2-positive operable breast cancer: an update of the initial randomized study population and data of additional patients treated with the same regimen. *Clin Cancer Res* 13: 228-233

Callahan R, Hurvitz S (2011) Human epidermal growth factor receptor-2-positive breast cancer: Current management of early, advanced, and recurrent disease. *Curr Opin Obstet Gynecol* 23: 37-43

Campiglio M, Bufalino R, Sasso M, Ferri E, Casalini P, Adamo V, Fabi A, Aiello R, Riccardi F, Valle E, Scotti V, Tabaro G, Giuffrida D, Tarenzi E, Bologna A, Mustacchi G, Bianchi F, Balsari A, Menard S, Tagliabue E (2013) Effect of adjuvant trastuzumab treatment in conventional clinical setting: an observational retrospective multicenter Italian study. *Breast Cancer Res Treat* 141: 101-110 doi: 10.1007/s10549-013-2658-z.

Cancer Genome Atlas Network (2012) Comprehensive molecular portraits of human breast tumours. *Nature* 490: 61-70

Carey, L. A., Berry, D. A., Ollila, D., Harris, L., Krop, I. E., Weckstein, D., Henry, N. L., Anders, C. K., Cirrincione, C., Winer, E. P., and Perou, C. M. Clinical and translational results of CALGB 40601: A neoadjuvant phase III trial of weekly paclitaxel and trastuzumab with or without lapatinib for HER2-positive breast cancer. J Clin Oncol 31 suppl, abstr 500. 2013.
Ref Type: Abstract

Castagnoli L, Iezzi M, Ghedini GC, Ciravolo V, Marzano G, Lamolinara A, Zappasodi R, Gasparini P, Campiglio M, Amici A, Chiodoni C, Palladini A, Lollini P, Triulzi T, Ménard S, Nanni P, Tagliabue E, Pupa SM (2014) Activated d16HER2 homodimers and Src kinase mediate optimal efficacy for trastuzumab. *Cancer Res* 74: 6248-6259 doi: 10.1158/0008-5472.CAN-14-0983.

Castiglioni F, Tagliabue E, Campiglio M, Pupa SM, Balsari A, Ménard S (2006) Role of exon-16-deleted HER2 in breast carcinomas. *Endocr Relat Cancer* 13: 221-232

Cescon DW, Bedard PL (2015) PIK3CA genotype and treatment decisions in human epidermal growth factor receptor 2-positive breast cancer. *J Clin Oncol* %20;33: 1318-1321

Cheang MC, Voduc D, Bajdik C, Leung S, McKinney S, Chia SK, Perou CM, Nielsen TO (2008) Basal-like breast cancer defined by five biomarkers has superior prognostic value than triple-negative phenotype. *Clin Cancer Res* 14: 1368-1376

Chen DS, Mellman I (2013) Oncology meets immunology: the cancer-immunity cycle. *Immunity* 39: 1-10

Cho HM, Rosenblatt JD, Tolba K, Shin SJ, Shin DS, Calfa C, Zhang Y, Shin SU (2010) Delivery of NKG2D ligand using an anti-HER2 antibody-NKG2D ligand fusion protein results in an enhanced innate and adaptive antitumor response. *Cancer Res* 70: 10121-10130

Citri A, Skaria KB, Yarden Y (2003) The deaf and the dumb: the biology of ErbB-2 and ErbB-3. *Exp Cell Res* 284: 54-65

Citri A, Yarden Y (2006) EGF-ERBB signalling: towards the systems level. *Nat Rev Mol Cell Biol* 7: 505-516

Clynes RA, Towers TL, Presta LG, Ravetch JV (2000) Inhibitory Fc receptors modulate in vivo cytoxicity against tumor targets. *Nat Med* 6: 443-446

Cortazar P, Zhang L, Untch M, Mehta K, Costantino JP, Wolmark N, Bonnefoi H, Cameron D, Gianni L, Valagussa P, Swain SM, Prowell T, Loibl S, Wickerham DL, Bogaerts J, Baselga J, Perou C, Blumenthal G, Blohmer J, Mamounas EP, Bergh J, Semiglazov V, Justice R, Eidtmann H, Paik S, Piccart M, Sridhara R, Fasching PA, Slaets L, Tang S, Gerber B, Geyer CE, Jr., Pazdur R, Ditsch N, Rastogi P, Eiermann W, von MG (2014) Pathological complete response and long-term clinical benefit in breast cancer: the CTNeoBC pooled analysis. *Lancet* 384: 164-172

Cox DR, Oakes D (1984) In *Analysis of Survival Data*, Chapman and Hall: London

Curtis C, Shah SP, Chin SF, Turashvili G, Rueda OM, Dunning MJ, Speed D, Lynch AG, Samarajiwa S, Yuan Y, Graf S, Ha G, Haffari G, Bashashati A, Russell R, McKinney S, Langerod A, Green A, Provenzano E, Wishart G, Pinder S, Watson P, Markowetz F, Murphy L, Ellis I, Purushotham A, Borresen-Dale AL, Brenton JD, Tavare S, Caldas C, Aparicio S (2012) The genomic and transcriptomic architecture of 2,000 breast tumours reveals novel subgroups. *Nature* 486: 346-352 doi: 10.1038/nature10983.

Damgaard RB, Nachbur U, Yabal M, Wong WW, Fiil BK, Kastirr M, Rieser E, Rickard JA, Bankovacki A, Peschel C, Ruland J, Bekker-Jensen S, Mailand N, Kaufmann T, Strasser A, Walczak H, Silke J, Jost PJ, Gyrd-Hansen M (2012) The ubiquitin ligase XIAP recruits LUBAC for NOD2 signaling in inflammation and innate immunity. *Mol Cell* 46: 746-758

Dawood S, Broglio K, Buzdar AU, Hortobagyi GN, Giordano SH (2010) Prognosis of women with metastatic breast cancer by HER2 status and trastuzumab treatment: an institutional-based review. *J Clin Oncol* 28: 92-98

De Cecco L, Bossi P, Locati L, Canevari S, Licitra L (2014) Comprehensive gene expression meta-analysis of head and neck squamous cell carcinoma microarray data defines a robust survival predictor. *Ann Oncol* 25: 1628-1635

de Ronde JJ, Rigaill G, Rottenberg S, Rodenhuis S, Wessels LF (2013) Identifying subgroup markers in heterogeneous populations. *Nucleic Acids Res* 41: e200

De P, Hasmann M, Leyland-Jones B (2013) Molecular determinants of trastuzumab efficacy: What is their clinical relevance? *Cancer Treat Rev* 39: 925-934

Deguine J, Breart B, Lemaitre F, Bousso P (2012) Cutting edge: tumor-targeting antibodies enhance NKG2D-mediated NK cell cytotoxicity by stabilizing NK cell-tumor cell interactions. *J Immunol* 189: 5493-5497

Di Modica M, Sfondrini L, Regondi V, Varchetta S, Oliviero B, Mariani G, Bianchi GV, Generali D, Balsari A, Triulzi T, Tagliabue E (2016) Taxanes enhance trastuzumab-mediated ADCC on tumor cells through NKG2D-mediated NK cell recognition. *Oncotarget* 7: 255-265

Du P, Kibbe WA, Lin SM (2008) Lumi: a pipeline for processing Illumina microarray. *Bioinformatics* 24:1547-1548.

Dushyanthen S, Beavis PA, Savas P, Teo ZL, Zhou C, Mansour M, Darcy PK, Loi S (2015) Relevance of tumor-infiltrating lymphocytes in breast cancer. *BMC Med* 13:202. doi: 10.1186/s12916-015-0431-3.: 202-0431

Egeblad M, Nakasone ES, Werb Z (2010) Tumors as organs: complex tissues that interface with the entire organism. *Dev Cell* 18: 884-901

Engel RH, Kaklamani VG (2007) HER2-positive breast cancer: current and future treatment strategies. *Drugs* 67: 1329-1341

Engelman JA (2009) Targeting PI3K signalling in cancer: opportunities, challenges and limitations. *Nat Rev Cancer* 9: 550-562

Eroglu Z, Tagawa T, Somlo G (2014) Human epidermal growth factor receptor family-targeted therapies in the treatment of HER2-overexpressing breast cancer. *Oncologist* 19: 135-150

Eroles P, Bosch A, Perez-Fidalgo JA, Lluch A (2012) Molecular biology in breast cancer: intrinsic subtypes and signaling pathways. *Cancer Treat Rev* 38: 698-707

Fischer L, Penack O, Gentilini C, Nogai A, Muessig A, Thiel E, Uharek L (2006) The anti-lymphoma effect of antibody-mediated immunotherapy is based on an increased degranulation of peripheral blood natural killer (NK) cells. *Exp Hematol* 34: 753-759

Franciszkiewicz K, Boissonnas A, Boutet M, Combadiere C, Mami-Chouaib F (2012) Role of chemokines and chemokine receptors in shaping the effector phase of the antitumor immune response. *Cancer Res* 72: 6325-6332

Fumagalli D, Venet D, Ignatiadis M, Azim HA Jr, Maetens M, Rothé F, Salgado R, Bradbury I, Pusztai L, Harbeck N, Gomez H, Chang TW, Coccia-Portugal MA, Di Cosimo S, de Azambuja E, de la Peña L, Nuciforo P, Brase JC, Huober J, Baselga J, Piccart M, Loi S, Sotiriou C (2016) RNA Sequencing to Predict Response to Neoadjuvant Anti-HER2 Therapy: A Secondary Analysis of the NeoALTTO Randomized Clinical Trial. JAMA Oncol. Sep 29.

Gabrilovich DI, Nagaraj S (2009) Myeloid-derived suppressor cells as regulators of the immune system. *Nat Rev Immunol* 9: 162-174

Gallardo A, Lerma E, Escuin D, Tibau A, Muñoz J, Ojeda B, Barnadas A, Adrover E, Sánchez-Tejada L, Giner D, Ortiz-Martínez F, Peiró G (2012) Increased signalling of EGFR and IGF1R, and deregulation of PTEN/PI3K/Akt pathway are related with trastuzumab resistance in HER2 breast carcinomas. *Br J Cancer* 106:1367-73

Gasparini P, Bertolini G, Binda M, Magnifico A, Albano L, Tortoreto M, Pratesi G, Facchinetti F, Abolafio G, Roz L, Tagliabue E, Daidone MG, Sozzi G (2010) Molecular cytogenetic characterization of stem-like cancer cells isolated from established cell lines. *Cancer Lett* 296: 206-215

Gasser S, Orsulic S, Brown EJ, Raulet DH (2005) The DNA damage pathway regulates innate immune system ligands of the NKG2D receptor. *Nature* 436: 1186-1190

Gavin PG, Song N, Kim SR, Pogue-Geile KL, Paik S (2015) Immune Signature to Predict Trastuzumab Benefit: Potential and Pitfalls. *J Clin Oncol* 33: 3671-3672

Gennari R, Ménard S, Fagnoni F, Ponchio L, Scelsi M, Tagliabue E, Castiglioni F, Villani L, Magalotti C, Gibelli N, Oliviero B, Ballardini B, Da Prada G, Zambelli A, Costa A (2004) Pilot study of the mechanism of action of preoperative trastuzumab in patients with primary operable breast tumors overexpressing HER2. *Clin Cancer Res* 10: 5650-5655

Gentleman RC, Carey VJ, Bates DM, Bolstad B, Dettling M, Dudoit S, Ellis B, Gautier L, Ge Y, Gentry J, Hornik K, Hothorn T, Huber W, Iacus S, Irizarry R, Leisch F, Li C, Maechler M, Rossini AJ, Sawitzki G, Smith C, Smyth G, Tierney L, Yang JY, Zhang J (2004) Bioconductor: open software development for computational biology and bioinformatics. *Genome Biol* 5: R80

Ghatak S, Misra S, Toole BP (2005) Hyaluronan constitutively regulates ErbB2 phosphorylation and signaling complex formation in carcinoma cells. *J Biol Chem* 280: 8875-8883

Ghosh R, Narasanna A, Wang SE, Liu S, Chakrabarty A, Balko JM, Gonzalez-Angulo AM, Mills GB, Penuel E, Winslow J, Sperinde J, Dua R, Pidaparthi S, Mukherjee A, Leitzel K, Kostler WJ, Lipton A, Bates M, Arteaga CL (2011) Trastuzumab has preferential activity against breast cancers driven by HER2 homodimers. *Cancer Res* 71: 1871-1882

Gianni, L., Eiermann, W., Pusztai, L., Semiglazov, V. F., Hoegel, B., Koehler, A., Manikhas, G., Bates, M., Valagussa, P., and Baselga, J. Biomarkers as potential predictors of pathologic complete response (pCR) in the NOAH trial of neoadjuvant trastuzumab in patients (pts) with HER2-positive locally advanced breast cancer (LABC). ASCO Annual Meeting Proceedings. J Clin Oncol 26 suppl, 15-Abstr 504. 2015.
Ref Type: Abstract

Gianni L, Eiermann W, Semiglazov V, Manikhas A, Lluch A, Tjulandin S, Zambetti M, Vazquez F, Byakhow M, Lichinitser M, Climent MA, Ciruelos E, Ojeda B, Mansutti M, Bozhok A, Baronio R, Feyereislova A, Barton C, Valagussa P, Baselga J (2010) Neoadjuvant chemotherapy with trastuzumab followed by adjuvant trastuzumab versus neoadjuvant chemotherapy alone, in patients with HER2-positive locally advanced breast cancer (the NOAH trial): a randomised controlled superiority trial with a parallel HER2-negative cohort. *Lancet* 375: 377-384

Gianni L, Pienkowski T, Im YH, Roman L, Tseng LM, Liu MC, Lluch A, Staroslawska E, de la Haba-Rodriguez J, Im SA, Pedrini JL, Poirier B, Morandi P, Semiglazov V, Srimuninnimit V, Bianchi G, Szado T, Ratnayake J, Ross G, Valagussa P (2012) Efficacy and safety of neoadjuvant pertuzumab and trastuzumab in women with locally advanced, inflammatory, or early HER2-positive breast cancer (NeoSphere): a randomised multicentre, open-label, phase 2 trial. *Lancet Oncol* 13: 25-32

Giuliano M, Trivedi MV, Schiff R (2013) Bidirectional crosstalk between the Estrogen Receptor and Human Epidermal Growth Factor Receptor 2 signaling pathways in Breast Cancer: molecular basis and clinical implications. *Breast Care (Basel)* 8: 256-262

Gluck S, Ross JS, Royce M, McKenna EF, Jr., Perou CM, Avisar E, Wu L (2012) TP53 genomics predict higher clinical and pathologic tumor response in operable early-stage breast cancer treated with docetaxel-capecitabine +/- trastuzumab. *Breast Cancer Res Treat* 132: 781-791

Goldhirsch, A., Piccart-Gebhart, M. J., Procter, M., De Azambuja, E., Weber, H. A., Untch, M., Smith, I., Gianni, L., Jackisch, C., Cameron, D., Bell, R., Dowsett, M., Gelber, R. D., Leyland-Jones, B., Baselga, J., and On behalf of the HERA Study Team. HERA TRIAL: 2years versus 1 year of trastuzumab after adjuvant chemotherapy in women with HER2-positive early breast cancer at 8 years of median follow up. Cancer Research 72[24 suppl.], 103s (S5-2). 2013a.
Ref Type: Abstract

Goldhirsch A, Winer EP, Coates AS, Gelber RD, Piccart-Gebhart M, Thurlimann B, Senn HJ (2013b) Personalizing the treatment of women with early breast cancer: highlights of the St Gallen International Expert Consensus on the Primary Therapy of Early Breast Cancer 2013. *Ann Oncol* 24: 2206-2223

Goldhirsch A, Wood WC, Coates AS, Gelber RD, Thurlimann B, Senn HJ (2011) Strategies for subtypes--dealing with the diversity of breast cancer: highlights of the St. Gallen International Expert Consensus on the Primary Therapy of Early Breast Cancer 2011. *Ann Oncol* 22: 1736-1747

Gu-Trantien C, Loi S, Garaud S, Equeter C, Libin M, de WA, Ravoet M, Le BH, Sibille C, Manfouo-Foutsop G, Veys I, Haibe-Kains B, Singhal SK, Michiels S, Rothe F, Salgado R, Duvillier H, Ignatiadis M, Desmedt C, Bron D, Larsimont D, Piccart M, Sotiriou C, Willard-Gallo K (2013) CD4(+) follicular helper T cell infiltration predicts breast cancer survival. *J Clin Invest* 123: 2873-2892

Guarneri V, Dieci MV, Frassoldati A, Maiorana A, Ficarra G, Bettelli S, Tagliafico E, Bicciato S, Generali DG, Cagossi K, Bisagni G, Sarti S, Musolino A, Ellis C, Crescenzo R, Conte P (2015) Prospective biomarker analysis of the randomized CHER-LOB study evaluating the dual Anti-HER2 treatment with Trastuzumab and Lapatinib plus chemotherapy as neoadjuvant therapy for HER2-positive breast cancer. *Oncologist* 20: 1001-1010

Guarneri V, Frassoldati A, Bottini A, Cagossi K, Bisagni G, Sarti S, Ravaioli A, Cavanna L, Giardina G, Musolino A, Untch M, Orlando L, Artioli F, Boni C, Generali DG, Serra P, Bagnalasta M, Marini L, Piacentini F, D'Amico R, Conte P (2012) Preoperative chemotherapy plus trastuzumab, lapatinib, or both in human epidermal growth factor receptor 2-positive operable breast cancer: results of the randomized phase II CHER-LOB study. *J Clin Oncol* 30: 1989-1995

Guiu S, Michiels S, Andre F, Cortes J, Denkert C, Di LA, Hennessy BT, Sorlie T, Sotiriou C, Turner N, van d, V, Viale G, Loi S, Reis-Filho JS (2012) Molecular subclasses of breast cancer: how do we define them? The IMPAKT 2012 Working Group Statement. *Ann Oncol* 23: 2997-3006

Hammond ME, Hayes DF, Dowsett M, Allred DC, Hagerty KL, Badve S, Fitzgibbons PL, Francis G, Goldstein NS, Hayes M, Hicks DG, Lester S, Love R, Mangu PB, McShane L, Miller K, Osborne CK, Paik S, Perlmutter J, Rhodes A, Sasano H, Schwartz JN, Sweep FC,

Taube S, Torlakovic EE, Valenstein P, Viale G, Visscher D, Wheeler T, Williams RB, Wittliff JL, Wolff AC (2010) American Society of Clinical Oncology/College of American Pathologists guideline recommendations for immunohistochemical testing of estrogen and progesterone receptors in breast cancer (unabridged version). *Arch Pathol Lab Med* 134: e48-e72

Hanahan D, Weinberg RA (2011) Hallmarks of cancer: the next generation. *Cell* 144: 646-674

Harris LN, You F, Schnitt SJ, Witkiewicz A, Lu X, Sgroi D, Ryan PD, Come SE, Burstein HJ, Lesnikoski BA, Kamma M, Friedman PN, Gelman R, Iglehart JD, Winer EP (2007) Predictors of resistance to preoperative trastuzumab and vinorelbine for HER2-positive early breast cancer. Clin Cancer Res 13: 1198-1207

Heagerty PJ, Lumley T, Pepe MS (2000) Time-dependent ROC curves for censored survival data and a diagnostic marker. *Biometrics* 56:337-344

Herschkowitz JI, Simin K, Weigman VJ, Mikaelian I, Usary J, Hu Z, Rasmussen KE, Jones LP, Assefnia S, Chandrasekharan S, Backlund MG, Yin Y, Khramtsov AI, Bastein R, Quackenbush J, Glazer RI, Brown PH, Green JE, Kopelovich L, Furth PA, Palazzo JP, Olopade OI, Bernard PS, Churchill GA, van DT, Perou CM (2007) Identification of conserved gene expression features between murine mammary carcinoma models and human breast tumors. *Genome Biol* 8: R76

Hicks DG, Kulkarni S (2008) HER2+ breast cancer: review of biologic relevance and optimal use of diagnostic tools. *Am J Clin Pathol* 129: 263-273

Holbro T, Beerli RR, Maurer F, Koziczak M, Barbas CF, III, Hynes NE (2003) The ErbB2/ErbB3 heterodimer functions as an oncogenic unit: ErbB2 requires ErbB3 to drive breast tumor cell proliferation. *Proc Natl Acad Sci USA* 100: 8933-8938

Hoshida Y, Brunet JP, Tamayo P (2007) Subclass mapping: Identifying common subtypes in independent disease data sets. *PLoS ONE* 2: e1195

Huang X, Gao L, Wang S, McManaman JL, Thor AD, Yang X, Esteva FJ, Liu B (2010) Heterotrimerization of the growth factor receptors erbB2, erbB3, and insulin-like growth factor-i receptor in breast cancer cells resistant to herceptin. *Cancer Res* 70: 1204-1214

Hynes NE, MacDonald G (2009) ErbB receptors and signaling pathways in cancer. *Curr Opin Cell Biol* 21: 177-184

Izumi Y, Xu L, di Tomaso E, Fukumura D, Jain RK (2002) Tumour biology: herceptin acts as an anti-angiogenic cocktail. *Nature* 416: 279-280

Jemal A, Siegel R, Xu J, Ward E (2010) Cancer statistics, 2010. *CA Cancer J Clin* 60: 277-300

Joensuu H, Bono P, Kataja V, Alanko T, Kokko R, Asola R, Utriainen T, Turpeenniemi-Hujanen T, Jyrkkio S, Moykkynen K, Helle L, Ingalsuo S, Pajunen M, Huusko M, Salminen T, Auvinen P, Leinonen H, Leinonen M, Isola J, Kellokumpu-Lehtinen PL (2009) Fluorouracil, epirubicin, and cyclophosphamide with either docetaxel or

vinorelbine, with or without trastuzumab, as adjuvant treatments of breast cancer: final results of the FinHer Trial. *J Clin Oncol* 27: 5685-5692

Joensuu H, Kellokumpu-Lehtinen PL, Bono P, Alanko T, Kataja V, Asola R, Utriainen T, Kokko R, Hemminki A, Tarkkanen M, Turpeenniemi-Hujanen T, Jyrkkio S, Flander M, Helle L, Ingalsuo S, Johansson K, Jaaskelainen AS, Pajunen M, Rauhala M, Kaleva-Kerola J, Salminen T, Leinonen M, Elomaa I, Isola J (2006) Adjuvant docetaxel or vinorelbine with or without trastuzumab for breast cancer. *N Engl J Med* 354: 809-820

Joensuu H, Sperinde J, Leinonen M, Huang W, Weidler J, Bono P, Kataja V, Kokko R, Turpeenniemi-Hujanen T, Jyrkkio S, Isola J, Kellokumpu-Lehtinen PL, Paquet A, Lie Y, Bates M (2011) Very high quantitative tumor HER2 content and outcome in early breast cancer. *Ann Oncol* 22: 2007-2013

Jones A (2003) Combining trastuzumab (Herceptin) with hormonal therapy in breast cancer: what can be expected and why? *Ann Oncol* 14: 1697-1704

Joyce JA, Pollard JW (2009) Microenvironmental regulation of metastasis. *Nat Rev Cancer* 9: 239-252

Knight DA, Ngiow SF, Li M, Parmenter T, Mok S, Cass A, Haynes NM, Kinross K, Yagita H, Koya RC, Graeber TG, Ribas A, McArthur GA, Smyth MJ (2013) Host immunity contributes to the anti-melanoma activity of BRAF inhibitors. *J Clin Invest* 123: 1371-1381

Kohler BA, Sherman RL, Howlader N, Jemal A, Ryerson AB, Henry KA, Boscoe FP, Cronin KA, Lake A, Noone AM, Henley SJ, Eheman CR, Anderson RN, Penberthy L (2015) Annual Report to the Nation on the Status of Cancer, 1975-2011, Featuring Incidence of Breast Cancer Subtypes by Race/Ethnicity, Poverty, and State. *J Natl Cancer Inst* 107: djv048

Konecny GE, Pegram MD, Venkatesan N, Finn R, Yang G, Rahmeh M, Untch M, Rusnak DW, Spehar G, Mullin RJ, Keith BR, Gilmer TM, Berger M, Podratz KC, Slamon DJ (2006) Activity of the dual kinase inhibitor lapatinib (GW572016) against HER-2-overexpressing and trastuzumab-treated breast cancer cells. *Cancer Res* 66: 1630-1639

Köstler WJ, Hudelist G, Rabitsch W, Czerwenka K, Müller R, Singer CF, Zielinski CC (2006) Insulin-like growth factor-1 receptor (IGF-1R) expression does not predict for resistance to trastuzumab-based treatment in patients with Her-2/neu overexpressing metastatic breast cancer. *J Cancer Res Clin Oncol* 132:9-18.

Koukourakis MI, Giatromanolaki A, Bottini A, Cappelletti MR, Zanotti L, Allevi G, Strina C, Ardine M, Milani M, Brugnoli G, Martinotti M, Ferrero G, Bertoni R, Ferrozzi F, Harris AL, Generali D (2014) Prospective neoadjuvant analysis of PET imaging and mechanisms of resistance to Trastuzumab shows role of HIF1 and autophagy. *Br J Cancer* 110: 2209-2216

Kreike B, van KM, Horlings H, Weigelt B, Peterse H, Bartelink H, van d, V (2007) Gene expression profiling and histopathological characterization of triple-negative/basal-like breast carcinomas. *Breast Cancer Res* 9: R65

Kroemer G, Senovilla L, Galluzzi L, Andre F, Zitvogel L (2015) Natural and therapy-induced immunosurveillance in breast cancer. *Nat Med* 21: 1128-1138

Krop IE (2013) Targeted therapies: HER2-positive breast cancer-sifting through many good options. *Nat Rev Clin Oncol* 10: 312-313

Laoui D, Van OE, Van Ginderachter JA (2013) Unsuspected allies: chemotherapy teams up with immunity to fight cancer. *Eur J Immunol* 43: 2538-2542

Lazennec G, Richmond A (2010) Chemokines and chemokine receptors: new insights into cancer-related inflammation. *Trends Mol Med* 16: 133-144

Lee HJ, Seo AN, Kim EJ, Jang MH, Kim YJ, Kim JH, Kim SW, Ryu HS, Park IA, Im SA, Gong G, Jung KH, Kim HJ, Park SY (2015) Prognostic and predictive values of EGFR overexpression and EGFR copy number alteration in HER2-positive breast cancer. *Br J Cancer* 112:103-11

Lee MT, Liebow C, Kamer AR, Schally AV (1991) Effects of epidermal growth factor and analogues of luteinizing hormone-releasing hormone and somatostatin on phosphorylation and dephosphorylation of tyrosine residues of specific protein substrates in various tumors. *Proc Natl Acad Sci USA* 88: 1656-1660

Li CI, Uribe DJ, Daling JR (2005) Clinical characteristics of different histologic types of breast cancer. *Br J Cancer* 93: 1046-1052

Lipton A, Goodman L, Leitzel K, Cook J, Sperinde J, Haddad M, Köstler WJ, Huang W, Weidler JM, Ali S, Newton A, Fuchs EM, Paquet A, Singer CF, Horvat R, Jin X, Banerjee J, Mukherjee A, Tan Y, Shi Y, Chenna A, Larson J, Lie Y, Sherwood T, Petropoulos CJ, Williams S, Winslow J, Parry G, Bates M (2013) HER3, p95HER2, and HER2 protein expression levels define multiple subtypes of HER2-positive metastatic breast cancer. *Breast Cancer Res Treat* 141(1):43-53.

Loi S (2014a) Tumor infiltrating lymphocytes in breast cancers. 37th annual SABCS

Loi S, Michiels S, Salgado R, Sirtaine N, Jose V, Fumagalli D, Kellokumpu-Lehtinen PL, Bono P, Kataja V, Desmedt C, Piccart MJ, Loibl S, Denkert C, Smyth MJ, Joensuu H, Sotiriou C (2014b) Tumor infiltrating lymphocytes is prognostic and predictive for trastuzumab benefit in early breast cancer: results from the FinHER trial. *Ann Oncol* 25: 1544-1550

Loi S, Sirtaine N, Piette F, Salgado R, Viale G, Van Eenoo F, Rouas G, Francis P, Crown JP, Hitre E, De Azambuja E, Quinaux E, Di Leo A, Michiels S, Piccart MJ, Sotiriou C (2013) Prognostic and predictive value of tumor-infiltrating lymphocytes in a phase III randomized adjuvant breast cancer trial in node-positive breast cancer comparing the addition of docetaxel to doxorubicin with doxorubicin-based chemotherapy: BIG 02-98. *J Clin Oncol* 31: 860-867

Loibl, S., Bruey, J., Von Minckwitz, G., Huober, J. B., Press, M. F., Darb-Esfahani, S., Solbach, C., Denkert, C., Tesch, H., Holms, F., Fehm, T. N., and Mehta, K. Validation of p95 as a predictive marker for trastuzumab-based therapy in primary HER2-positive brest cancer: A traditional investigation from the neoadjuvant GeparQuattro study. J

Clin Oncol suppl, Abstr 530. 2015a.
Ref Type: Abstract

Loibl, S., Majewski, I., Guarneri, V., Nekljudova, V., McCormick Holmes, E., Bria, E., Denkert, C., Eidtmann, H., Sotiriou, C., Loi, S., Andre, F., Untch, M., Conte, P. F., Piccart-Gebhart, M. J., Von Minckwitz, G., Baselga, J., and German Breast Group. Correlation of *PIK3CA* mutation with pathological complete response in primary HER2-positive breast cancer: Combined analysis of 967 patients from three prospective clinical trials. J Clin Oncol 33 suppl, Abstr 511. 2015b.
Ref Type: Abstract

Loibl S, von MG, Schneeweiss A, Paepke S, Lehmann A, Rezai M, Zahm DM, Sinn P, Khandan F, Eidtmann H, Dohnal K, Heinrichs C, Huober J, Pfitzner B, Fasching PA, Andre F, Lindner JL, Sotiriou C, Dykgers A, Guo S, Gade S, Nekljudova V, Loi S, Untch M, Denkert C (2014) PIK3CA mutations are associated with lower rates of pathologic complete response to anti-human epidermal growth factor receptor 2 (her2) therapy in primary HER2-overexpressing breast cancer. *J Clin Oncol* 32: 3212-3220

Lu Y, Zi X, Pollak M (2004) Molecular mechanisms underlying IGF-I-induced attenuation of the growth-inhibitory activity of trastuzumab (Herceptin) on SKBR3 breast cancer cells. *Int J Cancer* 108: 334-341

Majewski IJ, Nuciforo P, Mittempergher L, Bosma AJ, Eidtmann H, Holmes E, Sotiriou C, Fumagalli D, Jimenez J, Aura C, Prudkin L, az-Delgado MC, de la Pena L, Loi S, Ellis C, Schultz N, De Azambuja E, Harbeck N, Piccart-Gebhart M, Bernards R, Baselga J (2015) PIK3CA mutations are associated with decreased benefit to neoadjuvant human epidermal growth factor receptor 2-targeted therapies in breast cancer. *J Clin Oncol* 33: 1334-1339

Mamessier E, Sylvain A, Bertucci F, Castellano R, Finetti P, Houvenaeghel G, Charaffe-Jaufret E, Birnbaum D, Moretta A, Olive D (2011) Human breast tumor cells induce self-tolerance mechanisms to avoid NKG2D-mediated and DNAM-mediated NK cell recognition. *Cancer Res* 71: 6621-6632

Mantovani A, Allavena P, Sica A, Balkwill F (2008) Cancer-related inflammation. *Nature* 454: 436-444

Marmor MD, Skaria KB, Yarden Y (2004) Signal transduction and oncogenesis by ErbB/HER receptors. *Int J Radiat Oncol Biol Phys* 58: 903-913

Marzec M, Zhang Q, Goradia A, Raghunath PN, Liu X, Paessler M, Wang HY, Wysocka M, Cheng M, Ruggeri BA, Wasik MA (2008) Oncogenic kinase NPM/ALK induces through STAT3 expression of immunosuppressive protein CD274 (PD-L1, B7-H1). *Proc Natl Acad Sci U S A* 105: 20852-20857

McGranahan N, Furness AJ, Rosenthal R, Ramskov S, Lyngaa R, Saini SK, Jamal-Hanjani M, Wilson GA, Birkbak NJ, Hiley CT, Watkins TB, Shafi S, Murugaesu N, Mitter R, Akarca AU, Linares J, Marafioti T, Henry JY, Van Allen EM, Miao D, Schilling B, Schadendorf D, Garraway LA, Makarov V, Rizvi NA, Snyder A, Hellmann MD, Merghoub T, Wolchok JD, Shukla SA, Wu CJ, Peggs KS, Chan TA, Hadrup SR, Quezada SA, Swanton C (2016) Clonal

neoantigens elicit T cell immunoreactivity and sensitivity to immune checkpoint blockade. *Science* 351: 1463-1469

Ménard S, Pupa SM, Campiglio M, Tagliabue E (2003) Biologic and therapeutic role of HER2 in cancer. *Oncogene* 22: 6570-6578

Mercogliano MF, De Martino M, Venturutti L, Rivas MA, Proietti CJ, Inurrigarro G, Frahm I, Allemand DH, Deza EG, Ares S, Gercovich FG, Guzmán P, Roa JC, Elizalde PV, Schillaci R (2017) TNFα-Induced Mucin 4 Expression Elicits Trastuzumab Resistance in HER2-Positive Breast Cancer. *Clin Cancer Res* 23: Feb 1

Minuti G, Cappuzzo F, Duchnowska R, Jassem J, Fabi A, O'Brien T, Mendoza AD, Landi L, Biernat W, Czartoryska-Arlukowicz B, Jankowski T, Zuziak D, Zok J, Szostakiewicz B, Foszczynska-Kloda M, Tempinska-Szalach A, Rossi E, Varella-Garcia M (2012) Increased MET and HGF gene copy numbers are associated with trastuzumab failure in HER2-positive metastatic breast cancer. *Br J Cancer* 107: 793-799

Mitra D, Brumlik MJ, Okamgba SU, Zhu Y, Duplessis TT, Parvani JG, Lesko SM, Brogi E, Jones FE (2009) An oncogenic isoform of HER2 associated with locally disseminated breast cancer and trastuzumab resistance. *Mol Cancer Ther* 8: 2152-2162 doi: 10.1158/1535-7163.MCT-09-0295.

Miyan M, Schmidt-Mende J, Kiessling R, Poschke I, de BJ (2016) Differential tumor infiltration by T-cells characterizes intrinsic molecular subtypes in breast cancer. *J Transl Med* 14: 227-0983

Mohsin SK, Weiss HL, Gutierrez MC, Chamness GC, Schiff R, DiGiovanna MP, Wang CX, Hilsenbeck SG, Osborne CK, Allred DC, Elledge R, Chang JC (2005) Neoadjuvant trastuzumab induces apoptosis in primary breast cancers. *J Clin Oncol* 23: 2460-2468

Molina MA, Codony-Servat J, Albanell J, Rojo F, Arribas J, Baselga J (2001) Trastuzumab (herceptin), a humanized anti-HER2 receptor monoclonal antibody, inhibits basal and activated Her2 ectodomain cleavage in breast cancer cells. *Cancer Res* 61: 4744-4749

Montemurro F, Di CS, Arpino G (2013) Human epidermal growth factor receptor 2 (HER2)-positive and hormone receptor-positive breast cancer: new insights into molecular interactions and clinical implications. *Ann Oncol* 24: 2715-2724

Monti S, Tamayo P, Mesirov J (2003) Consensus clustering: A resampling based method for class discovery and visualization of gene expression microarray data. *Machine Learning* 52:91-118

Moretta A, Bottino C, Vitale M, Pende D, Cantoni C, Mingari MC, Biassoni R, Moretta L (2001) Activating receptors and coreceptors involved in human natural killer cell-mediated cytolysis. *Annu Rev Immunol* 19: 197-223

Mortenson ED, Park S, Jiang Z, Wang S, Fu YX (2013) Effective anti-neu-initiated antitumor responses require the complex role of CD4+ T cells. *Clin Cancer Res* 19: 1476-1486 doi: 10.1158/1078-0432.CCR-12-2522.

Motz GT, Coukos G (2013) Deciphering and reversing tumor immune suppression. *Immunity* 39: 61-73

Mozaffari F, Lindemalm C, Choudhury A, Granstam-Bjorneklett H, Helander I, Lekander M, Mikaelsson E, Nilsson B, Ojutkangas ML, Osterborg A, Bergkvist L, Mellstedt H (2007) NK-cell and T-cell functions in patients with breast cancer: effects of surgery and adjuvant chemo- and radiotherapy. *Br J Cancer* 97: 105-111

Nagata Y, Lan KH, Zhou X, Tan M, Esteva FJ, Sahin AA, Klos KS, Li P, Monia BP, Nguyen NT, Hortobagyi GN, Hung MC, Yu D (2004) PTEN activation contributes to tumor inhibition by trastuzumab, and loss of PTEN predicts trastuzumab resistance in patients. *Cancer Cell* 6: 117-127

Nagy P, Friedlander E, Tanner M, Kapanen AI, Carraway KL, Isola J, Jovin TM (2005) Decreased accessibility and lack of activation of ErbB2 in JIMT-1, a herceptin-resistant, MUC4-expressing breast cancer cell line. *Cancer Res* 65: 473-482

Nahta R, O'regan RM (2012) Therapeutic implications of estrogen receptor signaling in HER2-positive breast cancers. *Breast Cancer Res Treat* 135: 39-48

Nahta R, Takahashi T, Ueno NT, Hung MC, Esteva FJ (2004) P27(kip1) down-regulation is associated with trastuzumab resistance in breast cancer cells. *Cancer Res* 64: 3981-3986

Nahta R, Yuan LX, Du Y, Esteva FJ (2007) Lapatinib induces apoptosis in trastuzumab-resistant breast cancer cells: effects on insulin-like growth factor I signaling. *Mol Cancer Ther* 6: 667-674

Nausch N, Cerwenka A (2008) NKG2D ligands in tumor immunity. *Oncogene* 27: 5944-5958

Nocera NF, Lee MC, De La Cruz LM, Rosemblit C, Czerniecki BJ (2016) Restoring Lost Anti-HER-2 Th1 Immunity in Breast Cancer: A Crucial Role for Th1 Cytokines in Therapy and Prevention. *Front Pharmacol* 7: 356

Osborne CK, Schiff R (2005) Estrogen-receptor biology: continuing progress and therapeutic implications. *J Clin Oncol* 23: 1616-1622

Pardoll DM (2012) The blockade of immune checkpoints in cancer immunotherapy. *Nat Rev Cancer* 12: 252-264

Park S, Jiang Z, Mortenson ED, Deng L, Radkevich-Brown O, Yang X, Sattar H, Wang Y, Brown NK, Greene M, Liu Y, Tang J, Wang S, Fu YX (2010) The therapeutic effect of anti-HER2/neu antibody depends on both innate and adaptive immunity. *Cancer Cell* 18: 160-170 doi: 10.1016/j.ccr.2010.06.014.

Park S, Wang HY, Kim S, Ahn S, Lee D, Cho Y, Park KH, Jung D, Kim SI, Lee H (2014) Quantitative RT-PCR assay of HER2 mRNA expression in formalin-fixed and paraffin-embedded breast cancer tissues. *Int J Clin Exp Pathol* 7: 6752-6759

Parker JS, Mullins M, Cheang MC, Leung S, Voduc D, Vickery T, Davies S, Fauron C, He X, Hu Z, Quackenbush JF, Stijleman IJ, Palazzo J, Marron JS, Nobel AB, Mardis E, Nielsen TO, Ellis MJ, Perou CM, Bernard PS (2009) Supervised risk predictor of breast cancer based on intrinsic subtypes. *J Clin Oncol* 27: 1160-1167 doi: 10.1200/JCO.2008.18.1370.

Parsa AT, Waldron JS, Panner A, Crane CA, Parney IF, Barry JJ, Cachola KE, Murray JC, Tihan T, Jensen MC, Mischel PS, Stokoe D, Pieper RO (2007) Loss of tumor suppressor PTEN function increases B7-H1 expression and immunoresistance in glioma. *Nat Med* 13: 84-88

Pegram MD, Konecny GE, O'Callaghan C, Beryt M, Pietras R, Slamon DJ (2004) Rational combinations of trastuzumab with chemotherapeutic drugs used in the treatment of breast cancer. *J Natl Cancer I* 96: 739-749

Pegram MD, Reese DM (2002) Combined biological therapy of breast cancer using monoclonal antibodies directed against HER2/neu protein and vascular endothelial growth factor. *Semin Oncol* 29: 29-37

Penault-Llorca F, Bilous M, Dowsett M, Hanna W, Osamura RY, Ruschoff J, van d, V (2009) Emerging technologies for assessing HER2 amplification. *Am J Clin Pathol* 132: 539-548

Perez EA, Ballman KV, Tenner KS, Thompson EA, Badve SS, Bailey H, Baehner FL (2016) Association of stromal tumor-infiltrating lymphocytes with recurrence-free survival in the N9831 adjuvant trial in patients with early-stage HER2-positive breast cancer. *JAMA Oncol* 2: 56-64

Perez EA, Dueck AC, McCullough AE, Chen B, Geiger XJ, Jenkins RB, Lingle WL, Davidson NE, Martino S, Kaufman PA, Kutteh LA, Sledge GW, Harris LN, Gralow JR, Reinholz MM (2013) Impact of PTEN protein expression on benefit from adjuvant trastuzumab in early-stage human epidermal growth factor receptor 2-positive breast cancer in the North Central Cancer Treatment Group N9831 trial. *J Clin Oncol* 31: 2115-2122

Perez EA, Romond EH, Suman VJ, Jeong JH, Davidson NE, Geyer CE, Jr., Martino S, Mamounas EP, Kaufman PA, Wolmark N (2011) Four-year follow-up of trastuzumab plus adjuvant chemotherapy for operable human epidermal growth factor receptor 2-positive breast cancer: joint analysis of data from NCCTG N9831 and NSABP B-31. *J Clin Oncol* 29: 3366-3373

Perez EA, Romond EH, Suman VJ, Jeong JH, Sledge G, Geyer CE, Jr., Martino S, Rastogi P, Gralow J, Swain SM, Winer EP, Colon-Otero G, Davidson NE, Mamounas E, Zujewski JA, Wolmark N (2014) Trastuzumab Plus Adjuvant Chemotherapy for Human Epidermal Growth Factor Receptor 2-Positive Breast Cancer: Planned Joint Analysis of Overall Survival From NSABP B-31 and NCCTG N9831. *J Clin Oncol* 32: 3744-3752

Perez EA, Thompson EA, Ballman KV, Anderson SK, Asmann YW, Kalari KR, Eckel-Passow JE, Dueck AC, Tenner KS, Jen J, Fan JB, Geiger XJ, McCullough AE, Chen B, Jenkins RB, Sledge GW, Winer EP, Gralow JR, Reinholz MM (2015) Genomic analysis reveals that immune function genes are strongly linked to clinical outcome in the North Central Cancer Treatment Group n9831 Adjuvant Trastuzumab Trial. *J Clin Oncol* 33: 701-708

Perez EA, Ballman KV, Mashadi-Hossein A, Tenner KS, Kachergus JM, Norton N, Necela BM, Carr JM, Ferree S, Perou CM, Baehner F, Cheang MC, Thompson EA (2016) Intrinsic Subtype and Therapeutic Response Among HER2-Positive Breaty st Tumors from the NCCTG (Alliance) N9831 Trial.*JNCI* 109(2). pii: djw207. Print 2017 Feb.

Perou CM, Sorlie T, Eisen MB, van de Rijn M, Jeffrey SS, Rees CA, Pollack JR, Ross DT, Johnsen H, Akslen LA, Fluge O, Pergamenschikov A, Williams C, Zhu SX, Lonning PE, Borresen-Dale AL, Brown PO, Botstein D (2000) Molecular portraits of human breast tumours. *Nature* 406: 747-752 PMID:10963602

Peske JD, Woods AB, Engelhard VH (2015) Control of CD8 T-Cell Infiltration into Tumors by Vasculature and Microenvironment. *Adv Cancer Res* 128:263-307. doi: 10.1016/bs.acr.2015.05.001. Epub;%2015 Jun 1.: 263-307

Petrelli F, Borgonovo K, Cabiddu M, Ghilardi M, Barni S (2011) Neoadjuvant chemotherapy and concomitant trastuzumab in breast cancer: a pooled analysis of two randomized trials. *Anticancer Drugs* 22: 128-135

Piccart-Gebhart, M. J., Holmes, A. P., Baselga, J., De Azambuja, E., Dueck, A. C., Viale, G., Zujewski, J., Goldhirsch, A., Santillana, S., Pritchard, K. I., Wolff, A. C., Jackisch, C., Lang, I., Untch, M., Smith, I. E., Boyle, F., Xu, B., Gomez, H. L., Gelber, R. D., and Perez, E. A. First results from the phase III ALTTO trial (BIG 2-06; NCCTG [Alliance) N063D) comparing one year of anti-HER2 therapy with lapatinib alone (L), trastuzumab alone (T), their sequence (T--L), or thei compbination (T+L) in the adjuvant treatment of HER2-positive early breast cancer (EBC). J Clin Oncol 32 suppl, 5s-abstr LBA4. 2014.
Ref Type: Abstract

Pietras RJ, Pegram MD, Finn RS, Maneval DA, Slamon DJ (1998) Remission of human breast cancer xenografts on therapy with humanized monoclonal antibody to HER-2 receptor and DNA-reactive drugs. *Oncogene* 17: 2235-2249

Pogue-Geile KL, Kim C, Jeong JH, Tanaka N, Bandos H, Gavin PG, Fumagalli D, Goldstein LC, Sneige N, Burandt E, Taniyama Y, Bohn OL, Lee A, Kim SI, Reilly ML, Remillard MY, Blackmon NL, Kim SR, Horne ZD, Rastogi P, Fehrenbacher L, Romond EH, Swain SM, Mamounas EP, Wickerham DL, Geyer CE, Jr., Costantino JP, Wolmark N, Paik S (2013) Predicting Degree of Benefit From Adjuvant Trastuzumab in NSABP Trial B-31. *J Natl Cancer Inst* 105: 1782-1788

Pogue-Geile KL, Song N, Jeong JH, Gavin PG, Kim SR, Blackmon NL, Finnigan M, Rastogi P, Fehrenbacher L, Mamounas EP, Swain SM, Wickerham DL, Geyer CE, Jr., Costantino JP, Wolmark N, Paik S (2015) Intrinsic subtypes, PIK3CA mutation, and the degree of benefit from adjuvant trastuzumab in the NSABP B-31 trial. *J Clin Oncol* 33: 1340-1347

Pollack JR, Sorlie T, Perou CM, Rees CA, Jeffrey SS, Lonning PE, Tibshirani R, Botstein D, Borresen-Dale AL, Brown PO (2002) Microarray analysis reveals a major direct role of DNA copy number alteration in the transcriptional program of human breast tumors. *Proc Natl Acad Sci U S A* 99: 12963-12968

Prat A, Bianchini G, Thomas M, Belousov A, Cheang MC, Koehler A, Gomez P, Semiglazov V, Eiermann W, Tjulandin S, Byakhow M, Bermejo B, Zambetti M, Vazquez F, Gianni L,

Baselga J (2014a) Research-based PAM50 subtype predictor identifies higher responses and improved survival outcomes in HER2-positive breast cancer in the NOAH study. *Clin Cancer Res* 20: 511-521

Prat A, Carey LA, Adamo B, Vidal M, Tabernero J, Cortes J, Parker JS, Perou CM, Baselga J (2014b) Molecular features and survival outcomes of the intrinsic subtypes within HER2-positive breast cancer. *J Natl Cancer Inst* 106: dju152

Prat A, Perou CM (2011) Deconstructing the molecular portraits of breast cancer. *Mol Oncol* 5: 5-23

Prat A, Pineda E, Adamo B, Galvan P, Fernandez A, Gaba L, Diez M, Viladot M, Arance A, Munoz M (2015) Clinical implications of the intrinsic molecular subtypes of breast cancer. *Breast* 24 Suppl 2: S26-S35

R Development Core Team (2007) R: A language and environment for statistical computing. Vienna, Austria: R Foundation for Statistical Computing. URL http://www.R-project.org.

Rakha EA, Reis-Filho JS, Baehner F, Dabbs DJ, Decker T, Eusebi V, Fox SB, Ichihara S, Jacquemier J, Lakhani SR, Palacios J, Richardson AL, Schnitt SJ, Schmitt FC, Tan PH, Tse GM, Badve S, Ellis IO (2010) Breast cancer prognostic classification in the molecular era: the role of histological grade. *Breast Cancer Res* 12: 207

Rakhra K, Bachireddy P, Zabuawala T, Zeiser R, Xu L, Kopelman A, Fan AC, Yang Q, Braunstein L, Crosby E, Ryeom S, Felsher DW (2010) CD4(+) T cells contribute to the remodeling of the microenvironment required for sustained tumor regression upon oncogene inactivation. *Cancer Cell* 18: 485-498

Ravo M, Mutarelli M, Ferraro L, Grober OM, Paris O, Tarallo R, Vigilante A, Cimino D, De BM, Nola E, Cicatiello L, Weisz A (2008) Quantitative expression profiling of highly degraded RNA from formalin-fixed, paraffin-embedded breast tumor biopsies by oligonucleotide microarrays. *Lab Invest* 88: 430-440

Ritter CA, Perez-Torres M, Rinehart C, Guix M, Dugger T, Engelman JA, Arteaga CL (2007) Human breast cancer cells selected for resistance to trastuzumab in vivo overexpress epidermal growth factor receptor and ErbB ligands and remain dependent on the ErbB receptor network. *Clin Cancer Res* 13: 4909-4919

Rivenbark AG, O'Connor SM, Coleman WB (2013) Molecular and cellular heterogeneity in breast cancer: challenges for personalized medicine. *Am J Pathol* 183: 1113-1124

Robidoux A, Tang G, Rastogi P, Geyer CE, Jr., Azar CA, Atkins JN, Fehrenbacher L, Bear HD, Baez-Diaz L, Sarwar S, Margolese RG, Farrar WB, Brufsky AM, Shibata HR, Bandos H, Paik S, Costantino JP, Swain SM, Mamounas EP, Wolmark N (2013) Lapatinib as a component of neoadjuvant therapy for HER2-positive operable breast cancer (NSABP protocol B-41): an open-label, randomised phase 3 trial. *Lancet Oncol* 14: 1183-1192

Rody A, Holtrich U, Pusztai L, Liedtke C, Gaetje R, Ruckhaeberle E, Solbach C, Hanker L, Ahr A, Metzler D, Engels K, Karn T, Kaufmann M (2009) T-cell metagene predicts a

favorable prognosis in estrogen receptor-negative and HER2-positive breast cancers. *Breast Cancer Res* 11: R15

Roepman P, Horlings HM, Krijgsman O, Kok M, Bueno-de-Mesquita JM, Bender R, Linn SC, Glas AM, van d, V (2009) Microarray-based determination of estrogen receptor, progesterone receptor, and HER2 receptor status in breast cancer. *Clin Cancer Res* 15: 7003-7011

Ross JS, Slodkowska EA, Symmans WF, Pusztai L, Ravdin PM, Hortobagyi GN (2009) The HER-2 receptor and breast cancer: ten years of targeted anti-HER-2 therapy and personalized medicine. *Oncologist* 14: 320-368

Rousseeuw PJ (1987) Silhouettes: a graphical aid to the interpretation and validation of cluster analysis. Computational Applied Math 20: 53–56

Rouzier R, Perou CM, Symmans WF, Ibrahim N, Cristofanilli M, Anderson K, Hess KR, Stec J, Ayers M, Wagner P, Morandi P, Fan C, Rabiul I, Ross JS, Hortobagyi GN, Pusztai L (2005) Breast cancer molecular subtypes respond differently to preoperative chemotherapy. *Clin Cancer Res* 11: 5678-5685

Rubin I, Yarden Y (2001) The basic biology of HER2. *Ann Oncol* 12: S3-S8

Saha B, Jyothi PS, Chandrasekar B, Nandi D (2010) Gene modulation and immunoregulatory roles of interferon gamma. *Cytokine* 50: 1-14

Salgado R, Denkert C, Campbell C, Savas P, Nucifero P, Aura C, De AE, Eidtmann H, Ellis CE, Baselga J, Piccart-Gebhart MJ, Michiels S, Bradbury I, Sotiriou C, Loi S (2015a) Tumor-Infiltrating Lymphocytes and Associations With Pathological Complete Response and Event-Free Survival in HER2-Positive Early-Stage Breast Cancer Treated With Lapatinib and Trastuzumab: A Secondary Analysis of the NeoALTTO Trial. *JAMA Oncol* 1: 448-454

Salgado R, Denkert C, Demaria S, Sirtaine N, Klauschen F, Pruneri G, Wienert S, Van den EG, Baehner FL, Penault-Llorca F, Perez EA, Thompson EA, Symmans WF, Richardson AL, Brock J, Criscitiello C, Bailey H, Ignatiadis M, Floris G, Sparano J, Kos Z, Nielsen T, Rimm DL, Allison KH, Reis-Filho JS, Loibl S, Sotiriou C, Viale G, Badve S, Adams S, Willard-Gallo K, Loi S (2015b) The evaluation of tumor-infiltrating lymphocytes (TILs) in breast cancer: recommendations by an International TILs Working Group 2014. *Ann Oncol* 26: 259-271

Scaltriti M, Eichhorn PJ, Cortes J, Prudkin L, Aura C, Jimenez J, Chandarlapaty S, Serra V, Prat A, Ibrahim YH, Guzman M, Gili M, Rodriguez O, Rodriguez S, Perez J, Green SR, Mai S, Rosen N, Hudis C, Baselga J (2011) Cyclin E amplification/overexpression is a mechanism of trastuzumab resistance in HER2+ breast cancer patients. *Proc Natl Acad Sci U S A* 108: 3761-3766

Scaltriti M, Rojo F, Ocana A, Anido J, Guzman M, Cortes J, Di Cosimo S, Matias-Guiu X, Cajal S, Arribas J, Baselga J (2007) Expression of p95HER2, a truncated form of the HER2 receptor, and response to anti-HER2 therapies in breast cancer. *J Natl Cancer I* 99: 628-638

Schneeweiss A, Chia S, Hickish T, Harvey V, Eniu A, Hegg R, Tausch C, Seo JH, Tsai YF, Ratnayake J, McNally V, Ross G, Cortes J (2013) Pertuzumab plus trastuzumab in combination with standard neoadjuvant anthracycline-containing and anthracycline-free chemotherapy regimens in patients with HER2-positive early breast cancer: a randomized phase II cardiac safety study (TRYPHAENA). *Ann Oncol* 24: 2278-2284

Schumacher TN, Schreiber RD (2015) Neoantigens in cancer immunotherapy. *Science* 348: 69-74

Senkus E, Kyriakides S, Ohno S, Penault-Llorca F, Poortmans P, Rutgers E, Zackrisson S, Cardoso F (2015) Primary breast cancer: ESMO Clinical Practice Guidelines for diagnosis, treatment and follow-up. *Ann Oncol* 26 Suppl 5: v8-30

Serafini P, Meckel K, Kelso M, Noonan K, Califano J, Koch W, Dolcetti L, Bronte V, Borrello I (2006) Phosphodiesterase-5 inhibition augments endogenous antitumor immunity by reducing myeloid-derived suppressor cell function. *J Exp Med* 203: 2691-2702

Sharma RK, Chheda ZS, Jala VR, Haribabu B (2015) Regulation of cytotoxic T-Lymphocyte trafficking to tumors by chemoattractants: implications for immunotherapy. *Expert Rev Vaccines* 14: 537-549

Shattuck DL, Miller JK, Carraway KL, III, Sweeney C (2008) Met receptor contributes to trastuzumab resistance of Her2-overexpressing breast cancer cells. *Cancer Res* 68: 1471-1477

Shi Y, Fan X, Deng H, Brezski RJ, Rycyzyn M, Jordan RE, Strohl WR, Zou Q, Zhang N, An Z (2015) Trastuzumab triggers phagocytic killing of high HER2 cancer cells in vitro and in vivo by interaction with Fcgamma receptors on macrophages. *J Immunol* 194: 4379-4386

Shiu KK, Wetterskog D, Mackay A, Natrajan R, Lambros M, Sims D, Bajrami I, Brough R, Frankum J, Sharpe R, Marchio C, Horlings H, Reyal F, van d, V, Turner N, Reis-Filho JS, Lord CJ, Ashworth A (2014) Integrative molecular and functional profiling of ERBB2-amplified breast cancers identifies new genetic dependencies. *Oncogene* 33: 619-631

Siegel PM, Ryan ED, Cardiff RD, Muller WJ (1999) Elevated expression of activated forms of Neu/ErbB-2 and Erb-3 are involved in the induction of mammary tumors in transgenic mice: implications for human breast cancer. *EMBO J* 18: 2149-2164

Slamon D, Eiermann W, Robert N, Pienkowski T, Martin M, Press M, Mackey J, Glaspy J, Chan A, Pawlicki M, Pinter T, Valero V, Liu MC, Sauter G, Von Minckwitz G, Visco F, Bee V, Buyse M, Bendahmane B, Tabah-Fisch I, Lindsay MA, Riva A, Crown J (2011) Adjuvant trastuzumab in HER2-positive breast cancer. *N Engl J Med* 365: 1273-1283

Slamon DJ, Leyland-Jones B, Shak S, Fuchs H, Paton V, Bajamonde A, Fleming T, Eiermann W, Wolter J, Pegram M, Baselga J, Norton L (2001) Use of chemotherapy plus a monoclonal antibody against HER2 for metastatic breast cancer that overexpresses HER2. *N Engl J Med* 344: 783-792

Sliwkowski MX, Lofgren JA, Lewis GD, Hotaling TE, Fendly BM, Fox JA (1999) Nonclinical studies addressing the mechanism of action of trastuzumab (Herceptin). *Semin Oncol* 26: 60-70

Snyder A, Makarov V, Merghoub T, Yuan J, Zaretsky JM, Desrichard A, Walsh LA, Postow MA, Wong P, Ho TS, Hollmann TJ, Bruggeman C, Kannan K, Li Y, Elipenahli C, Liu C, Harbison CT, Wang L, Ribas A, Wolchok JD, Chan TA (2014) Genetic basis for clinical response to CTLA-4 blockade in melanoma. *N Engl J Med* 371: 2189-2199

Soria G, Ben-Baruch A (2008) The inflammatory chemokines CCL2 and CCL5 in breast cancer. *Cancer Lett* 267: 271-285

Sorlie T, Perou CM, Tibshirani R, Aas T, Geisler S, Johnsen H, Hastie T, Eisen MB, van de Rijn M, Jeffrey SS, Thorsen T, Quist H, Matese JC, Brown PO, Botstein D, Eystein LP, Borresen-Dale AL (2001) Gene expression patterns of breast carcinomas distinguish tumor subclasses with clinical implications. *Proc Natl Acad Sci USA* 98: 10869-10874

Sorlie T, Tibshirani R, Parker J, Hastie T, Marron JS, Nobel A, Deng S, Johnsen H, Pesich R, Geisler S, Demeter J, Perou CM, Lonning PE, Brown PO, Borresen-Dale AL, Botstein D (2003) Repeated observation of breast tumor subtypes in independent gene expression data sets. *Proc Natl Acad Sci USA* 100: 8418-8423

Sotiriou C, Neo SY, McShane LM, Korn EL, Long PM, Jazaeri A, Martiat P, Fox SB, Harris AL, Liu ET (2003) Breast cancer classification and prognosis based on gene expression profiles from a population-based study. *Proc Natl Acad Sci U S A* 100: 10393-10398

Spector NL, Blackwell KL (2009) Understanding the mechanisms behind trastuzumab therapy for human epidermal growth factor receptor 2-positive breast cancer. *J Clin Oncol* 27: 5838-5847

Spranger S, Spaapen RM, Zha Y, Williams J, Meng Y, Ha TT, Gajewski TF (2013) Up-regulation of PD-L1, IDO, and T(regs) in the melanoma tumor microenvironment is driven by CD8(+) T cells. *Sci Transl Med* 5: 200ra116

Staaf J, Ringner M, Vallon-Christersson J, Jonsson G, Bendahl PO, Holm K, Arason A, Gunnarsson H, Hegardt C, Agnarsson BA, Luts L, Grabau D, Ferno M, Malmstrom PO, Johannsson OT, Loman N, Barkardottir RB, Borg A (2010) Identification of subtypes in human epidermal growth factor receptor 2--positive breast cancer reveals a gene signature prognostic of outcome. *J Clin Oncol* 28: 1813-1820

Stagg J, Loi S, Divisekera U, Ngiow SF, Duret H, Yagita H, Teng MW, Smyth MJ (2011) Anti-ErbB-2 mAb therapy requires type I and II interferons and synergizes with anti-PD-1 or anti-CD137 mAb therapy. *Proc Natl Acad Sci USA* 108: 7142-7147

Stanton SE, Adams S, Disis ML (2016) Variation in the Incidence and Magnitude of Tumor-Infiltrating Lymphocytes in Breast Cancer Subtypes: A Systematic Review. *JAMA Oncol* 2: 1354-1360

Steiner JL, Murphy EA (2012) Importance of chemokine (CC-motif) ligand 2 in breast cancer. *Int J Biol Markers* 27: e179-e185

Stern HM, Gardner H, Burzykowski T, Elatre W, O'Brien C, Lackner MR, Pestano GA, Santiago A, Villalobos I, Eiermann W, Pienkowski T, Martin M, Robert N, Crown J, Nuciforo P, Bee V, Mackey J, Slamon DJ, Press MF (2015) PTEN Loss Is Associated with Worse Outcome in HER2-Amplified Breast Cancer Patients but Is Not Associated with Trastuzumab Resistance. *Clin Cancer Res* 21: 2065-2074

Subramanian A, Tamayo P, Mootha VK, Mukherjee S, Ebert BL, Gillette MA, Paulovich A, Pomeroy SL, Golub TR, Lander ES, Mesirov JP (2005) Gene set enrichment analysis: a knowledge-based approach for interpreting genome-wide expression profiles. *Proc Natl Acad Sci USA* 102: 15545-15550

Tagliabue E, Campiglio M, Pupa SM, Balsari A, Ménard S (2011) The HER2 world: better treatment selection for better outcome. *J Natl Cancer Inst Monogr* 2011: 82-85

Tagliabue E, Centis F, Campiglio M, Mastroianni A, Martignone S, Pellegrini R, Casalini P, Lanzi C, Ménard S, Colnaghi MI (1991) Selection of monoclonal antibodies which induce internalization and phosphorylation of $p185^{HER2}$ and growth inhibition of cells with HER2/*neu* gene amplification. *Int J Cancer* 47: 933-937

Taube JM, Anders RA, Young GD, Xu H, Sharma R, McMiller TL, Chen S, Klein AP, Pardoll DM, Topalian SL, Chen L (2012) Colocalization of inflammatory response with B7-h1 expression in human melanocytic lesions supports an adaptive resistance mechanism of immune escape. *Sci Transl Med* 4: 127ra37-doi: 10.1126/scitranslmed.3003689.

Topfer K, Kempe S, Muller N, Schmitz M, Bachmann M, Cartellieri M, Schackert G, Temme A (2011) Tumor evasion from T cell surveillance. *J Biomed Biotechnol* 2011:918471. doi: 10.1155/2011/918471. Epub;%2011 Nov 15.: 918471

Triulzi T, Bianchi GV, Tagliabue E (2016) Predictive biomarkers in the treatment of HER2-positive breast cancer: an ongoing challenge. *Future Oncol* 12: 1413-1428

Triulzi T, De Cecco L, Sandri M, Prat A, Giussani M, Paolini B, Carcangiu ML, Canevari S, Bottini A, Balsari A, Ménard S, Generali D, Campiglio M, Di Cosimo S, Tagliabue E (2015) Whole-transcriptome analysis links trastuzumab sensitivity of breast tumors to both HER2 dependence and immune cell infiltration. *Oncotarget* 6(29): 28173-28182.

Untch M, Rezai M, Loibl S, Fasching PA, Huober J, Tesch H, Bauerfeind I, Hilfrich J, Eidtmann H, Gerber B, Hanusch C, Kuhn T, Du bois A, Blohmer JU, Thomssen C, Dan CS, Jackisch C, Kaufmann M, Mehta K, von MG (2010) Neoadjuvant treatment with trastuzumab in HER2-positive breast cancer: results from the GeparQuattro study. *J Clin Oncol* 28: 2024-2031

Van Allen EM, Miao D, Schilling B, Shukla SA, Blank C, Zimmer L, Sucker A, Hillen U, Geukes Foppen MH, Goldinger SM, Utikal J, Hassel JC, Weide B, Kaehler KC, Loquai C, Mohr P, Gutzmer R, Dummer R, Gabriel S, Wu CJ, Schadendorf D, Garraway LA (2015) Genomic correlates of response to CTLA-4 blockade in metastatic melanoma. *Science* 350: 207-211

Varadan V, Gilmore H, Miskimen KL, Tuck D, Parsai S, Awadallah A, Krop IE, Winer EP, Bossuyt V, Somlo G, bu-Khalaf MM, Fenton MA, Sikov W, Harris LN (2016) Immune Signatures Following Single Dose Trastuzumab Predict Pathologic Response to

PreoperativeTrastuzumab and Chemotherapy in HER2-Positive Early Breast Cancer. *Clin Cancer Res* 22: 3249-3259

Varchetta S, Gibelli N, Oliviero B, Nardini E, Gennari R, Santo Silva L, Tagliabue E, Ménard S, Costa A, Fagnoni F (2007) Elements related to heterogeneity of antibody-dependent cell cytotoxicity (ADCC) in patients under trastuzumab therapy for primary operable breast cancer overexpressing HER2. *Cancer Res* 67: 11991-11999

Varfolomeev E, Goncharov T, Fedorova AV, Dynek JN, Zobel K, Deshayes K, Fairbrother WJ, Vucic D (2008) c-IAP1 and c-IAP2 are critical mediators of tumor necrosis factor alpha (TNFalpha)-induced NF-kappaB activation. *J Biol Chem* 283: 24295-24299

Vesely MD, Kershaw MH, Schreiber RD, Smyth MJ (2011) Natural innate and adaptive immunity to cancer. *Annu Rev Immunol* 29:235-71.

Viola A, Sarukhan A, Bronte V, Molon B (2012) The pros and cons of chemokines in tumor immunology. *Trends Immunol* 33: 496-504

Vivier E, Tomasello E, Baratin M, Walzer T, Ugolini S (2008) Functions of natural killer cells. *Nat Immunol* 9: 503-510

von MG, Loibl S, Untch M (2012) What is the current standard of care for anti-HER2 neoadjuvant therapy in breast cancer? *Oncology (Williston Park)* 26: 20-26

Waterman H, Alroy I, Strano S, Seger R, Yarden Y (1999) The C-terminus of the kinase-defective neuregulin receptor ErbB-3 confers mitogenic superiority and dictates endocytic routing. *EMBO J* 18: 3348-3358

Weigelt B, Geyer FC, Reis-Filho JS (2010) Histological types of breast cancer: how special are they? *Mol Oncol* 4: 192-208

Whiteside TL (2008) The tumor microenvironment and its role in promoting tumor growth. *Oncogene* 27: 5904-5912

Wilkerson MD, Hayes DN (2010) ConsensusClusterPlus: a class discovery tool with confidence assessments and item tracking. *Bioinformatics* 26: 1572-1573

Wirapati P, Sotiriou C, Kunkel S, Farmer P, Pradervand S, Haibe-Kains B, Desmedt C, Ignatiadis M, Sengstag T, Schutz F, Goldstein DR, Piccart M, Delorenzi M (2008) Meta-analysis of gene expression profiles in breast cancer: toward a unified understanding of breast cancer subtyping and prognosis signatures. *Breast Cancer Res* 10: R65

Wolff AC, Hammond ME, Hicks DG, Dowsett M, McShane LM, Allison KH, Allred DC, Bartlett JM, Bilous M, Fitzgibbons P, Hanna W, Jenkins RB, Mangu PB, Paik S, Perez EA, Press MF, Spears PA, Vance GH, Viale G, Hayes DF (2013) Recommendations for human epidermal growth factor receptor 2 testing in breast cancer: American Society of Clinical Oncology/College of American Pathologists clinical practice guideline update. *J Clin Oncol* 31: 3997-4013

Wolff AC, Hammond ME, Schwartz JN, Hagerty KL, Allred DC, Cote RJ, Dowsett M, Fitzgibbons PL, Hanna WM, Langer A, McShane LM, Paik S, Pegram MD, Perez EA, Press

MF, Rhodes A, Sturgeon C, Taube SE, Tubbs R, Vance GH, van d, V, Wheeler TM, Hayes DF (2007) American Society of Clinical Oncology/College of American Pathologists guideline recommendations for human epidermal growth factor receptor 2 testing in breast cancer. *J Clin Oncol* 25: 118-145

Yakes FM, Chinratanalab W, Ritter CA, King W, Seelig S, Arteaga CL (2002) Herceptin-induced inhibition of phosphatidylinositol-3 kinase and Akt is required for antibody-mediated effects on p27, cyclin D1, and antitumor action. *Cancer Res* 62: 4132-4141

Yarden Y (2001) The EGFR family and its ligands in human cancer. signalling mechanisms and therapeutic opportunities. *Eur J Cancer* 37: S3-S8

Yarden Y, Sliwkowski MX (2001) Untangling the ErbB signalling network. *Nat Rev Mol Cell Biol* 2: 127-137

Yasrebi H (2011) SurvJamda: an R package to predict patients' survival and risk assessment using joint analysis of microarray gene expression data. *Bioinformatics* 27: 1168-1169

Zhuang G, Brantley-Sieders DM, Vaught D, Yu J, Xie L, Wells S, Jackson D, Muraoka-Cook R, Arteaga C, Chen J (2010) Elevation of receptor tyrosine kinase EphA2 mediates resistance to trastuzumab therapy. *Cancer Res* 70: 299-308

Zitvogel L, Apetoh L, Ghiringhelli F, Kroemer G (2008) Immunological aspects of cancer chemotherapy. *Nat Rev Immunol* 8: 59-73

PUBLICATIONS

5.1. Publications related to my PhD project

- **Triulzi T**, Bianchi GV, Tagliabue E. Predictive biomarkers in the treatment of HER2-positive breast cancer: an ongoing challenge. Future Oncology, 2016 Jun;12(11):1413-28.
- Di Modica M, Sfondrini L, Regondi V, Varchetta S, Oliviero B, Mariani G, Bianchi GV, Generali D, Balsari A, **Triulzi T***, Tagliabue E*. Taxanes enhance trastuzumab-mediated ADCC on tumour cells through NKG2D-mediated NK cell recognition. Oncotarget, 2016 Jan 5;7(1):255-65.
- **Triulzi T***, De Cecco L*, Sandri M, Prat A, Giussani M, Paolini B, Carcangiu ML, Canevari S, Bottini A, Balsari A, Menard S, Generali D, Campiglio M, Di Cosimo S, Tagliabue E. Whole-transcriptome analysis links trastuzumab sensitivity of breast tumours to both HER2 dependence and immune cell infiltration. Oncotarget, 2015Sep 29;6(29):28173-82.

5.2. Other publications besides my PhD project

- Bianchi F., Sommariva M., De Cecco L., **Triulzi T**., Romero-Cordoba S., Tagliabue E., Sfondrini L., Balsari A. Expression and prognostic significance of the autoimmune regulator gene in breast cancer cells. Cell Cycle. In press
- M. Di Modica, V. Regondi, M. Sandri, MV Iorio, A. Zanetti, E. Tagliabue, P. Casalini and **T. Triulzi**. Breast cancer-secreted mir-939 downregulates VE-cadherin and destroys the barrier function of endothelial monolayers. Cancer Lett. 2016, Sep 28
- Castagnoli L, Ghedini GC, Koschorke A, **Triulzi T**, Dugo M, Gasparini P, Casalini P, Palladini A, Iezzi M, Lamolinara A, Lollini PL, Nanni P, Chiodoni C, Tagliabue E, Pupa SM. Pathobiological implications of the d16HER2 splice variant for stemness and aggressiveness of HER2-positive breast cancer. Oncogene, 2016

- Henne M, König N, **Triulzi T**, Baroni S, Forlani F, Scheibe R and Papenbrock J. Sulfurtransferase and thioredoxin specifically interact as demonstrated by bimolecular fluorescence complementation analysis and biochemical tests. FEBS Open Bio, 2015 Oct 8;5:832-843.
- Giussani M, De Maria C, Vasso M, Montemurro F, **Triulzi T**, Tagliabue E, Gelfi C, Vozzi G. Biomimicking of the breast tumour microenvironment. Curr Mol Biol Reports, 2015; 1(2):71-76.
- Castagnoli, M Iezzi, GC Ghedini, V Ciravolo, G Marzano, A Lamolinara, R Zappasodi, P Gasparini, M Campiglio, A Amici, C Chiodoni, A Palladini, PL Lollini, **T Triulzi**, S Menard, P Nanni, E Tagliabue and SM Pupa. Activated d16HER2 homodimers and Src kinase mediate optimal efficacy for trastuzumab. Cancer Res,2014 Nov 1;74(21):6248-59.
- Plantamura I, Casalini P, Dugnani E, Sasso M, D'Ippolito E, Tortoreto M, Cacciatore M, Guarnotta C, Ghirelli C, Barajon I, Bianchi F, **Triulzi T**,Agresti R, Balsari A, Campiglio M, Tripodo C, Iorio MV, Tagliabue E. PDGFRβ and FGFR2 mediate endothelial cell differentiation capability of triple negative breast carcinoma cells. Mol Oncol. 2014 Jul;8(5):968-81.